A multi-proxy study of planktonic foraminifera to identify past millennial-scale climate variability in the East Asian Monsoon and the Western Pacific Warm Pool

by

Stefanie Dannenmann

A Dissertation

Submitted to the University at Albany, State University of New York

in Partial Fulfillment of

the Requirements for the degree of

Doctor of Philosophy

College of Arts & Sciences

Department of Earth and Atmospheric Sciences

2001

University at Albany, State University of New York

COLLEGE OF ARTS & SCIENCES

The dissertation submitted by

Stefanie Dannenmann

under the title

A multi-proxy study of planktonic foraminifera to identify past millennial-scale climate variability in the East Asian Monsoon and the Western Pacific Warm Pool

has been read by the undersigned. It is hereby recommended for acceptance to the Faculty of the University in partial fulfillment of the requirement for the degree of Doctor of Philosophy.

_____	_____
Dr. B.K. Linsley	Date
_____	_____
Dr. A. G. Lapenis	Date
_____	_____
Dr. D.W. Oppo	Date
_____	_____
Dr. Y. Rosenthal	Date

Recommended by the Department of Earth & Atmospheric Sciences

_____, Chair

Recommendation accepted on behalf of the Graduate Academic Council.

_____	_____
	Date

ABSTRACT

High resolution paleo-climatological data from IMAGES core MD97-2141 (8.80° N, 121.31° E) located the Sulu Sea within the western tropical Pacific reveal the first evidence of continous millennial-scale variability in surface ocean conditions over the last 150,000 years. The millennial-scale planktonic foraminiferal oxygen isotope ($\delta^{18}O$) oscillations of *Globigerinoides ruber* (*G. ruber*) between 30,000-65,000 years (MIS3) are apparently in-phase with the Greenland ice core record and have amplitudes 1/3 to 2/3 the size of the Sulu Sea glacial-interglacial $\delta^{18}O$ amplitude of 1.3 ‰. In the same interval variations in planktonic foraminiferal Mg/Ca suggest that millennial-scale sea surface temperature (SST) variations were small (0.6-1°C) and out-of-phase with $\delta^{18}O$ indicating that $\delta^{18}O$ variability was mainly driven by changes in surface water salinity. This result implies that the linked East Asian monsoon and the western Pacific Intertropical Convergence Zones, both influencing the Sulu Sea, have fluctuated on the same millennial time scale as higher latitude climatic systems.

To further investigate the origin of the MIS3 $\delta^{18}O_{G.ruber}$ variations, the relative abundance of all planktonic foraminifer species and the $\delta^{18}O$ values of four planktonic foraminifer species was determined during MIS3. Combined, these data provide a detailed reconstruction of changes in the western tropical Pacific thermocline structure. The $\delta^{18}O$ composition of the mixed-layer foraminifera (*G. ruber* and *Globigerinoides sacculifer*) and upper thermocline species (*Neogloboquadrina dutertrei*) displays poor similarity with the $\delta^{18}O$ of the sub-thermocline dweller *Globorotalia crassaformis*. $\delta^{18}O_{G.crassaformis}$ shows larger $\delta^{18}O$ variations (~1 ‰) than the surface dwellers indicating past fluctuations in

the influence of high salinity North Pacific Tropical Waters that currently enter the Sulu Sea across the Mindoro Strait during the months of the winter monsoon. The faunal and isotopic data suggest a switch from winter to summer monsoon predominance after 55 kyr. However this predominance is interrupted by at least three episodes of increased winter monsoon between 42-46 kyr.

Comparison of the proxy SST and planktonic foraminiferal $\delta^{18}O$ profiles for the last glacial/interglacial sequence from fourteen cores in tropical and subtropical oceanic settings indicates that termination I in $\delta^{18}O$ coincides with SST change at some sites, while $\delta^{18}O$ lags SST by 3,000 years at other locations. A comparison of SST and $\delta^{18}O$ shows a linear increase in SST from glacial to interglacial conditions.. Sites where SST is leading the $\delta^{18}O$ record indicate fresher conditions during the LGM, and these sites are all located in areas influenced by increased atmospheric water vapor during times of today's La Niña.

DEDICATION

To my parents and my brother Tim

ACKNOWLEDGEMENTS

It has been an exceptional journey - one that I had never dreamed of. I am deeply indebted to my advisor Dr. B.K. Linsley for his encouragement, advice, mentoring, and research support throughout my doctoral studies. I also truly appreciate his engagement in the final stages of this dissertation. I am fortunate to have had Dr. Delia Oppo, Dr. Andrei Lapenis, and Dr. Yair Rosenthal as my committee members. I have enjoyed every moment to work with such a group of energetic people. This dissertation project also gave me the opportunity to work with great people at Woods Hole Oceanographic Institution and Rutgers University. Particularly, I would like to acknowledge Dr. Dick Norris for opening his world of foraminifera to me. Thanks to all of you for sharing your research ideas and enthusiasm about this project.

Thanks are also extended Dr. Win Means and Dr. Bill Kidd who have been tremendously helpful not only in their academic advisement but also in their personal openness. Steve Howe has been a great friend and extraordinary help in teaching my ways around the stable isotope lab, and editing the first draft of this dissertation. A big hug and special thanks go to Diana Paton for not going into early retirement. I could not have finished without her presence. I appreciate all their friendships and their collective encouragement to finish this dissertation.

I thank the IMAGES Program for allowing access to the great core MD97-2141. Thanks go to the WHOI-NOSAMS AMS facility that generated the AMS-data, and Liz Lukowski and Susan Trimarich for their technical support. This project has been funded by NSF Awards #OCE 9710156 to B.K. Linsley, #OCE

9710097 to D.W. Oppo for AMS analyses and lower 18 m $\delta^{18}O$ analyses, and #OCE 9987060 to Y. Rosenthal for Mg/Ca analyses.

I would especially like to thank my good friends Markus Landthaler, Chris Nemeth, Nicole Dentzien, Erich Nussbaum, my office-mate Barbara Fletcher and the Friday morning Quintessence breakfast club for helping me grow in various ways and for keeping this Ph.D. fun. I wish to acknowledge all of my other friends who have listened to me complain, cry and laugh through these past years. I could not ask for better friends.

There are not enough words to thank my boyfriend and best friend Stelios Matsopoulos for his love and support. His patience and understanding during this Ph.D. and particularly during difficult times was unselfish and appreciated more than he knows.

Finally, I owe a huge debt of gratitude to my parents' and my brother Tim's love and support, as well as their encouragement not only the course of my research career but throughout my entire life. This dissertation is dedicated to them.

To all of you, thank you

TABLE OF CONTENTS

LIST OF TABLES

LIST OF FIGURES

PREFACE

The research in this dissertation is based upon detailed analyses of marine sediments from the Sulu Sea in the Philippine archipelago of the tropical western Pacific. The primary goal of the research was to investigate the millennial-scale climate variability in this region and interpret the results within the context of the current understanding of the ocean-atmosphere system. Insights into the natural millennial-scale climatic variations will contribute to the developing understanding of forcing mechanisms and climatic interactions between widely separated regions. A new giant piston core in the Sulu Sea was collected to provide new material to study the millennial-scale events suggested by previous work on Ocean Drilling Program (ODP) site 769A [*Linsley and Thunell*, 1990; *Linsley*, 1996] in this unique and climatically important tropical setting.

This dissertation has been organized into a total of 4 chapters.

Chapter 1 presents background information about the regional area, and surface and deep water hydrography in the Sulu Sea.

Chapter 2 discusses millennial scale variability throughout the last 150,000 years in the Sulu Sea based on high resolution oxygen isotopic ($\delta^{18}O$) and Mg/Ca analyses of selected planktonic foraminifera. The findings in the Sulu Sea are then compared to millennial-scale climatic variations of high northern and southern latitudes.

Chapter 3 examines the specific climatic cause of marine isotope stage 3 (MIS3) millennial-scale oscillations by a faunal abundance study and the $\delta^{18}O$ composition of mixed layer, thermocline and subthermocline dwelling foraminifera. The $\delta^{18}O$ of these different foraminifera species is used to reconstruct the temporally varying upper column $\delta^{18}O$ gradient during MIS3.

Chapter 4 compares the Sulu Sea glacial-interglacial $\delta^{18}O$ record to 13 sediment cores from the Indian, Pacific and Atlantic oceans. It examines particularly the tropical climatological conditions during the last glacial maximum.

CHAPTER 1

Introduction to the Sulu Sea

1.1. Regional setting

The Sulu Sea is situated between Borneo, Palawan and the Philippines, and is approximately 600 km long and 400 km wide (Figure 1.1). The Sulu Sea is a small marginal basin with a maximum depth of more than 4,900 m. The basin exchanges surface water with surrounding basins over shallow sills, with the deepest sill connecting the Sulu Sea to the South China at 420 m through Mindoro Strait [*Wyrtki*, 1961].

IMAGES core MD97-2141 was collected in the Sulu Sea at 8.79° North latitude and 121.30° East longitude in 3,633 m water depth. This location is several kilometers northwest of Ocean Drilling Program Site 769A (ODP 769A) (8°47 North latitude, 121°13 East longitude, 3643 m water depth) (Figure 1.2). The bathymetric high where both cores were collected is ~1,200 m above the present local calcite compensation depth (4,800 m) and 200 m above the calcite lysocline (3,800 m) [*Linsley et al*., 1985].

1.2. Surface Water Hydrography

The East Asian Monsoon System (EAM) and the Western Pacific Warm Pool (WPWP) influence the surface hydrography of the South China and Sulu Seas. During the Northern Hemisphere summer, monsoon winds blow from the southeast. The winter component of the EAM has a stronger wind field, with northwesterly winds coming from Siberia [*Chen et al.,* 1997]. The high average annual atmospheric temperatures in the region induce evaporation of oceanic water, formation of low pressure cells and seasonally heavy rain. The overall hydrologic balance is a gain of freshwater from precipitation.

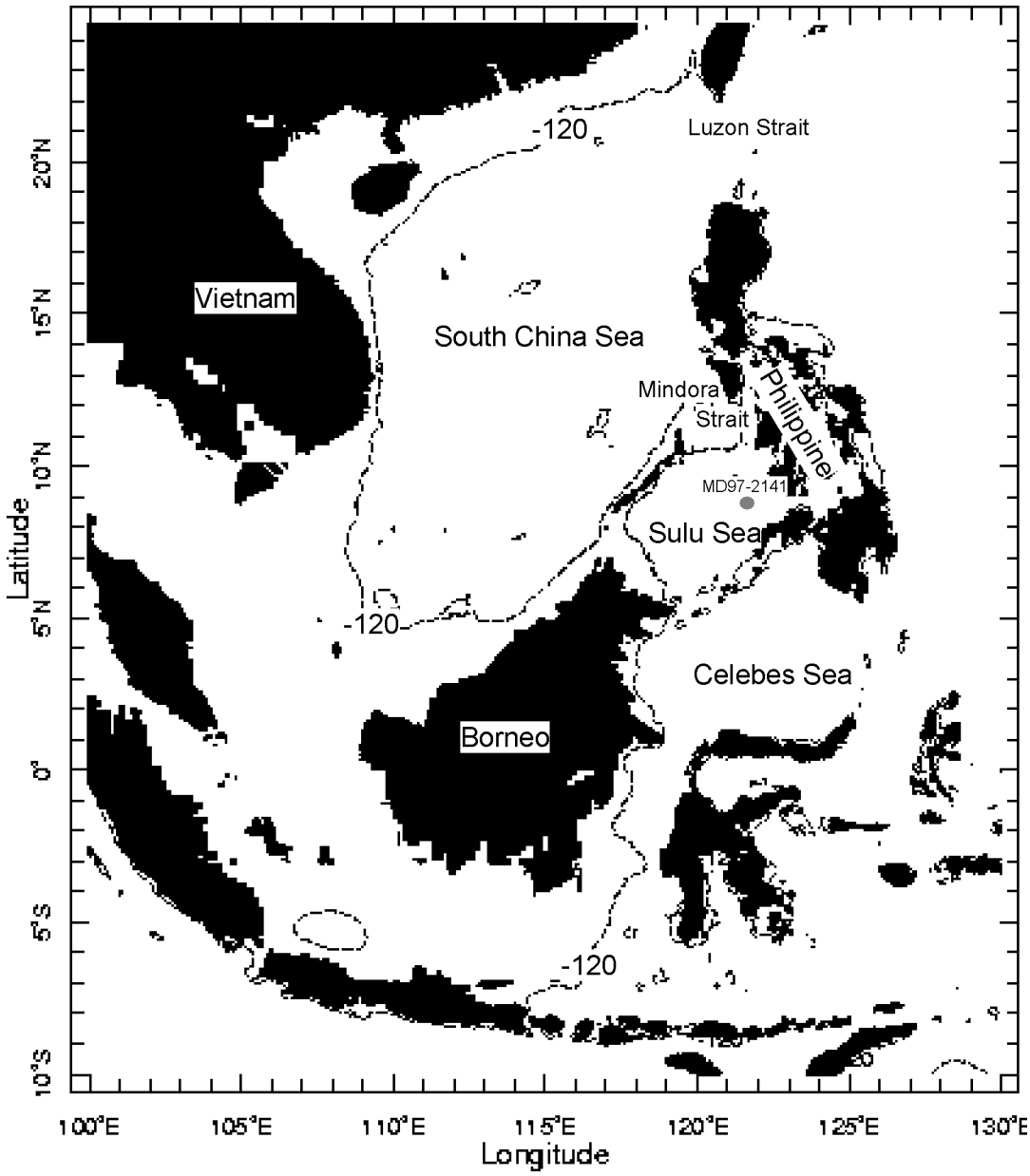

Figure 1.1: Map of western tropical Pacific showing the location of Sulu Sea. Bathymetric contour is the 120 m isobath indicating the approximate position of coast line during glacial maximum low sea level stand. A gray circle indicates location of IMAGES site MD97-2141.

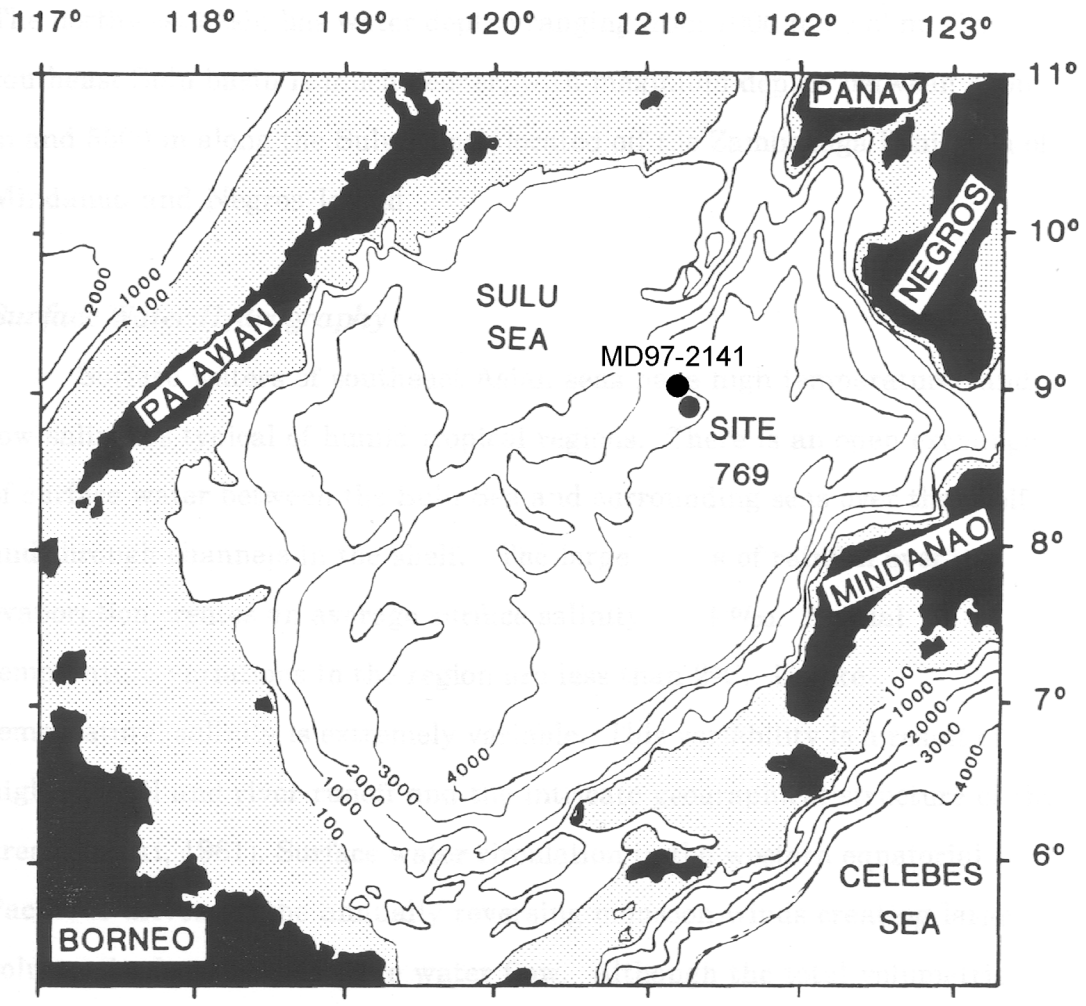

Figure 1.2: Detailed bathymetric map of the Sulu Sea. Bathymetric contour is presented in meters. Shelf shallower than 100 meter is marked by the shaded zone. Location of IMAGES site MD97-2141 (3,633 m) and ODP site 769A (3,643 m) are indicated by black circles.

In the Asian-Australian monsoon region, heavy convection is centered over the warm waters and adjacent land areas, with an eastward extension of high rainfall along the intertropical convergence zone (ITCZ) off the equator [*Rasmusson and Arkin*, 1993]. The ITCZ plays an important role in the climatic variability of the EAM region. The seasonal latitudinal variation of the ITCZ over this region is large. During the winter months in the Northern Hemisphere, the center of the warm pool lies south of the equator and during the summer months north of the equator. Areas with high sea surface temperatures (SST) (above 27.5 °C) correlate with oceanic regions of heavy rainfall. During the summer months, warm pool precipitation merges with the monsoon precipitation in the South China and Sulu Sea region.

Seasonal SST variability is greater in the northern South China Sea than the Sulu Sea, due to the inflow of cold water through the Luzon Strait and excess evaporation which both reduce SSTs during the months of the winter monsoon (Figure 1.3). Annually, SST varies about 2 ºC in the Sulu Sea and southern South China Sea (Figure 1.3) compared to 5 ºC in the northern South China Sea. The salinity in the entire region varies between 32.8 and 34.5 ‰ with the lowest salinities found during October as the result of freshwater inflow from rivers and direct monsoonal precipitation [*Wyrtki*, 1961]. *Wyrtki* [1961] gives a thorough review of the surface water hydrography of the Indonesian region.

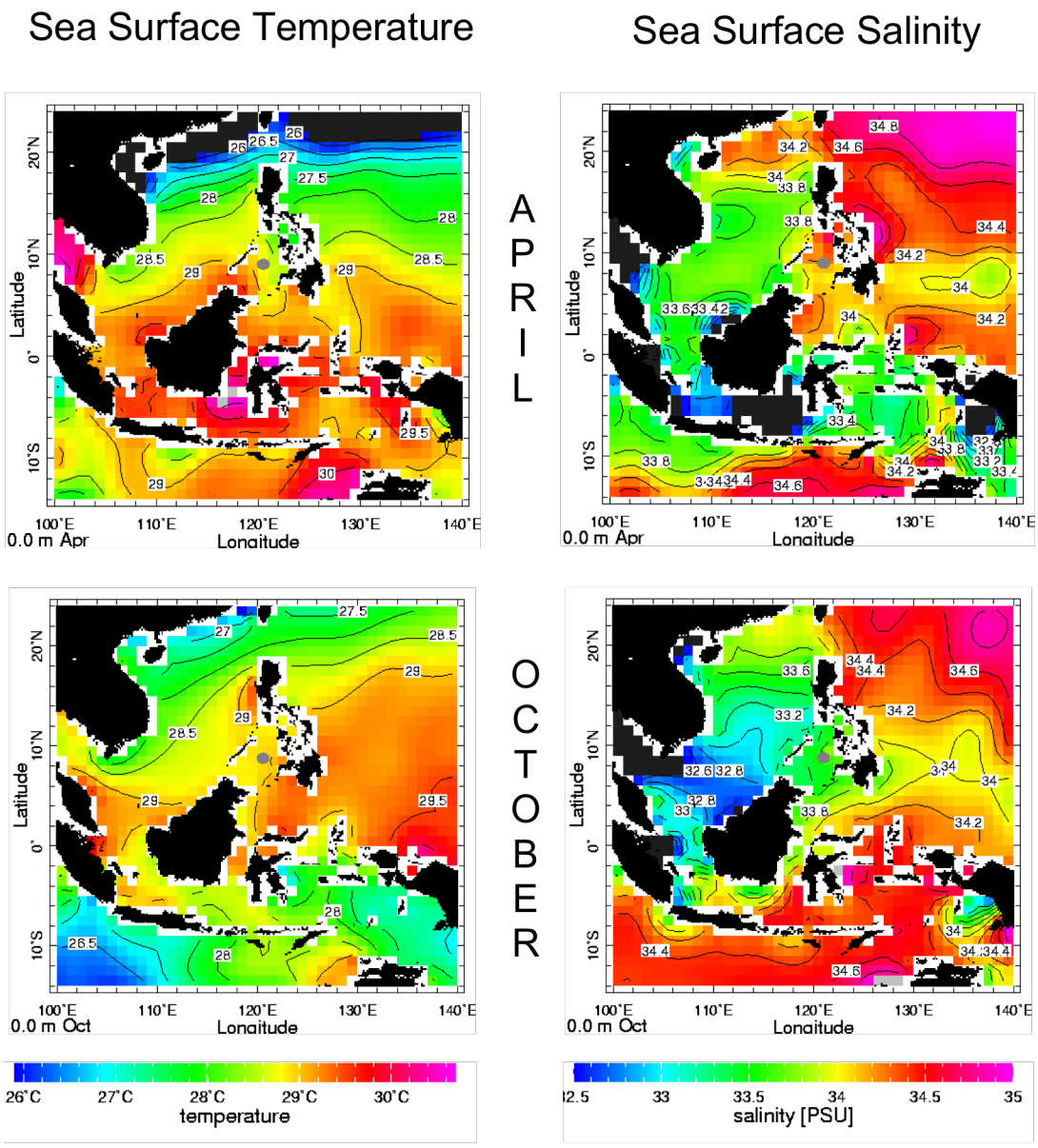

Figure 1.3: Average sea surface temperature and sea surface salinity in Indonesia and the western Pacific for the end of the winter monsoon (April) and the end of summer monsoon (October), highlighting maximal seasonal monsoon changes in surface conditions. Note the location of IMAGES core MD97-2141 that is marked by a gray circle. In the Sulu Sea the influence of East Asian Monsoon-driven river runoff and precipitation in Borneo and coastal regions of the mainland is evident as is the influence of the western Pacific on surface salinity [Data from *Conkright et al*., 1998].

1.3. Deep Water Hydrography

The semi-enclosed configuration of the Sulu Sea results in relatvely warm (10°), oxygen-depleted bottom water. This has resulted in a reduced depth of biological sediment mixing (1 to 3 cm), within the oxygen minimum zone compared to mixing depths in the South China Sea (10 cm) [*Kuehl et al.*, 1993]. High sediment accumulation rates [11 to 16 cm/1000 yr; *Linsley and Thunell*, 1990] and reduced benthic mixing have apparently resulted in the preservation of detailed paleoclimate records in certain areas and water depths of the Sulu Sea allowing past variations in the EAM and WPWP on millennial time scales to be examined.

Currently, the coldest water in the Sulu Sea is ~10 °C, and is found from ~600 m depth to the bottom. This relatively warm water fills the basin below the thermocline and contributes to the oxygen-deficient nature of the deep waters due to the stratification and biological utilization of oxygen. A detailed study of the hydrography in the Sulu Sea has been presented by *Nozaki et al.* [1999]. *Nozaki et al.* [1999] observed a salinity maximum (34.55 ‰) between 170 m and 310 m depths. They concluded that lateral flow of high salinity waters from the South China Sea produced this salinity maximum. *Wyrtki* [1961] named these high salinity waters the 'Subtropical Lower Waters', and *Qu et al.,* [2000] define these waters as high-salinity North Pacific Tropical Water (NPTW) which originates in the Kuroshio current outside the Southeast Asian seas. The Kuroshio current is part of western boundary current of the subtropical gyre in the North Pacific [*Shaw and Chao*, 1994; *Talley*, 1999]. Intrusion of the NPTW into the South China Sea occurs through the Luzon Strait, which has a sill depth of 2,500 m.

1.4. The Monsoon and the ENSO cycle

With growing global climate information and observations it became apparent that the monsoon system was a macro-scale phenomenon that was intertwined and interactive with global-scale circulation pattern [*Kutzbach*, 1987]. Of the many interrelated patterns found by Sir Gilbert Walker and others, the El Niño-Southern Oscillation (ENSO) was thought to be of particular relevance to the monsoon [e.g. *Walker*, 1923; *Walker*, 1928; *Walker and Bliss*, 1932; *Trenberth and Shea*, 1987; *Webster and Yank*, 1992; *Chen and Wu*, 2000]. For example the circum-Pacific climatic connection is revealed in an isocorrelation map of mean sea level pressure with Darwin, Australia [*Trenberth and Shea*, 1987]. A positive correlation exists between the northeastern and southeastern Pacific, and a strong negative correlation between the eastern and western Pacific. In the Sulu Sea and the surrounding basins, a quasi-permanent Indonesian low-pressure system influences regional oceanographic conditions. This low-pressure system affects the western Pacific climate, and also plays an important role on the ENSO system. It has been also suggested that ENSO may be initiated in the western equatorial Pacific [e.g. Wyrtki, 1975; Rasmusson and Carpenter, 1982; Li, 1989].

It is possible that ENSO effects are expressed over geological periods [*Anderson et al*., 1990; *Clement and Cane*, 1999; *Clement et al*., 2000], and it is therefore important to examine marine records affected by this phenomena in detail. Although this investigation does not establish a direct link between ENSO and Paleoclimatic variations in the western Pacific at lower than ENSO frequencies, it does help set the stage for establishing whether or not such linkage exists.

CHAPTER 2

Millennial-scale climate variability in the Tropical Western Pacific between 27,000 - 90,000 years B.P.

2.1 Abstract

Tropical oceanographic variabiity on millenial-time scales remains poorly understood. To develop a better understanding of past millenial-scale oceanographic variations in the western equatorial Pacific I have generated a continuously sampled record of variations in planktonic foraminiferal oxygen isotopes ($\delta^{18}O$) from a sediment core in the Sulu Sea (8°N, 122°E). This record reveals a distinct pattern of millennial-scale changes in surface ocean conditions, particularly between 27,000 and 60,000 years B.P. during marine isotope stage 3 (MIS3). This is the first evidence for persistent millenial-scale variability in MIS3 in the western tropical Pacific. The $\delta^{18}O$ oscillations during MIS3 appear to be in-phase with Dansgaard-Oeschger (D/O) air temperature variations in Greenland and have amplitudes 1/3 to 2/3 the size of the Sulu Sea glacial-interglacial $\delta^{18}O$ amplitude of 1.3 ‰. In the same interval, variations in planktonic foraminifera Mg/Ca indicate that surface ocean temperature variations were small (0.6-1°C) and not in phase with $\delta^{18}O$. This suggests that the MIS3 millennial $\delta^{18}O$ events in the Sulu Sea were driven by changes in surface water salinity indicating that the linked East Asian monsoon and western Pacific Intertropical Convergence Zones (ITCZ) have fluctuated on the same millennial time-scales as higher latitude climatic systems of the Northern Hemisphere.

2.2 Introduction

The fundamental question of the past variability of tropical surface temperatures and climate over glacial/interglacial and millennial time-scales remains controversial. There is conflicting information on the degree of tropical sea surface temperature (SST) cooling at the last glacial maximum (LGM) [e.g., *CLIMAP*, 1981; *Guilderson at el*., 1994; *Linsley*, 1996; *Wang et al*., 1999; *Lea et al.,* 2000; *Kienast et al*., 2001; *Rosenthal et al*., in prep], whereas terrestrial evidence consistently indicates a decrease of 4 to 5 °C in tropical surface temperatures during the LGM [e.g., *Rind and Peteet*, 1985; *Broecker and Denton*, 1989; *Stute et al.,* 1995]. On millennial time-scales, sparse evidence from the tropics is beginning to reveal a more variable late Pleistocene tropical climate than previously thought [e.g., *Linsley and Thunell*, 1990; *Sirocko et al*., 1999; *Wang et al*., 1999; *Kienast et al*., 2001; *Kudrass et al*., 2001; *deGaridel-Thoron et al.,* in press]. However, the number of tropical climate records that resolve millennial-scale climatic variations remains limited. This is particularly true for the tropical western Pacific, where developing a better understanding of past climatic variability is important because of the global influence of the Asian monsoon system and the Western Pacific Warm Pool (WPWP). Today, interannual and decadal variability in the monsoon and the WPMP has widespread and profound impacts on ecosystems, agriculture, and global economics. The South China and Sulu Seas are located in the northern part of the Asian-Australian monsoon region where during the summer months, increased precipitation is the result of the interaction of the ITCZ and the East Asian monsoon. In the Sulu Sea, monsoonal precipitation and river discharge

results in pronounced seasonal salinity variations with a minima in surface salinity occurring in October [*Wyrtki*, 1961; *Conkright et al*., 1998].

For this study I have analysed variations in planktonic foraminiferal $\delta^{18}O$ and Mg/Ca In MIS3 from Sulu Sea core MD97-2141 (IMAGES program) (8.8° N, 121.31° E, 3,633 m water depth) collected within several kilometers of Ocean Drilling Program (ODP) site 769A [*Linsley and Thunell*, 1990; *Linsley*, 1996]. At 1 cm sampling resolution for $\delta^{18}O$, the new record has four times greater temporal resolution (<100 years) than the previously published $\delta^{18}O$ record for *Globingerinoides ruber* ($\delta^{18}O_{G.\ ruber}$) from ODP site 769A [*Linsley,* 1996].

2.3 Methods

2.3.1 Oxygen isotopic analysis

Core MD97-2141 has a length of 36.3 m. The uppermost 18 m were slab-sampled every centimeter. The >150 μm size fraction was used for isotopic measurements. Each sample consisted of ~ 10 individual tests (~ 100 μg) of *Globingerinoides ruber* (white variety; 212-250 μm in diameter). Samples were reacted with 100 % H_3PO_4 at 90° C in a Mulitprep carbonate preparation device. The resulting CO_2 gas was analyzed with a Micromass Optima dual-inlet mass spectrometer at the University at Albany, State University of New York. The standard deviation of the National Institute of Science and Technology international reference standard NBS-19 analysed over an 8 month time period (n = 498) was 0.036 ‰ for $\delta^{18}O$. All isotopic data are reported relative to the Vienna Peedee Belemnite (VPDB) using the standard δ notation. The average

difference in $\delta^{18}O$ between duplicate analyses of the same sample of *G. ruber* (n=283) was 0.094 ‰.

2.3.2 Mg/Ca analysis

The cleaning procedure for the Mg/Ca analyses generally followed the protocol of *Rosenthal et al*. [1999]. Approximately 80 shells of *G. ruber* (212-250 µm sieve-size fraction) were picked and weighed with a Mettler M3 microbalance (nominal precision ± 1 µg). After weighing, each sample was gently crushed to open the chambers and split into two batches. The crushed samples were washed with deionized water, ultrasonicated and rinsed with methanol. The rinsed samples were treated with a hot basic oxidizing solution followed by multiple weak acid leaching (0.002 HNO_3). The cleaned samples were dissolved with HNO_3. Several authors [*Brown and Elderfield*, 1996; *Hastings et al.,* 1998] concluded that this cleaning procedure is sufficient for the Mg/Ca analysis in foraminifera. Mg/Ca ratios were determined using a Finnigan MAT Element Sector Field ICP-MS by a new method for precise, multi-elemental analysis of metal-to-calcium ratios [*Rosenthal et al*, 1999]. Samples between 30 and 60 kyr were analyzed for Mg/Ca and Sr/Ca only in order to decrease the external precision. The external precision of the Mg/Ca ratio was 0.1 % as determined by repeated measurements of three consistency standards. All other samples have been analyzed additionally for Mn/Ca, Cd/Ca, Ba/Ca and U/Ca and are described in greater detail in *Rosenthal et al* [in prep]. A more detailed analytical description and discussion about errors can be found in *Rosenthal et al.*, [1999].

2.3.3 Age model

The accelerator mass spectrometry (AMS) radiocarbon age measurements were made on the surface-dwelling planktonic foraminifera *G. ruber* and *G. sacculifer* at the Woods Hole AMS facility in Woods Hole, Massachusetts (Table 1). Calendar ages have been calculated using a 400 year reservoir correction and applying the *Stuiver and Braziunas* [1993] calibration curve for samples younger than 20,000 calendar years in age and a U/Th calibration curve for the samples older than 20,000 calendar years [*Bard et al*., 1993]. AMS-dates at the sample depths 400 cm and 421 cm indicate a gap of 11,000 years, and identify the probable presence of an erosional hiatus. A hiatus has not been observed in the ODP769A core [*Linsley*, 1996], but this might be due to the lower resolution AMS ^{14}C dating of this core. The general similarity of $\delta^{18}O$ records from both the ODP769A and MD97-2141 cores suggests that at least the upper 18 m of the MD97-2141 core is complete with the exception of the hiatus. All ages discussed in this paper are referred to calendar ages.

TABLE 1: Radiocarbon ages for MD97-2141

Depth in core (cm)	AMC ^{14}C Age (years)	Error* (years)	Calendar Age†, (years)	Species	Accession Number
1	4,560	± 50	4,798	*G. ruber (white)*	OS-16971
10.5	4,210	± 40	4,286	*G. ruber (white)*	OS-16926
14[a]	4,740	± 40	4,962	*G. ruber (white)*	OS-16410
29	4,700	± 55	4,873	*G. ruber (white)*	OS-16972
59[a]	6,020	± 40	6,416	*G. sacculifer (w/out sac*[b]*)*	OS-16411
73[a]	6,810	± 55	7,274	*G. sacculifer (w/out sac*[b]*)*	OS-16973
85	6,830	± 90	7,295	*G. sacculifer (w/out sac*[b]*)*	OS-18401
94	8,850	± 55	9,455	*G. sacculifer (w/out sac*[b]*)*	OS-16974
99	10,700	± 90	12,152	*G. sacculifer (w/out sac*[b]*)*	OS-16975
120[a]	9,380	± 160	10,001	*G. sacculifer (w/out sac*[b]*)*	OS-16977
150[a]	10,200	± 80	11,045	*G. ruber (white)*	OS-16978
158[a]	10,250	± 120	11,153	*G. sacculifer (w/out sac*[b]*)*	OS-16980
162	10,750	± 50	12,228	*G. sacculifer (w/out sac*[b]*)*	OS-16979
205.5[a]	11,750	± 130	13,258	*G. sacculifer (w/out sac*[b]*)*	OS-17238
212[a]	12,350	± 65	13,931	*G. ruber (white)*	OS-16412
226.5[a]	13,000	± 95	14,796	*G. ruber (white)*	OS-16970
244[a]	14,100	± 70	16,422	*G. ruber (white)*	OS-16413
269[a]	14,750	± 70	17,200	*G. ruber (white)*	OS-16361
282[a]	15,100	± 90	17,591	*G. sacculifer (w/out sac*[b]*)*	OS-17913
339[a]	17,150	± 140	19,749	*G. ruber (white)*	OS-17914
368[a]	17,650	± 85	20,430†	*G. ruber (white)*	OS-22672
400[a]	18,850	± 140	21847†	*G. sacculifer (w/out sac*[b]*)*	OS-17916
421	29,000	± 160	33,162†	*G. sacculifer (w/out sac*[b]*)*	OS-22673
440[a]	28,000	± 130	32,101†	*G. sacculifer (w/out sac*[b]*)*	OS-17882
487[a]	30,900	± 260	35,146†	*G. ruber (white)*	OS-17912
506.5	33,000	± 310	37,290†	*G. sacculifer (w/out sac*[b]*)*	OS-17917
543	33,600	± 590	37,893†	*G. sacculifer (w/out sac*[b]*)*	OS-17911
553[a]	34,300	± 390	38,790†	*G. sacculifer (w/out sac*[b]*)*	OS-17915
553-DUB	34,700	± 440	(average)	*G. sacculifer (w/out sac*[b]*)*	OS-17910
594[a]	36,900	± 460	41,134†	*G. sacculifer (w/out sac*[b]*)*	OS-17918

* Error is given in 1σ

† Calendar ages have been calculated using a 400 year reservoir correction and applying the *Stuiver and Braziunas* [1993] calibration curve for samples younger than 20,000 calendar year in age and a U/Th calibration curve for the samples older than 20,000 calendar years [*Bard et al*., 1993].

[a] included in age model

[b] without saccate like chamber

2.4 Results

The $\delta^{18}O$ analyses of *Globigerinoides ruber* ($\delta^{18}O_{G.\ ruber}$) from core MD97-2141 are listed in Appendix 1 and summarized in Figure 2.1. The MD97-2141 $\delta^{18}O$ record confirms the presence of an oscillation during the Younger Dryas Chronozone, and during MIS 5e [*Linsley and Thunell*, 1990; *Kudrass et al*., 1991; *Linsley*, 1996]. Most importantly the higher sampling density of this new $\delta^{18}O$ record documents additional millennial events with close to 0.5 ‰ amplitude, particularly in MIS3, that were previously not identified in ODP769A (Figure 2.1).

The $\delta^{18}O_{G.\ ruber}$ record from core MD97-2141 exhibits a glacial-interglacial (G-I) $\delta^{18}O_{G.\ ruber}$ amplitude of 1.3 ‰ (Figure 2.1), consistent with results from ODP site 769A [*Linsley*, 1996]. Previously, it was suggested that G-I changes in the $\delta^{18}O$ composition of planktonic foraminifera in the Sulu Sea could be totally explained by changes in the global ice volume with little or no change in surface temperature or local salinity [*Linsley*, 1996]. However recent Mg/Ca-based temperature estimates in the Sulu Sea record glacial cooling of 3°C indicating that surface waters were less saline at LGM, and that the apparent match between sea level and $\delta^{18}O$ may be fortuitous [*Rosenthal et al*., 2000a]. Lowered sea level during glacial times may have restricted the intrusion of relatively salty surface waters from the Celebes Sea and Western Pacific increasing the influence of low salinity South China Sea water entering the Sulu Sea across the Mindoro Strait [*Wyrtki*, 1961]. Lower SSS in the Sulu Sea during sea level lowstands also agrees with observations in the southern South China Sea, where SSS has been found to decrease by 2 ‰ during the LGM [*Wang et al*., 1999]. Furthermore, modelling studies indicate that wetter conditions are

found on the western side of New Guinea during the LGM [*Hostetler and Clark*, 2000]. These authors propose that the emerged land between Australia and Indonesia (currently Arafura Sea and Torres Strait) led to increased precipitation through increased surface heating. However, this conclusion is still controversial because pollen data in this area indicate cooler and drier conditions during the LGM *[Van der Kaars et al.*, 2000].

Mg/Ca analyses of *G. Ruber* are listed in Appendix II. Paired measurements of $\delta^{18}O$ and Mg/Ca on the same foraminifera species in the same samples permits the independent estimation of temperature from foraminiferal Mg/Ca [e.g., *Rosenthal et al*., 1997; *Hastings et al*., 1998], and theoretically allows the calculation of seawater $\delta^{18}O$ (Figure 2.1) and in turn, to estimate paleo-salinity [*Rosenthal et al*., 2000b]. Although Mg/Ca appears to be a robust tracer for temperature at several sites, there are also potential calibration problems. Recent studies suggest that in addition to the influence of temperature on the co-precipitation of Mg in planktonic foraminiferal shells, dissolution on the seafloor may alter the initial Mg composition of foraminifera tests, even at locations well above the calcite lysocline [*Braun & Elderfield*, 1996; *Rosenthal et al*., 2000b]. If partial dissolution occurs it will lower Mg/Ca values indicating a lower inferred temperature. Here, I use temporal variations in shell mass to assess dissolution effects on the Mg/Ca record (Figure 2.1). Based on the observed positive linear relationship between the shell's average weight, the shell's Mg/Ca, and the degree of bottom water calcite saturation, it

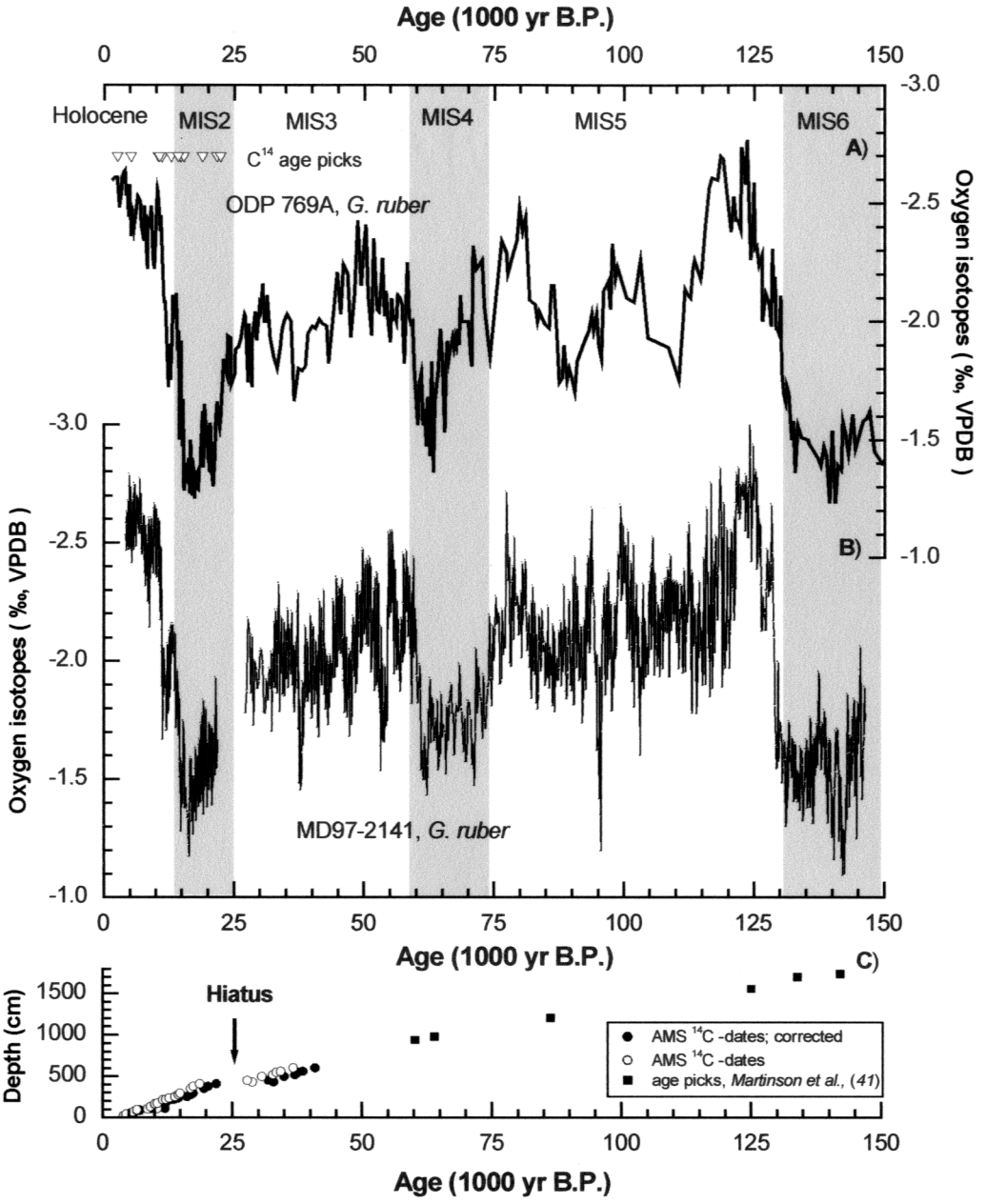

Figure 2.1: (A) Sulu Sea $\delta^{18}O$ record of *G. ruber* ($\delta^{18}O_{G.\ ruber}$) from ODP Site 769A (upper solid black line) [*Linsley*, 1996] with open down triangles indicating ^{14}C for this site, and from IMAGES core MD97-2141 (lower thin solid line) [this study]. Note that no attempt has been made to temporally align the ODP 769A and MD97-2141 $\delta^{18}O$ records. **(C)** Chronology for MD97-2141, consisting of 28 AMS radiocarbon age dates (solid black circles) and several correlation points with the *Martinson et al*. [1987] chronology (solid black squares).

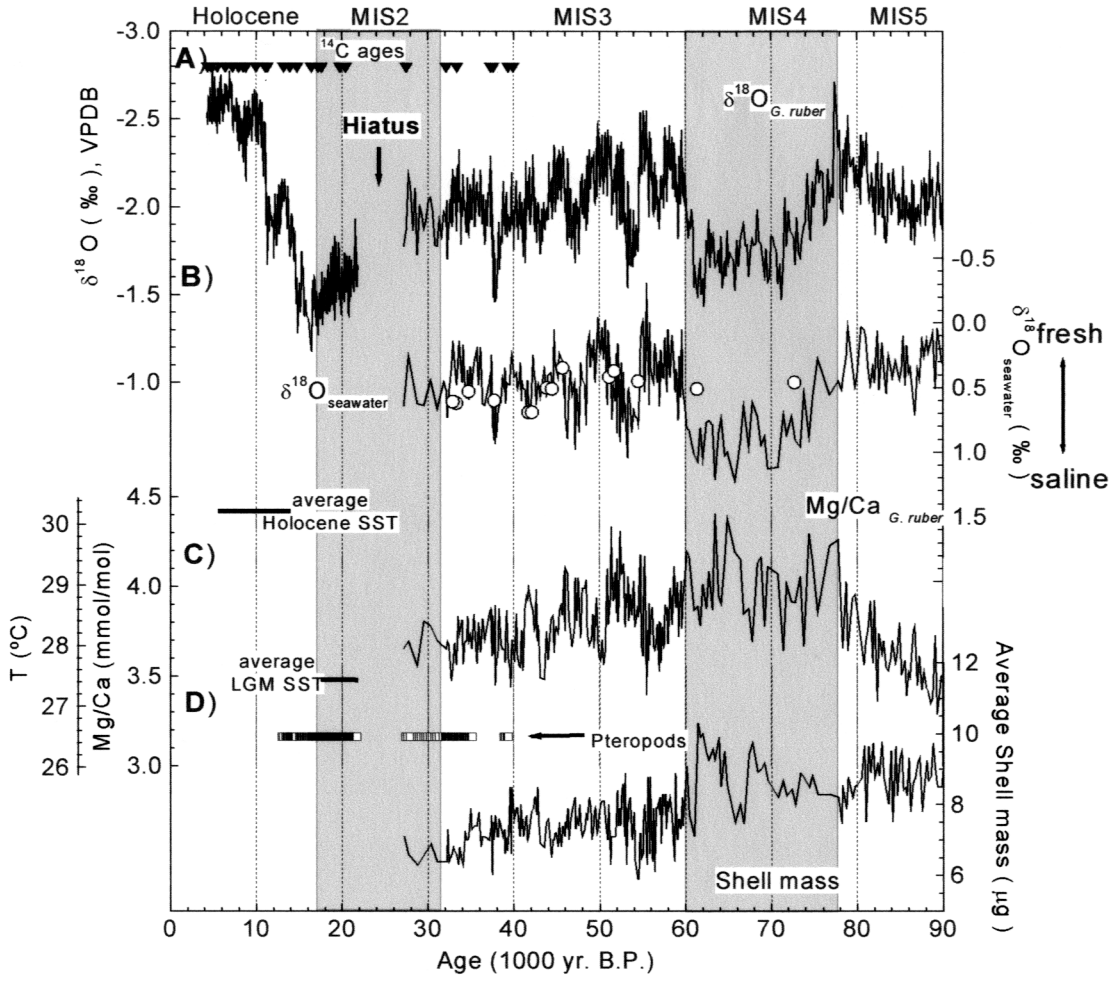

Figure 2.2: Data from the Sulu Sea during the last 90 kyr. Grey shaded areas represent marine isotope stages 2 and 4. **(A)** Sulu Sea $\delta^{18}O_{G.\ ruber}$; black down triangles indicate ^{14}C ages. **(B)** Sulu Sea $\delta^{18}O_{seawater}$; $\delta^{18}O_{seawater}$ has been calculated using the empirically derived temperature : $\delta^{18}O$ relationship based on planktonic foraminifera generated by *Erez & Luz* [1983] and the Mg/Ca –SST relationship reported by *Lea et al*. [2000]. Superimposed are sea level data (open circle) measured by *Fairbanks* [1989] and *Chappell et al*., [1996] **(C)** Sulu Sea Mg/Ca *G. ruber*; temperature estimates are calculated using *Lea et al.* [2000] equation. Horizontal lines indicate average Mg/Ca composition during Holocene and LGM [*from Rosenthal et al*., 2000a]. **(D)** Average shell mass in μg.

was suggested that variations in average shell mass may be used to monitor secondary dissolution effects [*Rosenthal et al*., 2000b].

Briefly, it was suggested that because planktonic foraminifera calcify over a relatively large water depth range, dissolution of primary calcite leads to a concomitant loss of shell's weight and Mg, thereby shifting the bulk shell chemistry toward the composition acquired in deeper and colder waters [*Rosenthal et al*., 2000b]. Variations in *G. ruber* shell mass in core MD97-2141 reveal a minimum in weight loss during MIS4, while the average shell's weight during MIS3 is 2μg lower compared to MIS4. However, the lack of correlation (r^2=1.6*10^{-6}) between the Mg/Ca and *G. ruber* shell mass during MIS3 suggests that in the Sulu sea dissolution does not strongly influence the Mg/Ca signal (Figure 2.1). This suggests that at this site foraminiferal Mg/Ca is primarily a record of variations in water temperature. In the Sulu Sea the carbonate compensation depth is currently at ~ 4,800 m, while the carbonate lysocline occurs near 3,800 m, and the aragonite lysocline near 1,400 m [*Linsley et al*., 1985]. Past studies indicate that calcite dissolution has not produced large G-I changes in either carbonate content or foraminiferal preservation in the Sulu Sea [*Miao et al*., 1994]. Additionally, the presence of pteropods in this core at 3,633 m during the LGM and during parts of MIS3 would seem to exclude a significant dissolution effect on Mg/Ca at this time in the Sulu Sea [Figure 2.1; *Miao et al*., 1994] .

Mg/Ca values of G. ruber during MIS3 range between 3.5 and 4.4 mmol/mol and suggest an apparent cooling trend of about 1°C from early to late MIS3, upon which millenial-scale events are superimposed. I estimated

$\delta^{18}O_{seawater}$ for MIS3 by subtracting the SST component of $\delta^{18}O$ change using 1°C = -0.22 ‰ [Figure 2.2B; *Epstein et al*., 1953]. A comparison to coral-based sea-level estimates converted to $\delta^{18}O$ [120m = 1‰; Chappell et al., 1996; and also *Schrag et al*., 1996] suggests that a portion of the $\delta^{18}O_{residual}$ may be accounted for by sea level change as already suggested by *Linsley* [1996]. However, additional $\delta^{18}O$ changes must be due to changes in SSS. Previous studies using temporally shorter cores from the northern South China Sea also found millennial-scale changes in precipitation and runoff that were potentially related to the East Asian monsoon [*Wang et al*., 1999]. Because the South China Sea and Sulu Sea are connected via two straits today and one strait at the LGM, monsoonally driven changes in the South China Sea salinity may influence SSS of the Sulu Sea. Because SSS in the Sulu Sea today is also influenced by the ITCZ, which is dynamically linked to the monsoon, it is also possible that millenial-scale changes in the ITCZ related rainfall/runoff modulated SSS changes in the Sulu Sea during MIS3. I conclude therefore that the large changes observed in Sulu Sea salinity in MIS3 indicate that the East Asian monsoon and/or ITCZ varied on millenial time scales during this time.

2.5 Discussion

An important question is whether these inferred tropical salinity changes are related to changes at higher latitudes. A comparison of the Sulu Sea $\delta^{18}O_{G.\ ruber}$ and Mg/Ca records to Greenland and Antarctic Byrd ice core $\delta^{18}O$ records [Figure 2.3; *Blunier & Brooks*, 2001] suggests that millennial-scale changes in foraminiferal $\delta^{18}O$ in the Sulu Sea generally correlate with variations in the Greenland air temperature. By contrast, the Sulu Sea Mg/Ca record does not correlate with either Antarctic or Greenland ice $\delta^{18}O$ records [Figure 2.3; *Blunier & Brooks*, 2001]. Although age model limitations do not allow detailed phasing determination, changes in the Sulu Sea planktonic $\delta^{18}O_{G.\ ruber}$ record occurred at approximately the same time as the Dansgaard-Oeschger events in the northern hemisphere. The semi-isolated configuration of the Sulu Sea may have worked to amplify monsoon and/or ITCZ fluctuations. Due to the lower sea level during MIS3, the Sunda shelf route of surface water circulation was at least in-part blocked and more of the fresh water discharge from rivers draining the South East Asia was focused in this region. The situation may have amplified millenial changes in either the East Asian Monsoon and/or ITCZ and could have caused a relative freshening of surface waters in the SCS and SS during MIS3. While recent investigations suggest a linkage between the North Atlantic and northern South China Sea precipitation via variations in the East Asian monsoon [*Wang et al*., 1996], my results from the Sulu Sea suggest that the link between Northern Hemisphere temperature and tropical precipitation is more widespread, and may involve parallel changes in the East Asian monsoon and western Pacific ITCZ.

The origin of global millennial-scale climate variations is not well understood. One hypothesis is that they are driven by millennial-scale changes in thermohaline circulation. This hypothesis successfully predicts anti-phased temperature changes in the high latitudes of the Northern and Southern Hemisphere [*Blunier and Brooks*, 2001]. Many coupled ocean-atmospheric models have examined the influence of the shut down of the conveyor circulation and/or the cooling of the North Atlantic SST [*Rind et al.,* 1986; *Manabe and Stauffer*, 1988]. The models indicate the strongest variations in areas close to the North Atlantic, and small changes elsewhere [*Manabe and Stauffer*, 1988; *Cane and Clement*, 1999]. However, the results from the Sulu Sea show apparently large amplitude millenial-scale climate events well outside of the North Atlantic.

Another proposed hypothesis is that millennial-scale variability originates from the tropics similar to the way current interannual El Niño Southern Oscillation (ENSO) variability originates in the tropics and propagates around the globe. Model experiments suggest that ENSO variability could have an influence on climatic change on millennial time-scales [*Clement and Cane*, 1999]. Under this scenario an interval of more numerous El Niño-warm mode events would favor the melting of Northern Hemisphere ice sheets [*Cane*, 1998; *Clement and Cane*, 1999]. The opposite is true in the Antarctic Peninsula where El Niño-warm events tend to be times of extensive sea ice [*Yuan & Martinson*, 2000]. Thus ENSO teleconnections may drive changes of opposite sign in the high latitude Northern and Southern Hemisphere.

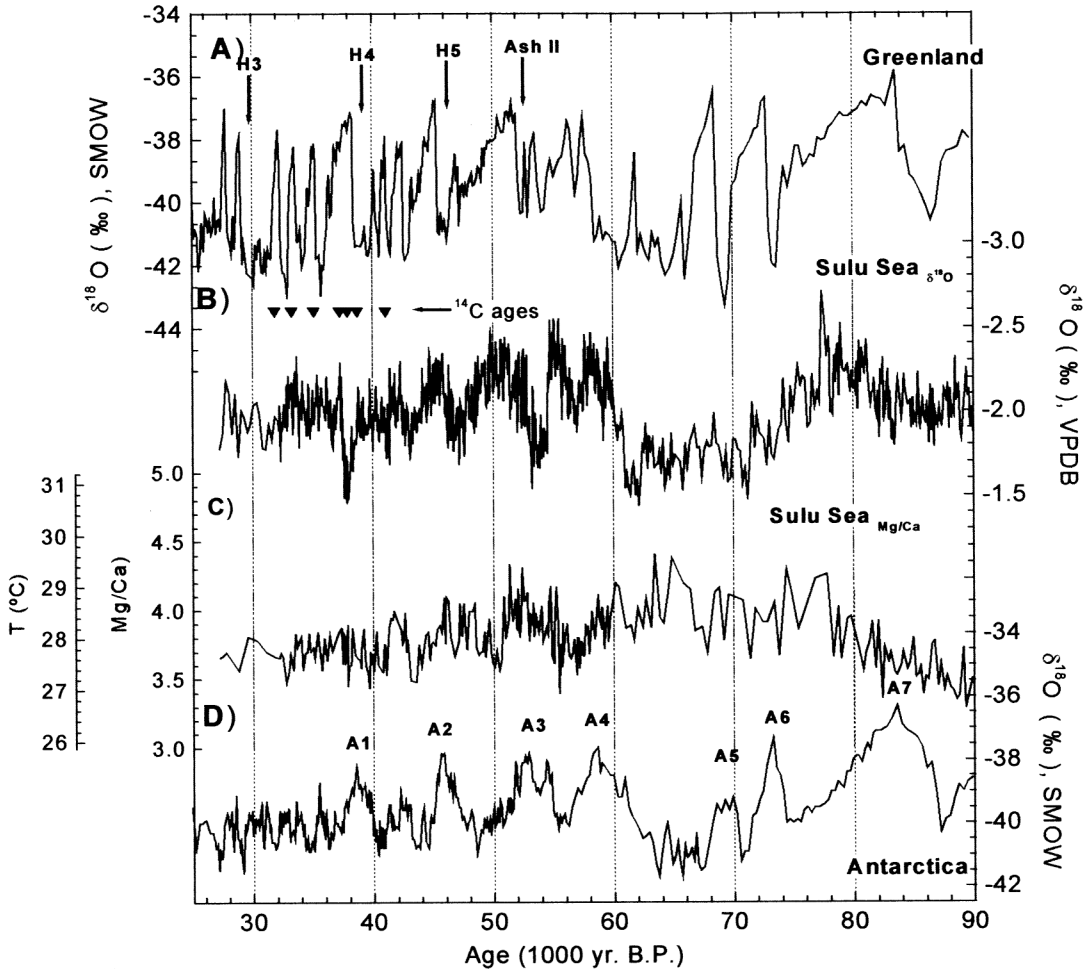

Figure 2.3: Comparison of the isotopic records from Greenland and Antarctica to isotopic and trace element data from the Sulu Sea between 27,000 and 90,000 years. The Greenland and Antarctica time scales between 25-90 kyr are based on correlating atmospheric methane records from these cores [*Blunier and Brooks*, 2001]. Sulu Sea data are on an independent time scale. **(A)** Greenland Ice core (GISP2) $\delta^{18}O$ data [*Blunier and Brooks,* 2001]. Occurrence of Heinrich events are indicated by H3-H5. **(B)** Sulu Sea $\delta^{18}O_{G.\ ruber}$; black triangles indicate ^{14}C ages. **(C)** Sulu Sea $Mg/Ca_{G.\ ruber}$; temperature estimates are calculated using *Lea et al.* [2000] equation. **(D)** Antarctica $\delta^{18}O$ data [*Blunier and Brooks,* 2001]. Antarctic warming events are indicated by A1-A7.

2.6 Conclusions

Although our new results from the Sulu Sea can not be used to prove or disprove either of the above models, we have demonstrated that in addition to millenial deglacial events, large millenial changes in Sulu Sea salinity have occurred in MIS3, and appear to be related to Greenland air temperature and not the Southern Hemisphere. We interpret these salinity changes to be due to fluctuations in the East Asian monsoon and/or ITCZ, and suggest that these key features of tropical climate may play an important role in transferring and/or regulating millenial-scale climate change in the latest Pleistocene.

CHAPTER 3

Variability of Marine Isotope Stage 3 Upper Water-Column Structure in the Sulu Sea: Isotopic and Faunal Evidence

3.1 Abstract

Oxygen isotopic analyses of *G. ruber* ($\delta^{18}O_{G.\ ruber}$) from IMAGES core MD97-2141 in the Sulu Sea have revealed several millennial-scale oscillations of 0.4-0.8 ‰ amplitude during this time period [see Chapter 2]. Here I use planktonic foraminifera faunal analysis and species specific isotopic analyses to provide a detailed reconstruction of changes in the western tropical Pacific thermocline structure between 35,000 and 55,000 years ago. The relative abundance of all planktonic foraminifer species and the $\delta\ ^{18}O$ values of four species (*Globigerinoides ruber* and *sacculifer*, mixed-layer dwellers; *Neogloboquadrina dutertrei*, a thermocline dweller; and *Globorotalia crassaformis*, a deep dweller) was determined in 35 samples between 35,000 and 55,000 years ago at Sulu Sea site MD97-2141. The $\delta^{18}O$ composition of the mixed-layer (*G. ruber*, *G. sacculifer*) and upper thermocline (*N. dutertrei*) species display little similarity to the $\delta^{18}O$ of the sub-thermocline dweller (*G. crassaformis*) which shows larger $\delta^{18}O$ (~1 ‰) variations than the surface dwellers. The observed changes in $\delta^{18}O_{G.\ crassaformis}$ could be explained by fluctuations in the influence of high salinity North Pacific Tropical Waters (NPTW), which currently enter the Sulu Sea at ~200 m depth across a 420 m deep sill during the months of the winter monsoon. High abundance of thermocline dwelling foraminifera coincides with the increase of NPTW influx. In the Sulu Sea, the combined oxygen isotopic and faunal abundance data suggest a switch from winter to summer monsoon predominance after 55 kyr indicating a reduced influence of the NPTW. However, this predominance is interrupted by at least three stronger winter monsoon episodes between 42-46 kyr.

3.2 Introduction

One of the most useful tools for reconstructing paleoceanographic conditions is the analysis of oxygen isotopic composition ($\delta^{18}O$) of planktonic foraminifera. Several species of planktonic foraminifera are in oxygen isotopic equilibrium with ambient seawater [e.g., *Erez and Honjo*, 1981; *Fairbanks et al*., 1982; *Curry et al*., 1983], and serve therefore as proxies for variations in the isotopic composition and temperature of seawater in which the tests grew [*Emiliani*, 1954]. The advantage of analyzing $\delta^{18}O$ of multiple foraminiferal species in the same sample from different calcification depths is that mixed layer, thermocline, and deep-water variations can be independently monitored, and separated from the total water column variability. Additionally, the character of planktonic foraminifer assemblages is determined by the thermal structure and nutrient distribution in the upper water column, and can be used to determine the vertical stratification of population maxima in the water column [e.g., Emiliani, 1954; Be, 1960; Shackleton and Vincent, 1978; Fairbanks and Wiebe, 1980; Fairbanks et al., 1980, 1982; Norris et al., 1993, 1994].

Previously, it has been suggested that the origin of millennial-scale events in the $\delta^{18}O$ record of *Globigerinoides ruber* ($\delta^{18}O_{G.\ ruber}$) in the Sulu Sea is mainly due to regional salinity changes [Chapter 2]. Based on the $\delta^{18}O_{G.\ ruber}$ and the Mg/Ca record, it was suggested that these events respond primarily to locally derived monsoon-related salinity changes throughout the last 150 kyr. However, millennial-scale variability in the western Pacific during marine isotope stage 3 (MIS3) is still poorly understood and published information concerning the thermocline structure during this time is lacking. Our knowledge of millenial changes in tropical climate for this interval is also limited, particularly for the

tropical western Pacific, where developing a better understanding of past climatic variations is important because of the global influence of the Asian monsoon system and the Western Pacific Warm Pool (WPWP).

The goal of collecting IMAGES core MD97-2141 (8.79° North latitude, 121.30° East longitude) was to provide new material to study the millennial-scale climatic events reported by previous work on Ocean Drilling Program Site 769A (ODP site 769A) in the Sulu Sea [*Linsley and Thunell*, 1990; *Linsley*, 1996]. The specific climatic cause of MIS3 millennial-scale oscillations in surface hydrography suggested in Chapter 2 is further investigated here using the $\delta^{18}O$ composition of surface- and thermocline-dwelling foraminifera and the relative abundance data for planktonic foraminifer species.

To assess the vertical upper water column changes in the Sulu Sea during MIS3, the $\delta^{18}O$ composition of four planktonic foraminifera species (*G. ruber*, *Globigerinoides sacculifer*, *Neogloboquadrina dutertrei* and *Globorotalia crassaformis*) known to calcify at different water depths was analysed in the same sample. By comparing the isotopic results, changes in the vertical water column structure and the influence of deeper-water currents should be detectable. The isotope records of *G. crassaformis* should reflect changes below the thermocline, *N. dutertrei* within the thermocline, and *G. sacculifer*, and *G. ruber* the mixed layer [*Shackleton and Vincent*, 1978; *Fairbanks and Wiebe*, 1980; *Fairbanks et al*., 1980; *Hemleben et al.*, 1989; *Ravelo and Fairbanks*, 1992].

3. 3 Area Description

IMAGES core MD97-2141 is located in the Sulu Sea (8.79° North latitude, 121.30° East longitude, 3,588 m water depth) several kilometers northwest of the ODP site 769A (8°8 North latitude, 121°13 East longitude, 3,633 m water depth) (Figure 3.1). The Sulu Sea basin exchanges surface water with surrounding basins over shallow sills [*Wyrtki*, 1961]. Currently, the coldest water entering the Sulu Sea is 10 °C, which fills the basin below the thermocline (Figure 3.2). This restricted circulation results in reduced oxygen levels in deep waters compared to the South China Sea or the open western Pacific. The bathymetric high where the core was collected is well above the present local calcite compensation depth at 4,800 m and just above the calcite lysocline at 3,800 m [*Linsley et al*., 1985; *Exon et al*., 1981].

3.4 Deep Water Hydrography

A detailed study of current hydrography in the Sulu Sea has been presented by *Nozaki et al.* [1999]. They observed a salinity maximum between 170 m and 310 m depths and concluded that lateral flow of high salinity waters from the South China Sea produced this peak. *Wyrtki* [1961] named this high density current the 'Subtropical Lower Water'. *Qu et al.,* [2000] define these waters as high-salinity North Pacific Tropical Water (NPTW). The NPTW originates outside the Southeast Asian seas in the Kuroshio current which is part of western boundary current of the subtropical gyre in the North Pacific [*Shaw and Chao*, 1994; *Talley*, 1999]. Intrusion of the NPTW in the South China Sea occurs through the Luzon Strait, which has a sill depth of 2500 m (Figure 3.1).

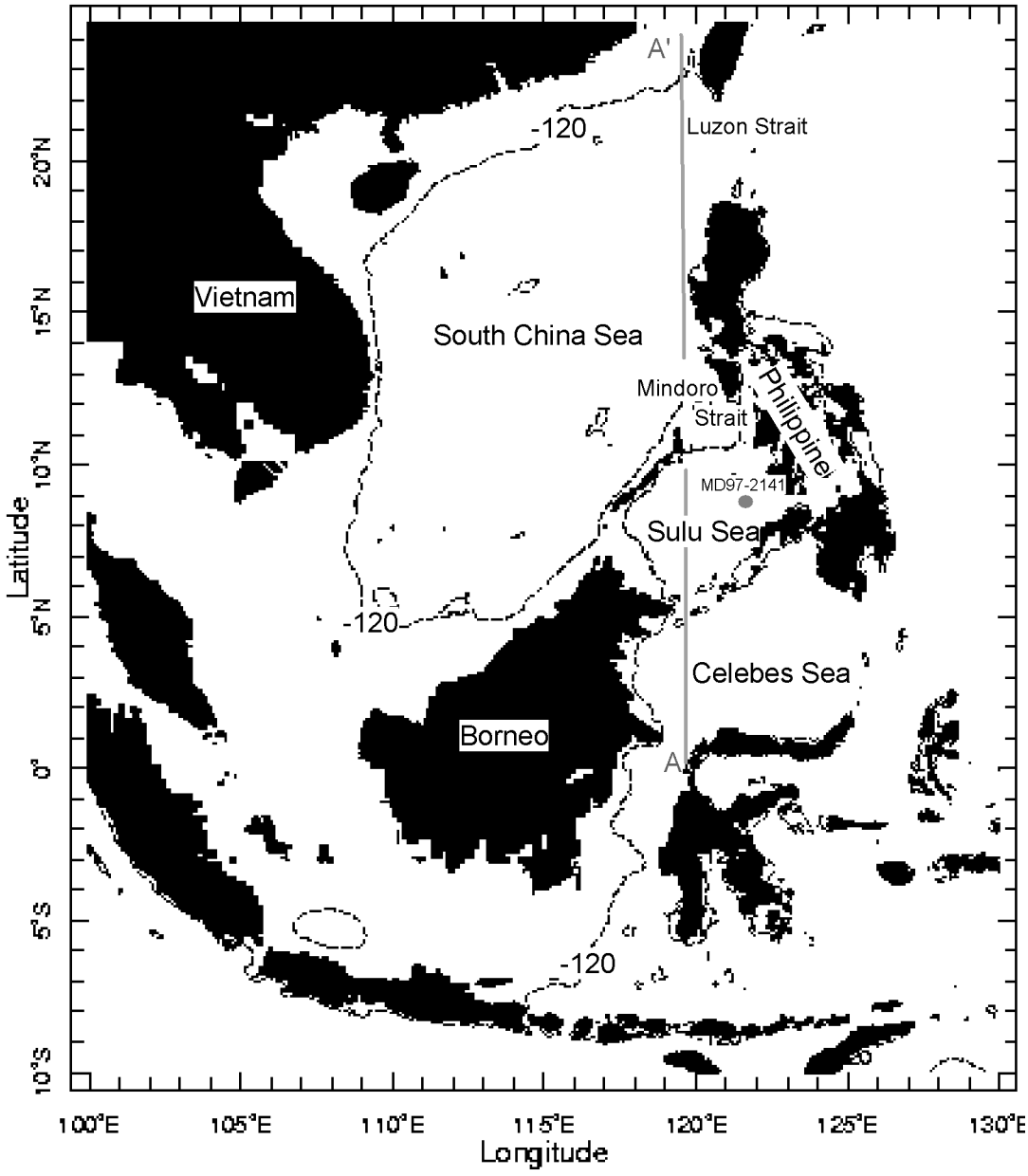

Figure 3.1: Map of western tropical Pacific showing location of the Sulu Sea and the location of IMAGES core MD97-2141 (gray circle). Bathymetric contour is the 120 m isobath indicating the approximate position of coast line during glacial maximum low sea level stand. A - A' cross section illustrated in **Figure 3.2**.

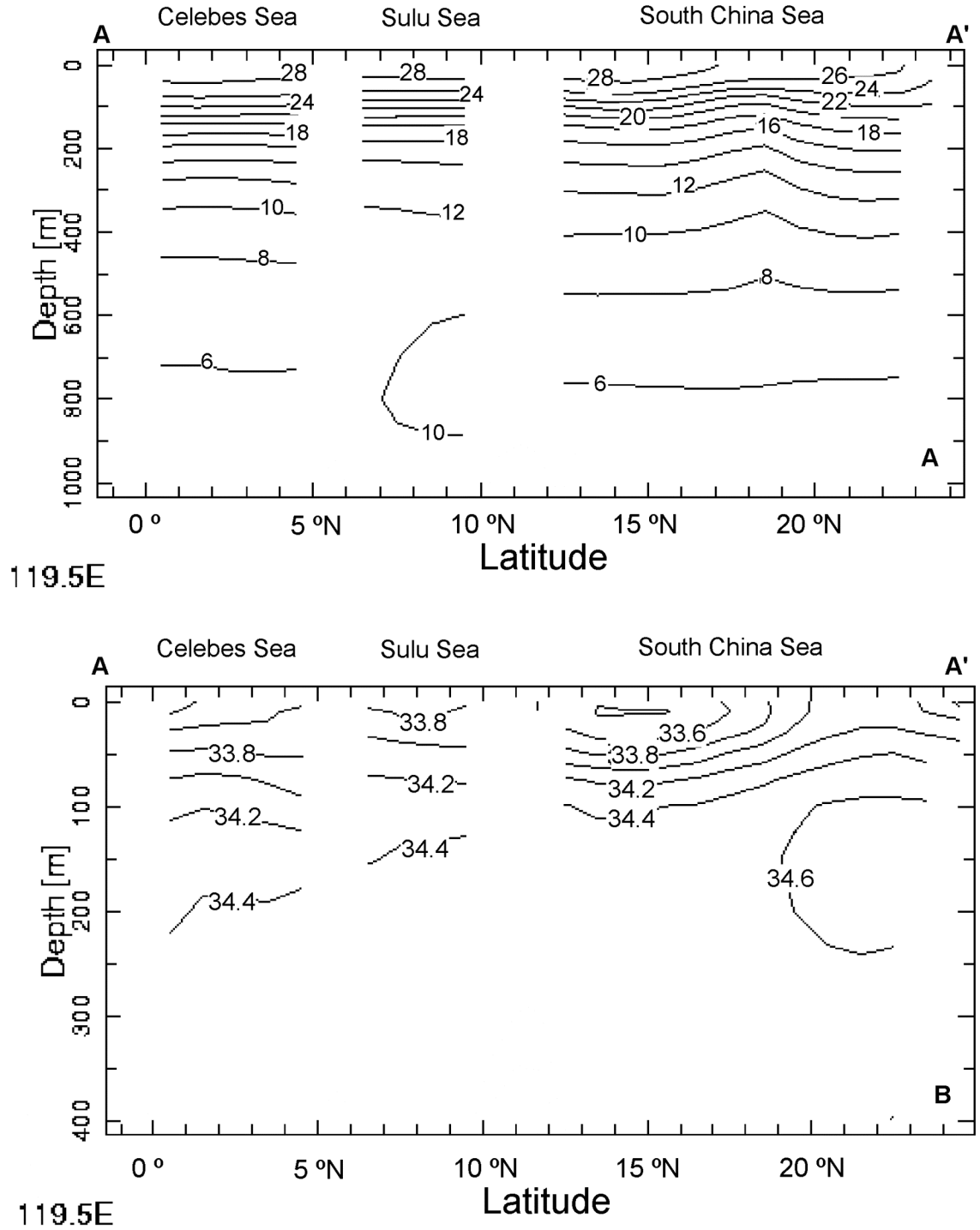

Figure 3.2: Vertical profiles of annual averaged **(A)** temperature (upper 1000m) and **(B)** salinity (upper 400m) along north-south line A-A' shown in Figure 3.1 (119.5º E) [Data from *Conkright et al*., 1998]. Note the warm (10°C) bottom waters in the Sulu Sea.

The South China Sea has a salinity maximum in the Subtropical Lower Water at 150 m depth and salinity minimum in the northern Intermediate Water at 600 m depth [*Wyrtki*, 1961]. The Sulu Sea is connected to the South China Sea by a sill depth of 420 m called the Mindoro Strait [*Wyrtki*, 1961], and only water masses above this sill depth can enter the Sulu Sea. In the South China Sea the NPTW is characterized by a salinity maximum between 34.5 -34.9 ‰. In the Sulu Sea, NPTW with salinity content of 34.55 ‰ and temperatures ranging between 13-16°C is observed at about 200 m depth [*Wyrtki*, 1961; *Nozaki et al.*, 1999]. In the South China Sea, *Shaw et al*. [1996] proposed that upwelling occurs northwest of Luzon between October and January based on the distribution of temperature, salinity, and dissolved oxygen concentration. At the end of the upwelling season, cold water spreads southwestward into the central basin of the South China Sea at approximately 200 m due to the offshore Ekman drift and a converging northward undercurrent [*Shaw & Chao*, 1994; *Shaw et al*. 1996]. Cold and high salinity waters are then able to enter the Sulu Sea at about 200 m depth across the Mindoro Strait.

3.5 Depth ecology of planktonic foraminifera

Ravelo and Fairbanks [1992] introduced the idea of describing surface-water hydrography across the tropical Atlantic using $\delta^{18}O$ content of *G. sacculifer*, *N. dutertrei*, and *Globorotalia tumida*. They noticed that the observed temperature difference between the surface and the bottom of the photic zone was proportional to the range of $\delta^{18}O$ values recorded in foraminiferal calcite. I have adopted this approach here, but have measured *G. crassaformis* instead of

G. tumida because it is more abundant, and it calcifies at approximately 200 m water depth, the depth where high salinity water intrudes into the Sulu Sea through the Mindoro Strait. Therefore it is possible to monitor the influence of the NPTW during MIS3. Information about calcification depth, calcification temperature, temperature and salinity tolerance for each species is summarized in Table 2.

Table 2. Summary of modern living habitat for *G. ruber*, *G. sacculifer*, *N. dutertrei*, and *G. crassaformis*

	G. ruber	***G. sacculifer***	***N. dutertrei***	***G. crassaformis***
calcification depth (meters)	< 25m	< 25m	125m	200 - 300 m
calcification temperature	~24°C	~26°C	15°C	10°C
temperature tolerance	16°C - 31°C	14°C - 31°C	13°C - 33°C	rarely been observed in the living state
salinity tolerance	22‰ - 49‰	24‰ - 47‰	25‰ - 46‰	-
Comments	mixed layer	mixed layer	thermocline	sub-thermocline

100 μm 200 μm 200 μm 200 μm

Hemleben et al [1989]

G. ruber (white) is the dominant species of tropical and subtropical planktic foraminifera. *G. sacculifer* is also abundant in tropical water masses. These species both live in the surface mixed layer [e.g., *Shackleton and Vincent*, 1978]. A potential complicating factor when interpreting *G. sacculifer* $\delta^{18}O$ is secondary calcification and partial dissolution [*Lohmann*, 1995]. Some forms of *G. sacculifer* develop a distinct saccate-like chamber in their terminal stage. These forms of *G. sacculifer* have been excluded from this study.

N. dutertrei lives in a wide range of tropical and subtropical environments [*Fairbanks et al*., 1980; *Fairbanks and Wiebe*, 1980]. In tropical Atlantic plankton tows, the highest abundance of *N. dutertrei* is found below the mixed layer [*Fairbanks et al*., 1980], and hence the oxygen isotopic composition of *N. dutertrei* tests is thought to reflect conditions in the thermocline.

Less is known about the ecology of *G. crassaformis* as it has rarely been observed in the living state. However, published results indicate that *G. crassaformis* starts to calcify at temperatures >10 °C and resides at about 200 meters in the water column [*Hemleben et al.*, 1989]. In plankton tows, the species occurs below the seasonal thermocline and the deep chlorophyll maximum [*Ravelo and Fairbanks*, 1992].

3.6. Material and Methods

For all foraminiferal faunal and isotopic analysis a split of each bulk sample was dry-weighed, disaggregated in tap water, and subsequently wet-sieved through a 63 μm screen. Dry coarse fraction (>63 μm) residues were weighed and sieved through a 150 μm screen. The > 150 μm size fraction was also weighed (see Appendix VII) and split in half, one half for isotopic analyses and one half for faunal analyses.

3.6.1 Oxygen Isotope Analysis

Stable oxygen isotopic measurements were made on several planktonic foraminifer species from the same samples in the Sulu Sea core MD97-2141. Samples consisted of ~ 100 μg of *G. ruber* (white variety; 212-250 μm; ~14 individuals), *G. sacculifer* (without saccate like chamber; 300-355 μm; ~ 9 individuals), or *N. dutertrei* (250-300 μm; ~ 5 individuals), or *G. crassaformis* (300-355 μm; ~ 3-4 specimens). *G. ruber* and *G. sacculifer* have been analyzed throughout the upper 18 m of the core at 1 cm and 10 cm intervals, respectively. However, only the data for MIS3 are presented in this chapter. *N. dutertrei* and *G. crassaformis* have only been analyzed for selected samples during MIS3. Samples were reacted with 100 % H_3PO_4 at 90° C in a Mulitprep carbonate preparation device. The resulting CO_2 gas was analyzed with a Micromass Optima dual-inlet mass spectrometer at the University at Albany, State University of New York. The standard deviation of the National Institute of Science and Technology international reference standard NBS-19 analysed over

an 8 month time period (n = 498) was 0.036 ‰ for $\delta^{18}O$. The average difference in $\delta\ ^{18}O$ between duplicate analyses of the same samples for *G. ruber* was (n=283) 0.094 ‰, *G. sacculifer* (n=24) 0.077 ‰, *N. dutertrei* (n=12) 0.042 ‰, and *G. crassaformis* (n=12) 0.152 ‰.

3.6.2 Faunal Abundance

From the > 150 p.m split for foraminifera faunal analysis an aliquot was separated that contained an average of 387 specimens per sample. For each sample aliquot, I recorded specimen counts of each planktonic foraminifer species and the total planktonic foraminifer fragments (see Appendix VI).

3.6.3 Chronology

The chronology for this IMAGES core is based on 28 radiocarbon measurements obtained on either *G. ruber* or *G. sacculifer* at the Woods Hole Accelerator Mass Spectrometer facility. Before 43,000 year B.P. the $\delta^{18}O_{G.\ ruber}$ chronology has been correlated to the $\delta^{18}O$ chronology of *Martinson et al.* [1987]. All ages in this paper are represent calendar ages. A detailed description of the age model can be found elsewhere [Chapter 2].

3.7 Results

3.7.1 Oxygen isotopic composition of G. ruber and G. sacculifer

The $\delta^{18}O$ analyses of *G. ruber* and *G. sacculifer* from core ND97-2141 are listed in Appendix I and III, respectively, and summarized in Figure 3.3 for MIS3. Due to the higher sampling density this newly obtained $\delta^{18}O_{G.\ ruber}$ record has four times the temporal resolution (< 100 years) than does the $\delta^{18}O_{G.\ ruber}$ record from ODP site 769A [*Linsley,* 1996]. Most importantly, $\delta^{18}O$ variations during MIS3 include several previously unidentified oscillations in $\delta^{18}O_{G.\ ruber}$ which range from 0.4 - 0.8 ‰ in amplitude with the largest oscillation at the beginning of MIS3 (Figure 3.3A). Similar events have been observed in the $\delta^{18}O_{G.\ sacculifer}$ record from this core. Due to the lower sampling resolution of *G. sacculifer* not all events are as well defined as in the $\delta^{18}O_{G.\ ruber}$ record. However, the relationship between $\delta^{18}O_{G.\ ruber}$ and $\delta^{18}O_{G.\ sacculifer}$ for the whole core is very good (r^2 = 0.74, Table 3a). This degree of correlation is expected, because both species dwell in the mixed layer [e.g., *Shackleton and Vincent*, 1978]. A more detailed description of MD97-2141 $\delta^{18}O_{G.\ ruber}$ results have been presented in Chapter 2.

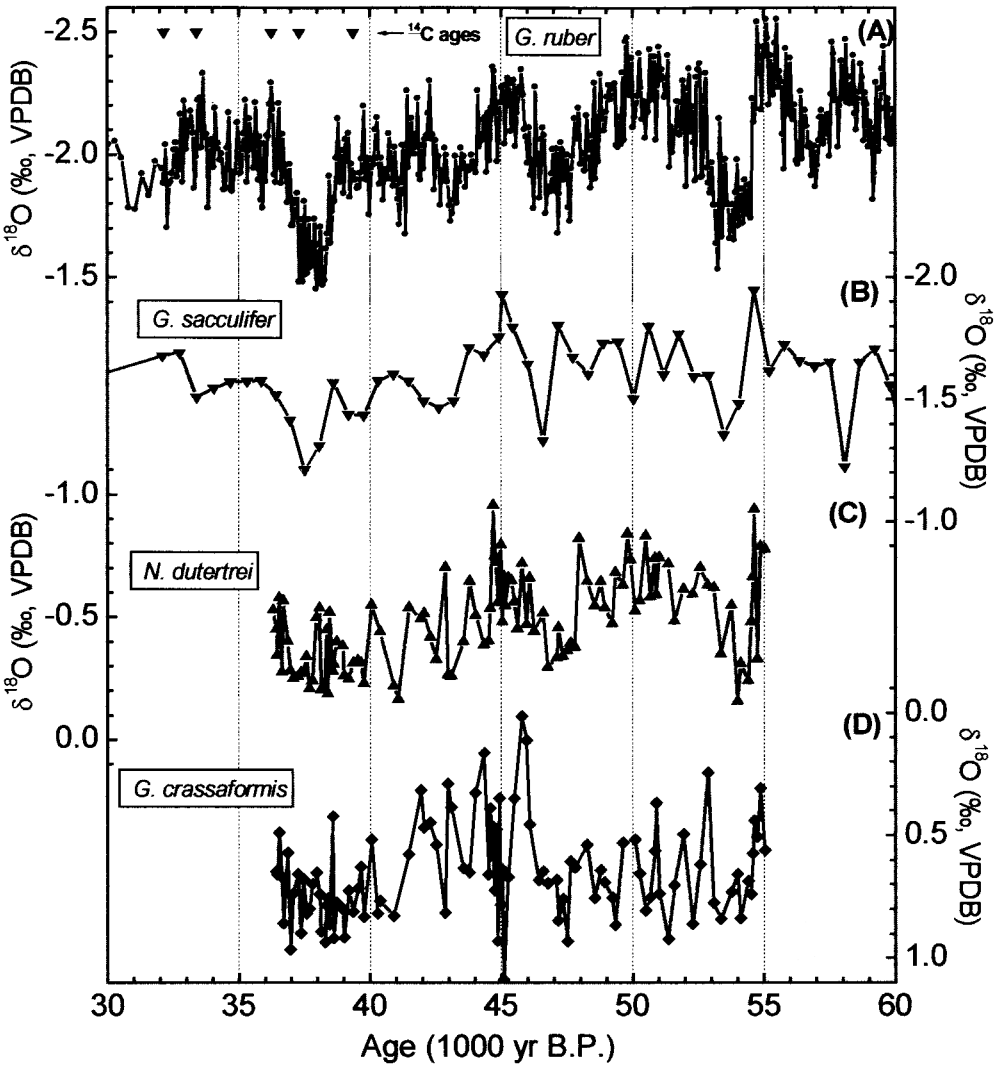

Figure 3.3: Planktonic foraminiferal $\delta^{18}O$ records plotted against time for each species analyzed in IMAGES core MD97-2141 during marine isotope stage 3. **(A)** *Globigerinoides ruber* (circles); black triangles indicate ^{14}C ages. **(B)** *Globigerinoides sacculifer* (down triangles) **(C)** *Neogloboquadrina dutertrei* (up triangles) **(D)** *Globorotalia crassaformis* (diamonds). Note that the y-axis scale range for all plots is 1.2 ‰.

Table 3a: Similarity coefficients (r^2) for planktonic foraminifera $\delta^{18}O$ results during last 150 kyr.

	$\delta^{18}O$ *G.ruber*	$\delta^{18}O$ *G.sacculifer*
$\delta^{18}O$ *G.ruber*	1.00	
$\delta^{18}O$ *G.sacculifer*	**0.74**	1.00

Table 3b: Similarity coefficients (r^2) for planktonic foraminifera $\delta^{18}O$ results during MIS 3 (30-60 kyr).

	$\delta^{18}O$ *G.ruber*	$\delta^{18}O$ *N.dutertrei*	$\delta^{18}O$ *G.crassaformis*
$\delta^{18}O$ *G.ruber*	1.00		
$\delta^{18}O$ *N.dutertrei*	**0.38**	1.00	
$\delta^{18}O$ *G.crassaformis*	0.05	0.03	1.00

3.7.2 Oxygen isotopic composition of deeper-dwellering foraminifera

The $\delta^{18}O$ analyses of *N. dutertrei* and *G. crassaformis* from core MD97-2141 are listed in Appendix IV and V, respectively, and summarized in Figure 3.3 for MIS3. The $\delta^{18}O_{N.\ dutertrei}$ record follows a pattern similar to that of $\delta^{18}O_{G.\ ruber}$ (Figure 3.3C). The $\delta^{18}O_{N.\ dutertrei}$ values are approximately 1.5 ‰ more enriched than the mixed layer dwellers. Starting 44 kyr, $\delta^{18}O_{N.\ dutertrei}$ record increases to -0.2 ‰ over a period of 3 kyr. Not all $\delta^{18}O_{G.\ ruber}$ excursions are found in the $\delta^{18}O_{N.\ dutertrei}$ record and this is reflected in the relatively low similarity coefficient of 38 % (r^2 = 0.38, Table 3b).

In contrast, $\delta^{18}O_{G.\ crassaformis}$ is not significantly correlated to $\delta^{18}O_{G.\ ruber}$ or $\delta^{18}O_{N.\ dutertrei}$ (r^2: 0.05 and 0.03, respectively, Table 3b). The magnitude of the

$\delta^{18}O$ changes in $\delta^{18}O_{G.\ crassaformis}$ are in general larger (up to 1 ‰) than those of the shallower dwelling foraminifera (up to 0.6 ‰) studied. The largest amplitude changes in $\delta^{18}O_{G.\ crassaformis}$ are observed between 47 and 45 kyr. A decrease in 1‰ $\delta^{18}O_{G.\ crassaformis}$ begins at 47 kyr reaching its lowest $\delta^{18}O_{G.\ crassaformis}$ value of 0.0 ‰ near 46 kyr increasing again to about 1.1 ‰ in less then 500 years before decreasing again to 0.02 ‰ in less than 500 years.

3.7.3 Faunal abundance

Seasonal changes in the upper ocean conditions can also influence the species composition of planktonic foraminiferal assemblages [Bé, 1960; Curry et al., 1983; Ravelo et a!., 1990; Thune!! and Sautter, 1992]. Twenty-three different planktonic foraminifera species were counted throughout the MD97-2141 section containing MIS3. One specimen of these taxa was recorded in at least one of the 35 samples analyzed between 35 - 60 kyr. Eleven species dominate the downcore fauna and make up nearly 89 % of the average species population. In total, 13 species have maximum relative abundance that exceed 5 % (Table 4). Downcore variations in the relative abundance of 8 different planktonic foraminifera (four mixed layer species, two thermocline species, and two sub-thermocline species) highlight the complex relationship between species abundance and $\delta^{18}O_{G.\ ruber}$ in MIS 3 (Figure 3.4). The four most abundant species (*G. ruber, G!obigerinita glutinata, N. dutertrei and Globigerinoides bul!oides*) show fluctuations with amplitudes in the 10 % - 20 % ranges. Abundance maxima for *G. saccu!ifer* and *N. dutertrei* occur between 42-44 kyr.

Globorotalia tumida, N. pachyderma (r.), and *G. crassaformis* occur in trace amounts. *G. crassaformis* reaches its maximum abundance of ~5.5 % at 39 kyr.

The downcore inter-relationships among abundant species are not straightforward. The abundance maxima and minima are not related in a simple manner to the MIS 3 $\delta^{18}O_{G.\ ruber}$ oscillations. The species' abundance changes abruptly and most species are not highly correlated with each other. *N. dutertrei* and *G. ruber* indicate the highest correlation with r^2 of 0.29.

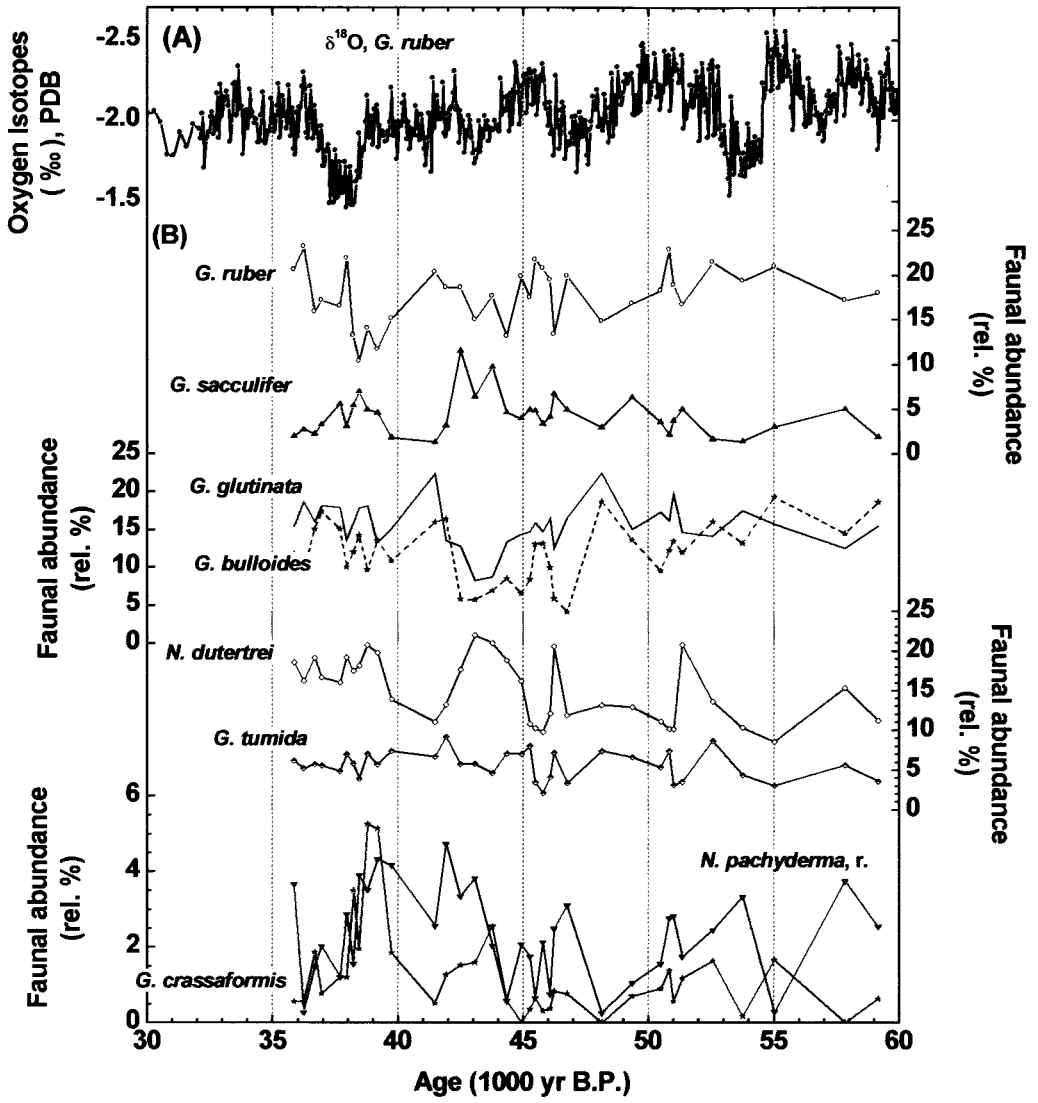

Figure 3.4: (A) The $\delta^{18}O$ values of planktonic *G. ruber* for MIS3. **(B):** Downcore variations in the percent relative abundance of 8 planktonic foraminifera species during MIS3 at MD97-2141. Four mixed-layer species: *G. ruber, G. sacculifer, G. glutinata, G. bulloides*; two thermocline species: *N. dutertrei, G. tumida*; and two sub-thermocline species: *N. pachyderma (r.)*, and *G. crassaformis.*

Table 4: Planktonic Foraminifer taxonomic categories used in present study along with their means, standard deviations, and minimum and maximum occurrences between 35-60 kyr in MD97-2141

Planktonic foraminifer species	Mean (relative %)	SD (relative%)	Minimum (relative %)	Maximum (relative%)
Globerinoides ruber (d'Orbigny), white	18.0	3.2	15.8	23.1
Globiqerinita glutinata (Egger)	15.4	3.0	15.4	22.4
Neogloboquadrina dutertrei (d'Orbigny)	15.3	4.0	16.0	22.0
Globierina bulloides (d'Orbigny)	12.2	4.0	9.9	19.3
Globigerina calida (Parker)	6.6	2.1	5.2	11.3
Globorotalia tumida (Brady)	5.7	1.7	4.8	9.1
Globigerinella aequilateralis (Brady)	3.9	2.0	2.7	11.4
Globigerinoides tenellus (Parker)	3.4	1.6	2.4	9.1
Globigerina rubescens (Hofker)	3.1	2.3	1.9	10.3
Globerinoides sacculifer (d'Orbigny). without sac	3.1	1.9	1.4	10.6
Neogloboquadrina pachyderma (Ehrenberg), right coiling	2.4	1.3	0.3	4.7
Orbulina universa (d'Orbigny)	1.6	1.0	1.3	3.8
Globigerina falconensis (Blow)	1.1	1.7	0.0	6.9
Pulleniatina obliquiioculata (Parker and Jones)	0.9	0.6	0.2	2.3
Globorotalia crassaformis (Galloway and Wissler)	0.8	1.2	0.5	5.2
Globorotalia scitula (Brady)	0.7	2.3	0.0	10.6
Globerinoides sacculifer (d'Orbigny), with sac	0.6	0.8	0.2	3.3
Globorotalia menardii (d'Orbigny)	0.3	0.5	0.0	2.1
Globigerina diqitata (Brady)	0.3	0.3	0.0	1.3
Globoquadrina conglomerata (Schwager)	0.0	0.4	0.0	2.5
Globorotalia inflata (d'Orbigny)	0.0	0.1	0.0	0.5
Globorotalia truncatulinoides (d'Orbiqny), right coiling	0.0	0.4	0.0	2.4
Globiqerinita uvula (Ehrenberg)	0.0	1.1	0.0	4.0
"Mixed layer" species: *G. ruber, G. sacculifer, G. glutinata*	37.4	4.0	33.8	43.7
"Thermocline" species: *G. menardii, P.obliquiloculata, N.dutertrei, and G. tumida*	23.2	4.8	21.5	28.7

Notes: Number of samples = 35; SD = standard deviation

3.8 Discussion

The mixed layer in the Sulu Sea has a depth of less than 10 meters during the summer months and is deepest (25 m) during winter months [*Levitus*, 1994]. Using surface sediments in the tropical Atlantic, *Ravelo et al*. [1990] and *Ravelo and Fairbanks* [1992] have related spatial variations in foraminifera faunas to changes in the hydrographic conditions of the overlying surface layer. In the tropical Atlantic the planktonic foraminiferal assemblage is dominated primarily by thermocline species when the upper ocean is well-stratified during winter months while mixed layer species are more abundant during summer months when they are living in a compressed depth habitat [*Ravelo and Fairbanks*, 1992]. They also observed that the tropical Atlantic faunal assemblages are more correlated to the depth of the mixed layer, thermocline depth, rather than to colder and warmer sea surface temperatures. In their study, *Ravelo and Fairbanks* [1992] summed the relative fauna abundance of *G. ruber, G. glutinata*, and *G. sacculifer* (species known to calcify in the mixed layer). The sum of these species correlates well to the mixed layer depth [*Ravelo and Fairbanks*, 1992]. A second factor assemblage (containing *Globorotalia menardii, Pu!leniatina obliquiloculata, N. dutertrei, and G. tumida*) reflects changes in the thermocline where the chlorophyll maximum is located, and therefore, whose primary production is at a maximum [*Fairbanks and Wiebe*, 1980; *Fairbanks et al*., 1980, 1982; *Ortner et al.,* 1980]. These species are most abundant in regions where surface temperature seasonality is low and where the thermocline moves into the photic zone. I have adopted the approach of *Ravelo and Fairbanks* [1992] for this study to examine possible changes in the thermocline structure based on the faunal assemblage. In MD97-2141, the

mixed layer species explain 73% variance of the data set (Table 4), and indicate greater variability between ~ 35-47 kyr (Figure 3.5). In contrast, "thermocline" species only explain 11% variance of faunal data, and display a mirror image to the mixed layer species (Figure 3.5). Changes from maxima to minima abundance for mixed layer and thermocline species vary from 5-15 % and 10-15 %, respectively. Overall, the changes in the thermocline species are larger for a single event compared to changes in the mixed layer species.

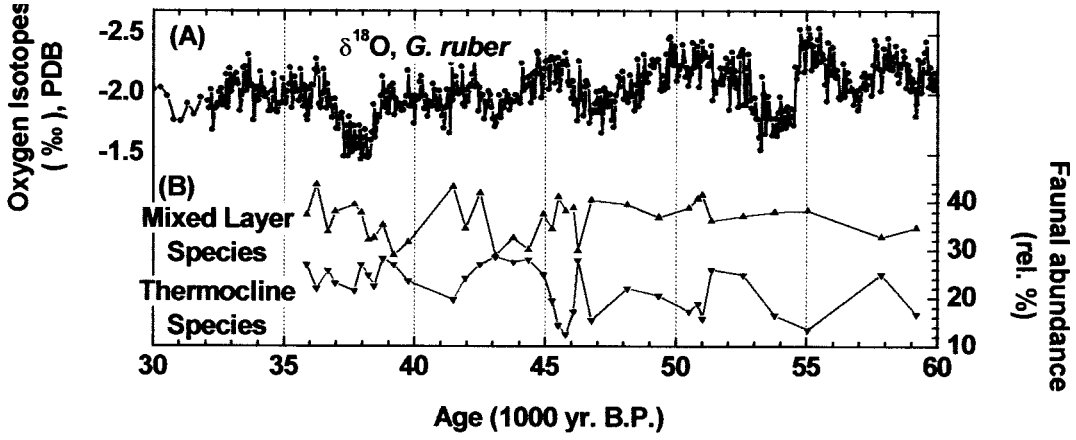

Figure 3.5: (A) $\delta^{18}O_{G.\ ruber}$ during MIS3. **(B):** Time series of the relative abundance sums of "mixed-layer" species *Globigerinoides ruber, Globigerinita glutinata, Globigerinoides sacculifer* and the relative abundance sum of "thermocline" dwellers *Globorotalia menardii, Pulleniatina obliquiloculata, Neogloboquadrina dutertrei, and Globorotalia tumida.*

How much of the observed changes in the $\delta^{18}O$ of the mixed layer dwellers can be explained by changes in the thermocline and sub-thermocline? To address this question *Chaisson and Ravelo* [1997] introduced the strategy to

use the difference between $\delta^{18}O$ time series from the mixed layer species and the thermocline species as a proxy for the temperature difference between the depths of calcification for the different foraminifera species. Their study is based on the assumption that the $\delta^{18}O$ signal includes both global ice volume and local temperature components, however, each species records the temperature and salinity ($\delta^{18}O_{seawater}$) of its immediate environment uniquely. Therefore, the isotope "difference curve" represents the temperature and local salinity difference of their respective records [*Berger et al.,* 1978; *Chaisson and Ravelo*, 1997]. ML $\Delta\ \delta^{18}O$ represents the temperature and local salinity range between the sea surface and thermocline:

$$ML\ \Delta\ \delta^{18}O = \delta^{18}O_{N.\ dutertrei} - \delta^{18}O_{G.\ ruber}$$

TH $\Delta\ \delta^{18}O$ represents the changes in the temperature and local salinity from the thermocline to the water layer below it:

$$TH\ \Delta\ \delta^{18}O = \delta^{18}O_{G.\ crassaformis} - \delta^{18}O_{N.\ dutertrei}$$

During MIS3 in the Sulu Sea, the difference between $\delta^{18}O_{N.\ dutertrei}$ and $\delta^{18}O_{G.\ ruber}$ (ML $\Delta\ \delta^{18}O$) averages 1.5 ‰ (Figure 3.6A). Two intervals of smaller ML $\Delta\ \delta^{18}O$ changes are observed at 38 kyr and between 52-54 kyr. No obvious relationship exists with the $\delta^{18}O_{G.\ ruber}$ oscillations. The most prominent changes observed in TH $\Delta\ \delta^{18}O$ are between 42.5 - 45.8 kyr and 49 - 52 kyr (Figure 3.6B). During these intervals $\Delta\ \delta^{18}O$ fluctuates more than 1.1 ‰ in less than 1,000 years, mostly due to changes in $\delta^{18}O_{G.\ crassaformis}$ (see Figure 3.3D). The oscillations in $\delta^{18}O_{G.\ crassaformis}$ do not appear to be directly related to the

observed changes in shallower dwelling foraminifera but are possibly influenced by sub-thermocline oceanic currents.

If the 1 ‰ depletion of $\delta^{18}O_{G.\ crassaformis}$ at 47 kyr (Figure 3.3D) is entirely due to temperature, this would require temperature fluctuations of 4.5 °C assuming -0.22 ‰ per °C [*Epstein et al.,* 1953]. This is higher than the glacial-interglacial temperature change of about 3 °C discussed in Chapter 2. Since $\delta^{18}O_{G.\ crassaformis}$ changes are out of phase with the $\delta^{18}O$ changes of shallower-dwelling foraminifera, these fluctuations are better explained by the varying influence of the colder high salinity NPTW. My interpretation is that starting at approximately 50 kyr the influence of NPTW decreased gradually until 46 kyr in the Sulu Sea (Figure 3.6B) as these waters were prevented from entering the Sulu Sea due to increased summer monsoon strength. NPTW is only able to spread to the southern South China Sea during a fully developed northeast monsoon [*Qu et al*., 2000]. Therefore, at times of intense summer monsoon activity NPTW is unable to spread southward. In the Sulu Sea, however, the intensity of the summer monsoon may have weakened starting at 46 kyr, while the northeast monsoon may have strengthened at least three times between 45 and 42.5 kyr, allowing the NPTW to spread southward into the Sulu Sea. The Sulu Sea isotopic data in this study are also in agreement with a study in the southern South China Sea by *Pelejero et al.* [1999], in which they observed that a low sea surface salinity episode caused by inferred extreme tropical precipitation and an enhanced summer monsoon between 47-40 kyr. This model is also consistent in a broadly stronger southwest monsoon between 50-30 kyr suggested by magnetic susceptibility data for Chinese paleo loess records [*Chen et al.*, 1997]. Additionally, most of the observed oscillations in the oxygen isotope

record and the overall trend of the thermocline abundance record between 40-50 kyr seem to correlate well with the magnetic susceptibility peaks (Figure 3.7). This indicates increased East Asian summer monsoon conditions, and therefore reduced influenced of the NPTW.

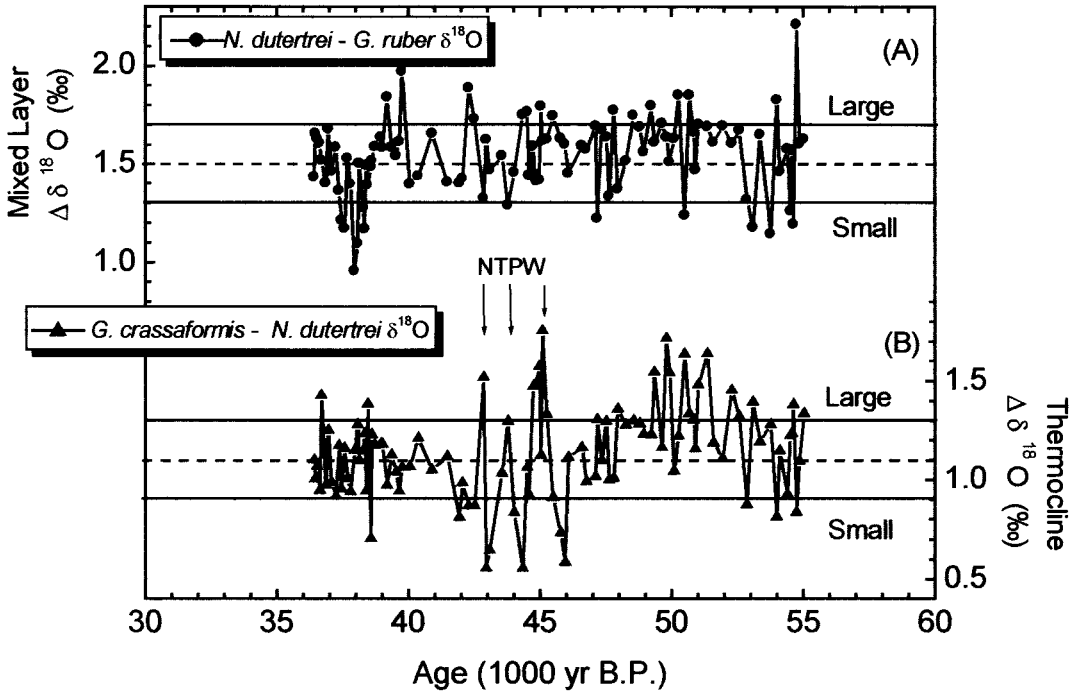

Figure 3.6: Oxygen isotope "difference" curves. **(A)** *Neogloboquadrina dutertrei* $\delta^{18}O$ - *Globigerinoides ruber* $\delta^{18}O$. **(B)** *Globorotalia Crassaformis* $\delta^{18}O$ - *Neogloboquadrina dutertrei* $\delta^{18}O$. Dashed horizontal lines represent average values. Solid lines represent average standard deviation. Possible influence of North Pacific Tropical Water (NPTW) is indicated by arrows.

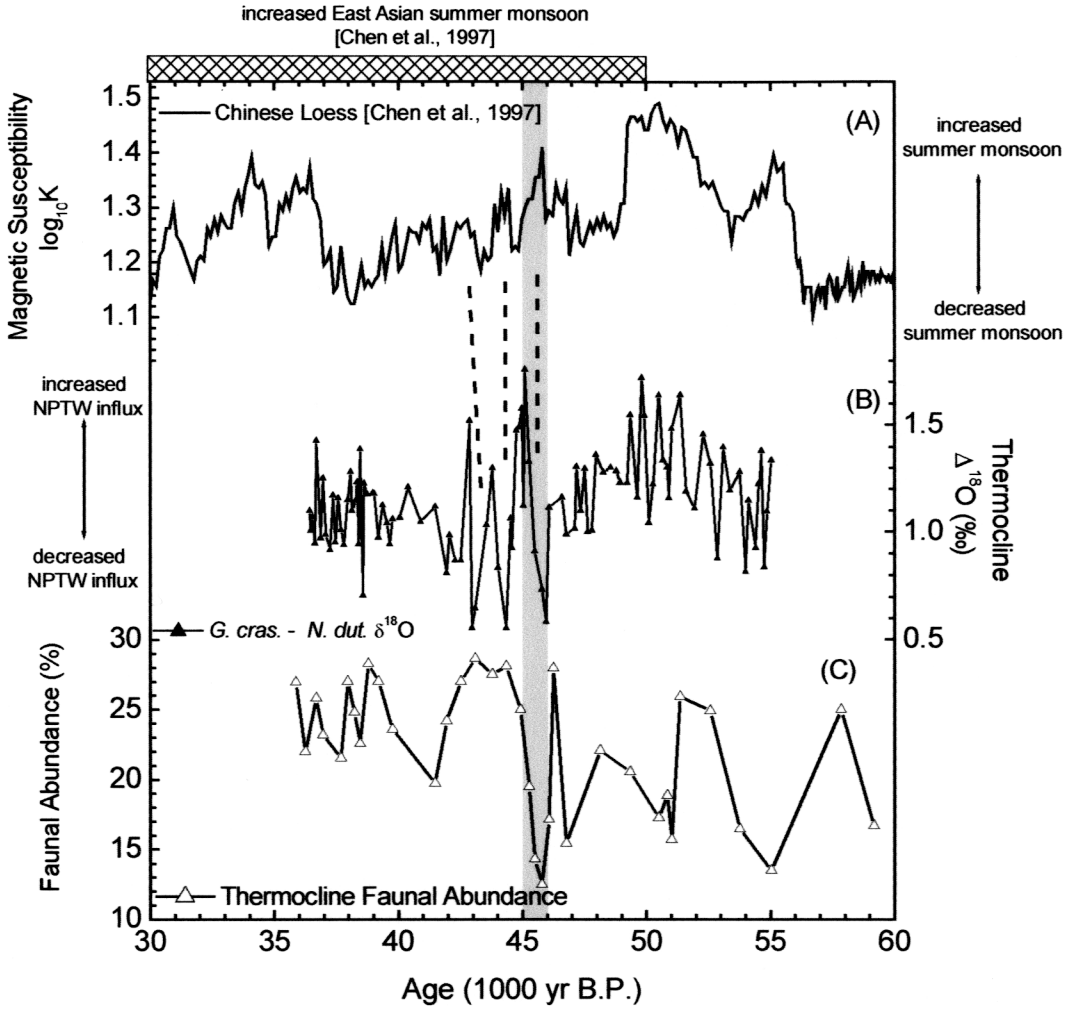

Figure 3.7: Comparison between Chinese loess and Sulu Sea data. **(A)** Chinese loess magnetic susceptibility data used as an index for East Asian monsoon activity [*Chen et al*., 1997]. **(B)** Same figure as in Figure 3.6B. Dashed vertical lines represent possible correlation between the Chinese loess and Sulu Sea record during enhanced East Asian summer monsoon peaks. (C) Time series of the relative abundance sums of "thermocline" dwellers. *G. menardii, P. obliquiloculata, N. dutertrei, and G. tumida*. Greyshaded area indicates one example of a possible correlation of all three data sets between 45 and 46 kyr (see also Figure 3.5B).

3.9 Conclusions

The planktonic foraminiferal stable isotopic and fauna assemblage data presented here clearly demonstrate that significant oceanographic changes occurred in the Sulu Sea between 60,000 and 30,000 years. Most of the observed $\delta^{18}O_{G.\ ruber}$ excursions in MIS3 occurred within the surface mixed layer, and are not influenced by changes below the thermocline. The deeper-dweller $\delta^{18}O$ and faunal study exhibits greater variability of thermocline faunal abundance and $\delta^{18}O$ within the sub-thermocline species indicating episodes of reduced influence of North Pacific Tropical Water into the Sulu Sea driven by enhanced summer monsoon activity.

CHAPTER 4

The relationship between changes in temperature and precipitation in tropical oceans during the Last Glacial Maximum

4.1 Abstract

Comparison of published proxy sea surface temperature (SST) and oxygen isotope ($\delta^{18}O$) profiles for glacial/interglacial sequences from fourteen tropical and subtropical oceanic settings enables assessment of the spatial differences in the timing and progression of ocean warming following the last glacial maximum (LGM: 18,000 - 21,000 calendar years). These stratigraphic records indicate that on average SST has increased ~2.5-3 °C since the LGM in the tropical and subtropical regions. At 5 sites the $\delta^{18}O$ termination is synchronous with SST changes inferred from foraminiferal Mg/Ca and alkenones, while at 9 sites it lags SST by approximately 3,500 years. A comparison of SST and residual $\delta^{18}O$ (ice volume component removed) over the glacial-interglacial period indicates a linear increase in SST with younger age. At sites where the $\delta^{18}O$ and SST transition coincide $\delta^{18}O$ continuously decreases over time reaching a plateau at ~ 7 kyr. This indicates that $\delta^{18}O_{residual}$ is mainly influenced by changes in SST. At sites where SST is leading the $\delta^{18}O$ record, foraminiferal $\delta^{18}O_{residual}$ increases for approximately 3,000 years up to 17 kyr, and then continuously decreases to the mid-Holocene, indicating large regional changes in precipitation-evaporation balance. The sites where SST is leading the $\delta^{18}O$ record are all located in areas that are currently influenced by increased atmospheric water vapor under La Niña like conditions.

4.2 Introduction

Understanding paleoclimate patterns during the Last Glacial Maximum (LGM) is important because the LGM represents a global climate state with vastly different boundary conditions from those of today, and thus provides a useful test of climate models. Although other extreme states of climate may also exist, the clearly documented influence of global ice sheets on climate [*Clark et al*., 1999] justifies a thorough understanding of the climate state dominated by ice. One key weakness in our understanding is how the tropical ocean responded to climatic changes during the LGM.

Recent evidence from ocean sediments indicates that sea surface temperature (SST) changes at the LGM termination (18-21,000 calendar years) lead the planktonic oxygen isotopic record ($\delta^{18}O$) by approximately 3,500 years (Figure 4.1) [*Charles et al*., 1996; *Lea et al.,* 2000; Chapter 2; *Rosenthal et al*., in prep]. It has been inferred from tropical paleo-records that SST changes in the tropics coincide with changes in Antarctic air temperature, and precede changes in continental ice volume by ~ 3,000 years, suggesting that tropical cooling must have played a major role in driving the ice-age climate [*Charles et al*., 1996; *Lea et al*., 2000; Chapter 2]. Additionally, it has been proposed that the transport of water vapor into the western Pacific was enhanced during the LGM based on the extraction of a salinity proxy from magnesium/calcium (Mg/Ca) and $\delta^{18}O$ planktonic foraminiferal records [*Lea et al*., 2000; Chapter 2]. However, this conclusion is in conflict with the idea of a colder and drier glacial climate with reduced precipitation [e.g., *Thompson et al*., 2000]. Furthermore, not all sediment cores indicate this same lead-lag relationship between SST and $\delta^{18}O$

[e.g., *Schneider et al*., 1996; *Rühlemann et al*., 1999; *Wang et al*., 1999; *Kudrass et al*., 2001].

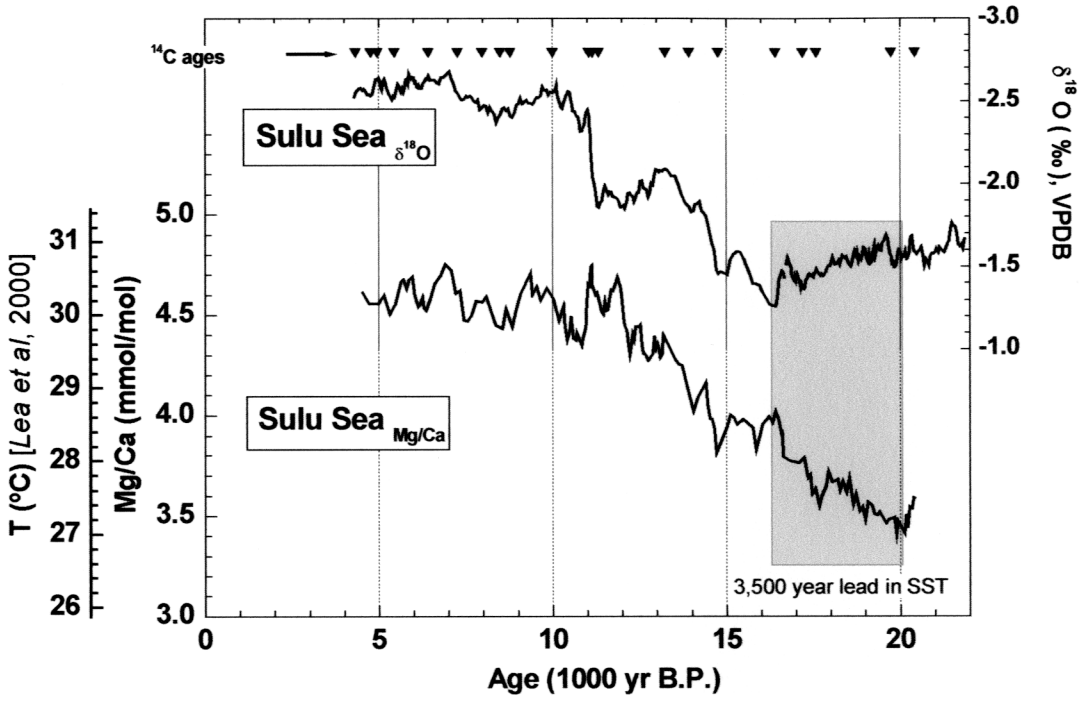

Figure 4.1: δ^{18}O and SST estimates based on Mg/Ca in the Sulu Sea for the last 21,000 years. This figure is used as an example to demonstrate the 3,500 year lead in SST between 17 and 20 kyr (Last Glacial Maximum). The data are smoothed with a 5 point running average. Down triangles indicate radiocarbon ages for this site. [Data from Chapter 2 and *Rosenthal et al*., in prep].

This study examines in greater detail the relationship between inferred temperature changes and foraminiferal planktonic δ^{18}O in tropical oceans during the LGM and across the transition to the Holocene. Published reconstruction of SST and δ^{18}O data collected within the same sediment cores in mainly tropical

oceanic settings have been compiled in order to describe the regional extent of the relationship between SST and $\delta^{18}O$ at the LGM and termination I.

4.3 Methods

In this study we have compiled oxygen isotope data from mixed layer planktonic foraminifera and published proxy-derived SST data measured from the same fourteen cores in the Atlantic, Pacific, and Indian Oceans (Figure 4.2 and Table 5) for the last 20,000 years. SST reconstructions were derived from Mg/Ca analyses [see Chapter 2; *Rosenthal et al*., in prep, *Lea at al*., 2000; *Nürnberg et al*., 2000] or alkenone analyses [*Sikes and Keigwin*, 1994; *Schneider et al*., 1995; *Chapmann et al.,* 1996; *Schneider et al*., 1996; *Sonzogni et al*., 1998; *Rühlemann et al*., 1999; *Wang et al*., 1999; *Kudrass et al*., 2001]. At all sites, the data were used with the chronology provided in the original literature. The data have been box averaged into 1,000 year constant time steps using the Arand software package to compensate for age model discrepancies between the different records. Therefore, major conclusions do not rely on observations made from single data points, and the age-model discrepancies do not significantly affect the findings in this study.

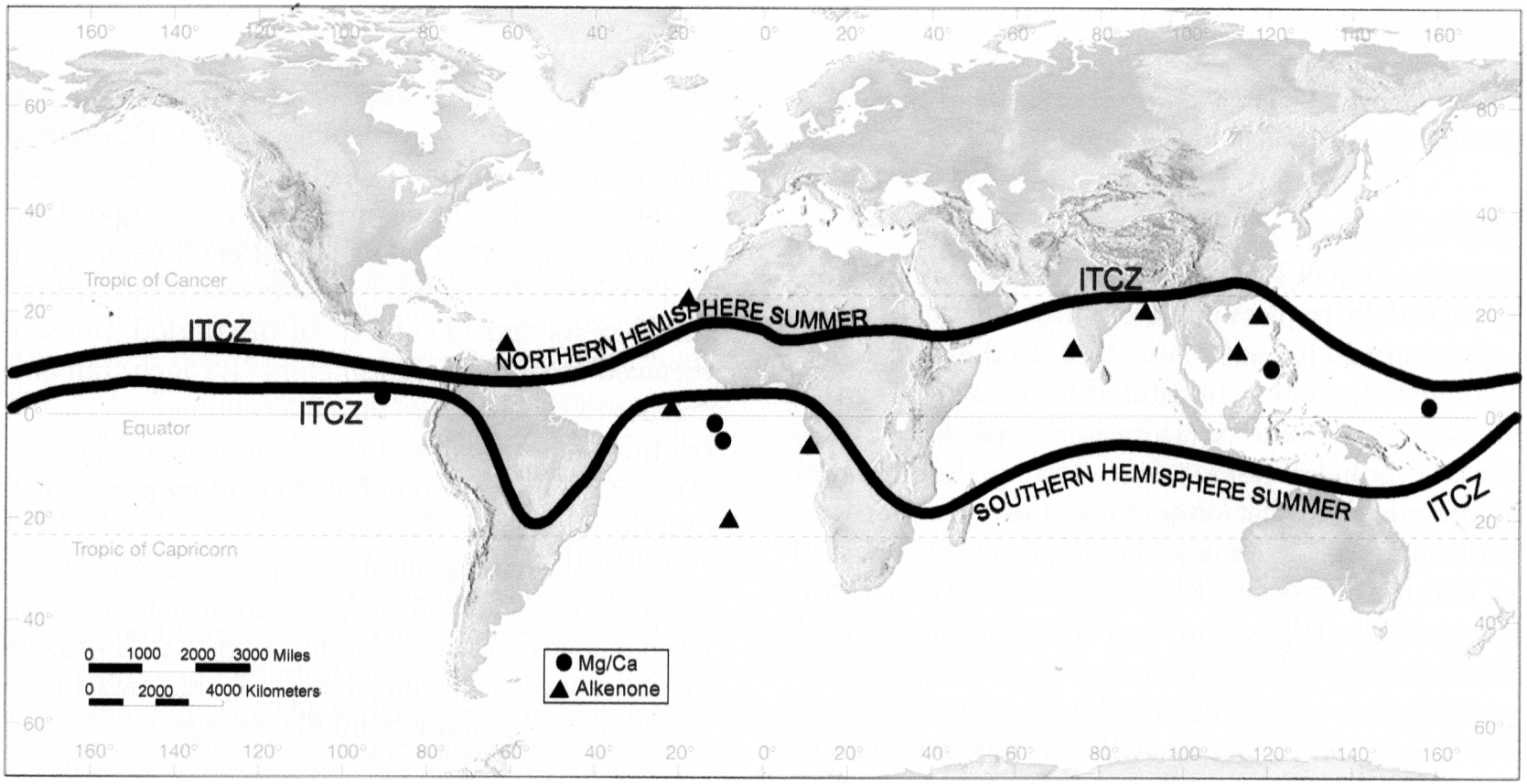

Figure 4.2: Location of ocean sediment cores used to examine glacial-interglacial sea surface temperature and salinity changes by means of Mg/Ca (circle) and alkenones (triangle) analyses. See Table 4 for location details and references.

Table 5: Background information of cores used in this study

location	latitude	longitude	core name	Mg/Ca	Alkenone	$\delta^{18}O$	Reference
Sulu Sea	8.78 N	121.28 E	MD97-2141	*G. ruber*	-	*G. ruber*	this study
Cocos Ridge	2.26 N	90.95 W	TR163-19	*G. ruber*	√ *	*G. ruber*	*Lea et al.* [2000]
Ontong Java Plateau	0.32 N	159.36 E	ODP 806B	*G. ruber*	√*	*G. ruber*	*Lea et al.* [2000]
Equatorial Divergence Zone	1.67 S	12.43 W	GeoB1105	*G. sacculifer*	-	*G. sacculifer*	*Nürnberg et al.* [2000]
Guinea Basin (South Equ. Current)	5.77 S	10.75 W	GeoB1112	*G. sacculifer*	-	*G. sacculifer*	*Nürnberg et al.* [2000]
Northeast Atlantic	20.16 N	19.00 W	BOFS31/1K		√	*G. bulloides*	*Chapmann et al.* [1996]
Angola Basin	6.58 S	10.32 E	GeoB1008-3		√	*G. ruber, pink*	*Schneider et al.* [1995]
Walfish-Ridge	20.1 S	9.18 W	GeoB1028-5		√	*G. ruber*	*Schneider et al.* [1996]
Bengal Fan	19.97 N	90.03 E	SO93-126KL		√	*G. ruber*	*Kudrass et al.* [2001]
Indian Ocean	10.47 N	75.23 E	MD77-194		√	*G. ruber*	*Duplessy* [1981]; *Sonzogni et al.* [1999]
South China Sea	8.51 N	112.33 E	GIK17961-2		√	*G. ruber*	*Wang et al.* [1999]
South China Sea	20.12 N	117.38 E	GIK17940		√	*G. ruber*	*Wang et al.* [1999]
Equatorial Atlantic	0.04 N	23 W	86014-12PC51		√	*G. sacculifer*	*Sikes and Kegwin* [1994]
Tropical Atlantic	12.09 N	61.24 W	M35003-4		√	*G. ruber, pink*	*Rühlemann et al.* [1999]

Note: * = agree with Mg/Ca result according to Tim Herbert (Brown University)

The oxygen isotope record preserved in planktonic foraminifera buried in sediments is a function of SST, precipitation-evaporation (P-E) balance, and global ice volume all of which are affected by global radiative forcing. I have subtracted the generally accepted 1 ‰ [*Schrag et al*., 1996] glacial-interglacial $\delta^{18}O$ signal of global ice volume from the planktonic $\delta^{18}O$ time series in each record in order to better evaluate the influence of SST and P-E at each location assuming a 120 m drop in sea level at the LGM. All available sea-level data [*Fairbanks*, 1989; *Fairbanks*, 1990; *Chappell & Polach*, 1991; *Edwards et al.*, 1993; *Guilderson et al*., 2000; *Hanebuth et al*., 2000] were compiled, corrected for their estimated tectonic uplift, and converted into calendar ages using INTCAL98/Calib4 [*Stuiver et al*., 1998a, b]. However if available, U/Th ages have been used instead of ^{14}C ages (Figure 4.3). The best fit is expressed in the polynomial function:

$$\text{sea level} = 1.25 + (5.39*yr) - (2.29*yr)^2 + (0.39*yr)^3 - (0.022*yr)^4 + (0.00038*yr)^5$$

The sea level curve has been converted into permil units assuming 0.008 ‰ per meter sea level change [*Schrag et al*., 1996], and subtracted from each available $\delta^{18}O$ record. The $\delta^{18}O$ record minus the sea level record will be hereafter referred to as $\delta^{18}O_{residual}$.

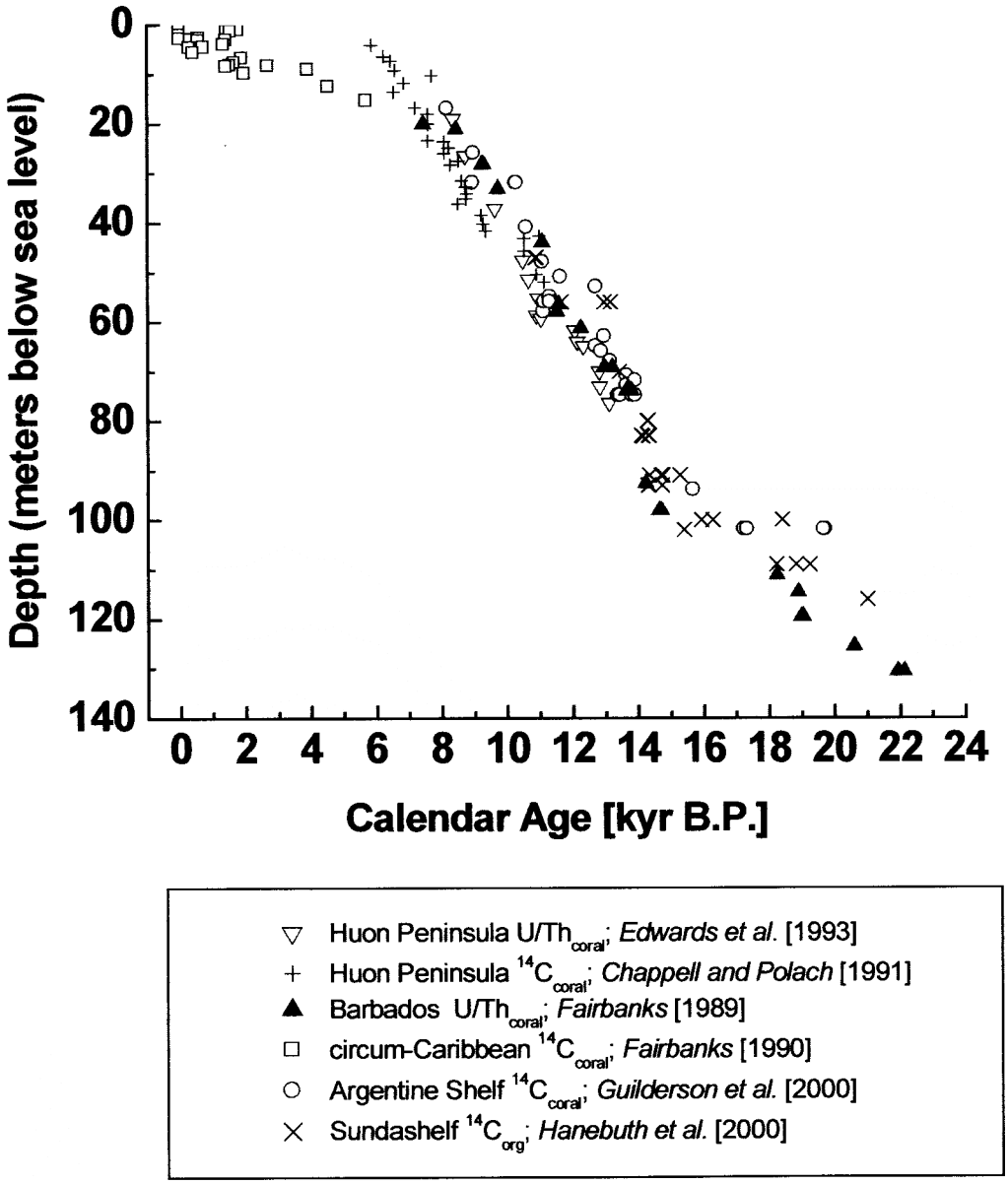

Figure 4.3: Compilation of sea-level data used to remove ice volume signal from planktonic $\delta^{18}O$ time series. All data have been corrected for their tectonic uplift and are converted into calendar ages using INTCAL98/Calib4 [*Stuiver et al.,* 1998a, b]. However U/Th ages have been used instead of ^{14}C ages if available.

4.4 Results

Cores known to exhibit a lead in SST over $\delta^{18}O$ at the LGM (Figure 4.4A and B) have been separated from cores where SST changes are synchronous with $\delta^{18}O$ during this period (Figure 4.4C & D). All cores where SST estimates were based on Mg/Ca analyses ($SST_{Mg/Ca}$) indicate a lead in $\delta^{18}O_{residual}$, whereas only three cores with SST derived from alkenones (SST_{Alk}) indicate a lead with respect to $\delta^{18}O_{residual}$. In those cores where SST leads the $\delta^{18}O_{residual}$, $\delta^{18}O_{residual}$ increases approximately 0.3 to 0.4 ‰ between 20 to 17 kyr, and decreases thereafter by 1 ‰ (Figure 4.4A). In those cores with SST leading, SST continuously increases by 2 °C until it reaches a maximum at approximately 10 kyr, after which SST drops 0.5 °C (Figure 4.4B). However, this drop in SST after 10 kyr is only true for $SST_{Mg/Ca}$. SST_{Alk} increases continuously during this time period. One of the main focuses of this study will be to examine the cause of the $\delta^{18}O_{residual}$ increase by 0.3-0.4 ‰ in cores where SST is leading the $\delta^{18}O$ record (Figure 4.4A).

In cores where SST is synchronous with $\delta^{18}O_{residual}$, $\delta^{18}O_{residual}$ continuously decreases by 0.7 ‰ until 10 kyr, then increases by 0.4 ‰ (Figure 4.4C). Over this same interval SST increases by 1.5 °C (Figure 4.4D). Note that the SST record in Figure 4.4D is based only on alkenones. Comparison of all SST records indicates a linear relationship between 20-10 kyr. However, starting at 10 kyr, $SST_{Mg/Ca}$ indicates minimal change or even a slight reduction in temperature.

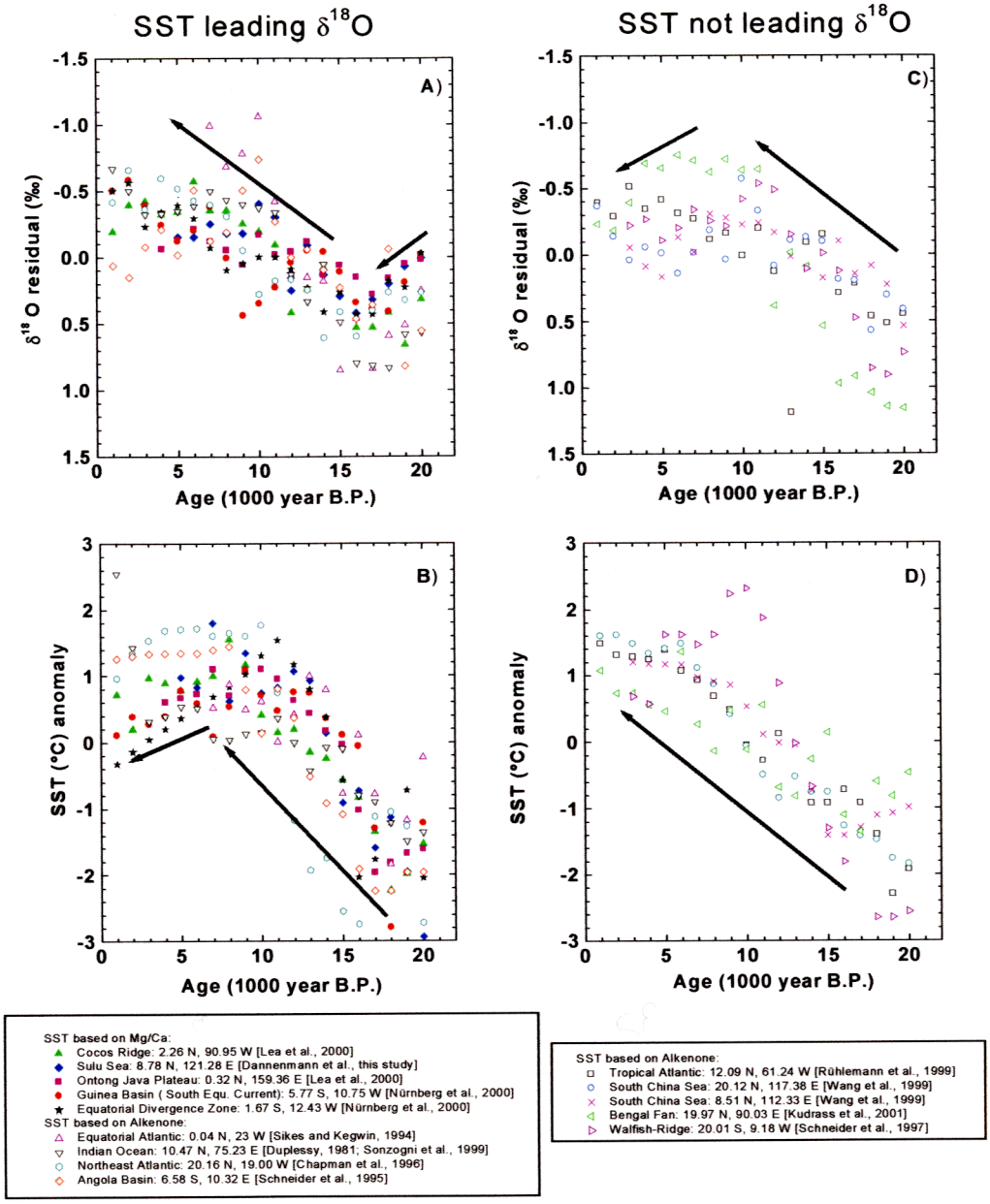

Figure 4.4: Oxygen isotope ($\delta^{18}O$) and SST data age in 1000 yrs B.P.. Ice volume change of 1.0 ‰ for glacial-interglacial range has been subtracted from the $\delta^{18}O$ record. **A)** Compilation of $\delta^{18}O$ of cores where SST is leading the $\delta^{18}O$ record. **B)** Compilation of SST from cores where SST is leading $\delta^{18}O$. **C)** Compilation of $\delta^{18}O$ from cores where SST is not leading $\delta^{18}O$. **D)** Compilation of SST from cores where SST is not leading $\delta^{18}O$.

4.5 Discussion

The oxygen isotopic ratio of planktonic foraminifera is mainly a function of sea surface temperature (SST), ice volume and sea surface salinity (SSS),

$$\delta^{18}O_{foraminifera} = \delta^{18}O \text{ (SSS, SST, ice volume)}$$

where SSS is a function of Precipitation (P) minus Evaporation (E), and where evaporation is a function of wind speed and water vapor saturation. Foraminiferal $\delta^{18}O$ potentially is a function of water temperature due to temperature-dependent equilibrium oxygen isotopic fractionation (~ 0.22‰ $\delta^{18}O$ per °C [*Epstein et al.*, 1953]. Additionally the $\delta^{18}O$ of ocean water responds to changes in rainfall, which adds isotopically light (more negative $\delta^{18}O$) water. Therefore, $\delta^{18}O$ will increase as SST decreases and as SSS (defined as P-E) decreases. Since the ice volume signal has been subtracted from the $\delta^{18}O$ records in Figure 4.4A and Figure 4.4C, changes in the $\delta^{18}O_{residual}$ must be due to changes in local SST and SSS. Furthermore, assuming the $\delta^{18}O_{residual}$ is only a function of SST, SSS it is possible to subtract SST from the $\delta^{18}O_{residual}$ record using the SST estimates based on Mg/Ca and alkenone analyses. Thus, it is potentially possible to isolate and assess the influence of SSS for each sediment core location.

4.5.1 Cores with SST synchronous with $\delta^{18}O$

In cores where the glacial-interglacial SST change is synchronous with $\delta^{18}O$, SST displays a linear increase through the glacial-interglacial transition (Figure 4.4D). In the same cores, the $\delta^{18}O_{residual}$ indicates a continuous decrease to ~10 kyr) (Figure 4.4 C), and increases thereafter by 0.3-0.4 ‰. If $\delta^{18}O_{residual}$ is

driven mainly by changes in SST, it would be expected that Figure 4.4C and Figure 4.4D would portray the same trend. SST and $\delta^{18}O_{residual}$ do indicate a similar trend until about 10 kyr, but then they differ during the Holocene. However, SST based on Mg/Ca measurements in Figure 4.4B shows a similar pattern to $\delta^{18}O_{residual}$ (Figure 4.4C) suggesting that $\delta^{18}O_{residual}$ is influenced mainly by changes in SST. This difference in inferred temperature changes derived from Mg/Ca and alkenones is puzzling. Since in this study only *G. ruber* and *G. sacculifer* have been included (with the exception of one *G. bulloides* record) the difference between these SST curves might be due to changes in conditions under which *G. ruber* and *G. sacculifer* calcify. Alkenones are known to reflect temperature changes over the first 10 m of the water column [*Prahl et al.,* 1988; *Müller et al*., 1998; *Herbert*, 2001], whereas *G. ruber* and *G. sacculifer* can calcify from the surface to a depth of ~70 m [e.g., *Ravaelo and Fairbanks*, 1992; *Nikolaev et al*., 1998]. Typically, the average calcification depth of *G. ruber* is within the uppermost 25 m [*Ravaelo and Fairbanks*, 1992]. The isotopic composition of modern oceanic waters partially reflects a dynamic balance between vertical and horizontal mixing, causing homogenization of the isotopic composition in the upper 70 m [*Nikolaev et al*., 1998]. Because the depth at which *G. ruber* and *G. sacculifer* calcify is not exactly known, it is therefore possible to get erroneous SST estimates since we are measuring an average temperature of at least the upper 25 m. A different thermocline structure during glacial and interglacial times could also influence temperature estimates based on foraminiferal Mg/Ca and $\delta^{18}O_{residual}$. For example due to the large temperature gradient in the thermocline, depending on the depth at which *G. ruber* calcifies, the average temperature of the uppermost 25 m during an interglacial period could be close to the average temperature during glacial times (Figure 4.5).

Therefore, I argue that as temperature proxies foraminiferal Mg/Ca and $\delta^{18}O_{residual}$ are independently affected by thermocline changes. This also suggests that for the purpose of reconstructing past changes in SSS, it is better to use SST estimates based on Mg/Ca rather than alkenones because both Mg/Ca and $\delta^{18}O$ are measured on the same species of foraminifera in the same sample, and thus by subtracting the $SST_{Mg/Ca}$ from the $\delta^{18}O_{residual}$ the additional temperature difference based on the calcification depths in each record will theoretically cancel each other out, and the estimate of $\delta^{18}O_{seawater}$ will be more accurate.

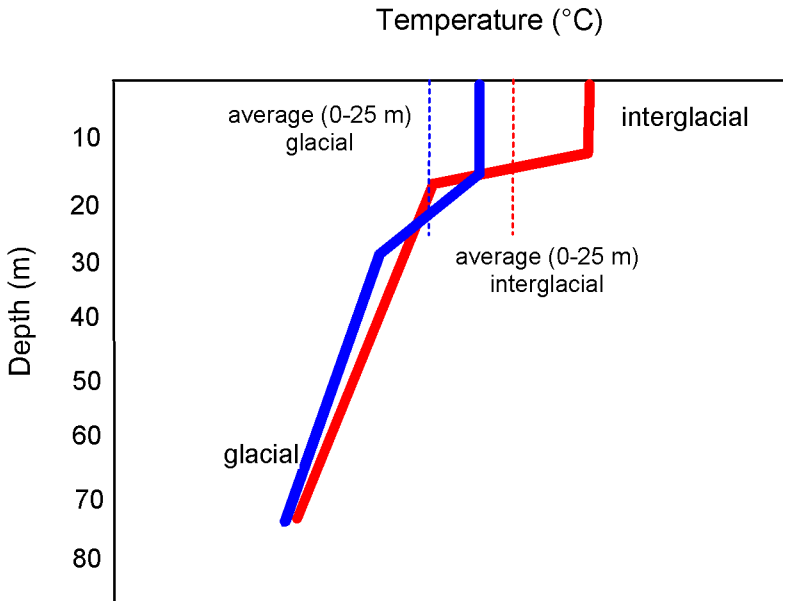

Figure 4.5: Hypothetical thermocline reconstruction for the last glacial maximum and interglacial. Horizontal bars indicate average temperature change for the uppermost 25 meters.

4.5.2 Cores where SST leads $\delta^{18}O$

$\delta^{18}O_{residual}$ and reconstructed SST for cores where SST leads $\delta^{18}O$ are presented in Figures 4.4A and B. Of particular interest is the observed 0.4 ‰ $^{18}O_{residual}$ enrichment between 20-17 kyr in cores where SST is leading $\delta^{18}O$ at the termination (Figure 4.4A). The independent SST proxies in Figure 4.4B record the same increase in SST during this time period indicating that the $^{18}O_{residual}$ enrichment between 20-17 kyr is not related to temperature changes. Since the ice volume signal has already been extracted from the $\delta^{18}O$ record (Figure 4.4A), planktonic foraminiferal $\delta^{18}O_{residual}$ must be lower at the LGM (20 kyr) due to an increase in P-E. For the purpose of calculating $\delta^{18}O$ of seawater, only cores with SST estimates based on Mg/Ca, and not on alkenone data, have been included in Figure 4.6 for reasons mentioned in the previous section. Figure 4.6A emphases the 0.4 ‰ $^{18}O_{residual}$ enrichment between 20-17 kyr, and thereafter the continuous lowering of $^{18}O_{residual}$ into the Holocene. The $\delta^{18}O_{seawater}$ (SSS) has been calculated using the empirically derived temperature : $\delta^{18}O$ relationship based on planktonic foraminifera generated by *Erez and Luz* [1983] for *G. sacculifer* (Figure 4.6C). The $\delta^{18}O_{seawater}$ record shows a 0.6 ‰ enrichment between the LGM and 14 kyr, suggesting a continuous change from less saline surface oceans during the LGM to more saline conditions at 14 kyr. This trend reverses at 14 kyr, indicating a decrease in SSS.

The P-E state of the tropics at the LGM remains controversial. However, the conclusion that the ^{18}O depletion at the LGM is due to an increase in P-E appears to be in agreement with observations from forty lake paleo-records

Farrera et al., [1999]. A more positive mean annual LGM P-E is recorded in the now-arid basins of western North America, on the southern Andean Altiplano [*Baker et al.,* 2001], in the Mediterranean region [*Prentice et al*., 1992; *Harrison and Digerfeldt*, 1993], in the Middle East [*Roberts and Wright*, 1993], and in southern Africa [*Farrera et al*., 1999]. Modelling studies indicate that wetter conditions are found on the western side of New Guinea during the LGM [*Hostetler and Clark*, 2000]. These authors proposed that the land that emerged between Australia and Indonesia (presently the Arafura Sea and the Torres Strait) led to increased precipitation through increased surface heating. However, in equatorial East Africa, lakes show conditions similar to, or drier than present west of 34 °E, and similar to, or wetter than present to the east of 34 °E [*Farrera et al*., 1999]. Additionally, there are many examples where regions register drier conditions during the LGM (e.g., Australian subtropics, northwestern Sahara [*Conrad* 1969; *Causse et al*. 1988]. Additionally, ice core analyses from the Sajama Mountains in Bolivia indicate increased regional accumulation during the LGM which is consistent with the higher water levels in regional paleolakes [*Thompson et al*., 1998]. *Thompson et al.*, [1998] concluded that the occurrence of less dust in tropical glacial ice cores indicates that climate conditions must have been wetter, and therefore greater snow cover is possible.

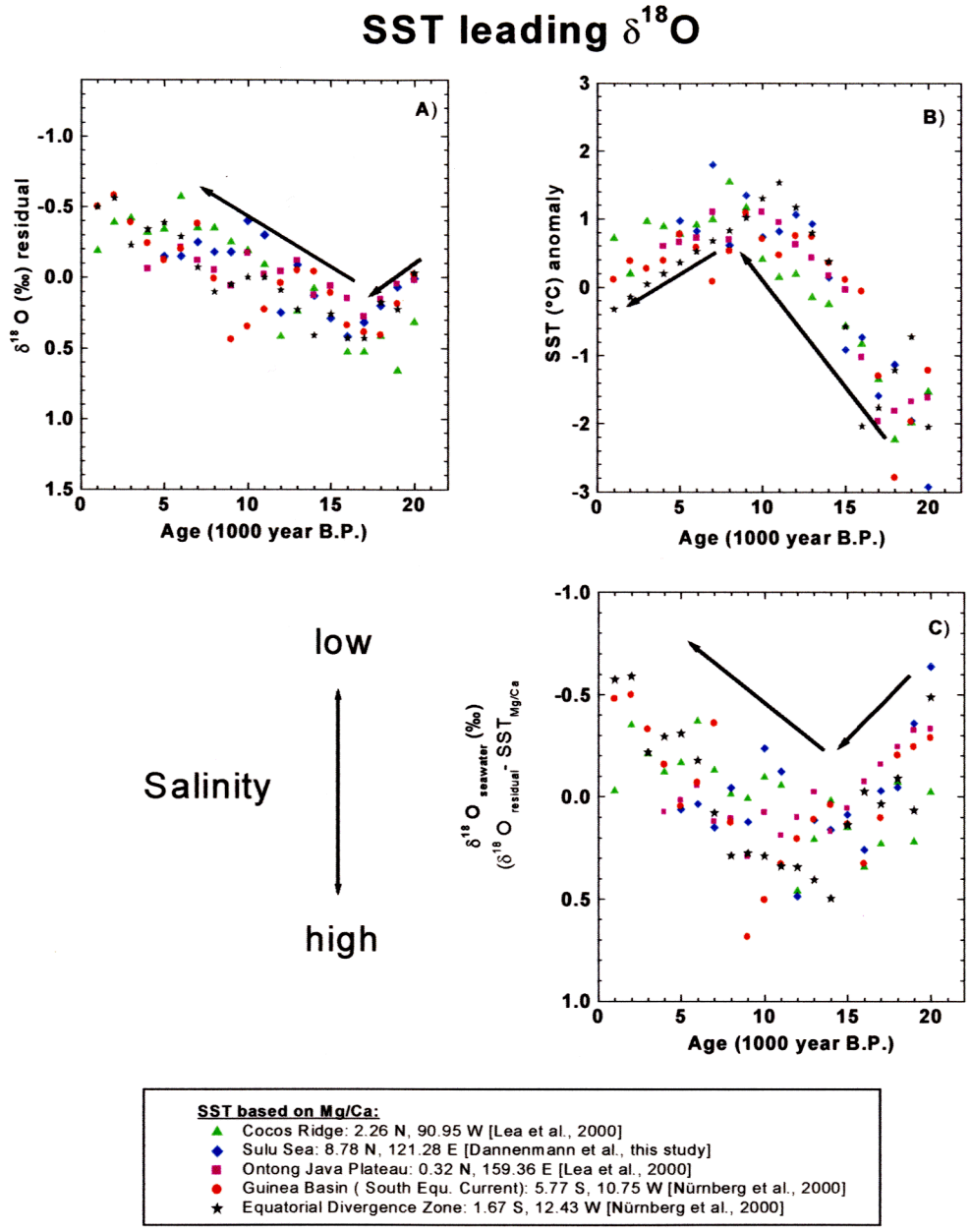

Figure 4.6: (A) Oxygen isotope ($\delta^{18}O$) and **(B)** SST data versus ages in 1000 years B.P.. Sea level change of 1.0 ‰ for glacial-interglacial range has been subtracted from the $\delta^{18}O$ record ($\delta^{18}O_{residual}$). Only data of cores where SST leads $\delta^{18}O$ and is based on Mg/Ca measurements are shown. Compare with Figures 4.4A and B, respectively. **(C)** $\delta^{18}O_{seawater}$ calculated using the equation by *Erez and Luz* [1983].

I argue that lower salinity conditions in certain regions of the tropical oceans at the LGM and higher lake levels at high altitudes are linked. Under colder glacial climate, less precipitation is expected because there is less moisture in the air. The apparent wetness of high elevations may have been due to strong cooling and reduced evaporative demand more than an increase in precipitation at these elevations [*Farrera et al*., 1999]. Generally reduced precipitation in the tropics and sub-tropics and enhanced precipitation in the path of southward-shifted jet streams in the Northern Hemisphere are also consistent features of the Paleoclimate Modeling Intercomparison Project simulations for the LGM [*Pinot et al*.,1999].

It has been suggested that El Niño-Southern Oscillation (ENSO) variability has existed for at least the past 130,000 years [*Tudhope et al*., 2001; *Cane and Clement*, 1999; *Clement et al*., 2000]. *Cane and Clement* [1999] further suggested that the ENSO system could go through periods of more numerous El Niño or La Niña conditions. Glacial conditions would favor prolonged intervals of La Niña conditions. Today, during times of La Niña, cooler conditions occur in the East Pacific when the easterly trade winds over the Pacific increase, allowing more upwelling of water along the equator. Teleconnections through air-sea interactions and the atmosphere spread the effects of La Niña over the globe. For example, the water vapor pattern in the middle troposphere during a strong La Niña month in 1989 (Figure 4.7) indicated that moist air was found predominantly in the Western Pacific. A ENSO-like change in the present water vapor spatial pattern could be the reason why some areas indicate greater P-E changes during the LGM while others do not show this increase. The ocean sediment cores examined in this study that indicate

fresher conditions during the LGM are found within the predominantly moist areas depicted in Figure 4.7. Even though La Niña in 1989 is only one example, a schematic map of spatial and temporal responses of global hydro-climatological variables during strong La Niña phases indicates overall the same correlation (Figure 4.8) [*Halbert and Ropelewski*, 1992].

In view of the strong tropical jet streams at the LGM, atmospheric transport alone is probably sufficient to spread the influence of a strong regional atmospheric event over the entire extratropical hemisphere in which it occurs. Water vapor has a rapid response time, and because it is such an effective greenhouse gas, it has leverage over climate [*Pierrehumbert*, 1999]. Reorganizations of tropical convection could have a profound effect on the water vapor pattern of the tropical Pacific. The water vapor pattern can be influenced by changes in the location and surface area of the convective moisture-source region (Walker circulation), but also by changes in the intensity of subsidence of the air (Hadley circulation), which alters the dryness of the nonconvective regions [*Pierrehumbert*, 2000]. The Hadley and Walker cells are large-scale features of tropical atmospheric circulation that overturn meridionally and zonally, respectively. These two interacting circulations cannot always be separated into distinct components. Strong atmospheric convection over the Pacific occurs throughout the extensive region associated with the Western Pacific Warm Pool and also in the narrow belt of the intertropical convergence zone (ITCZ).

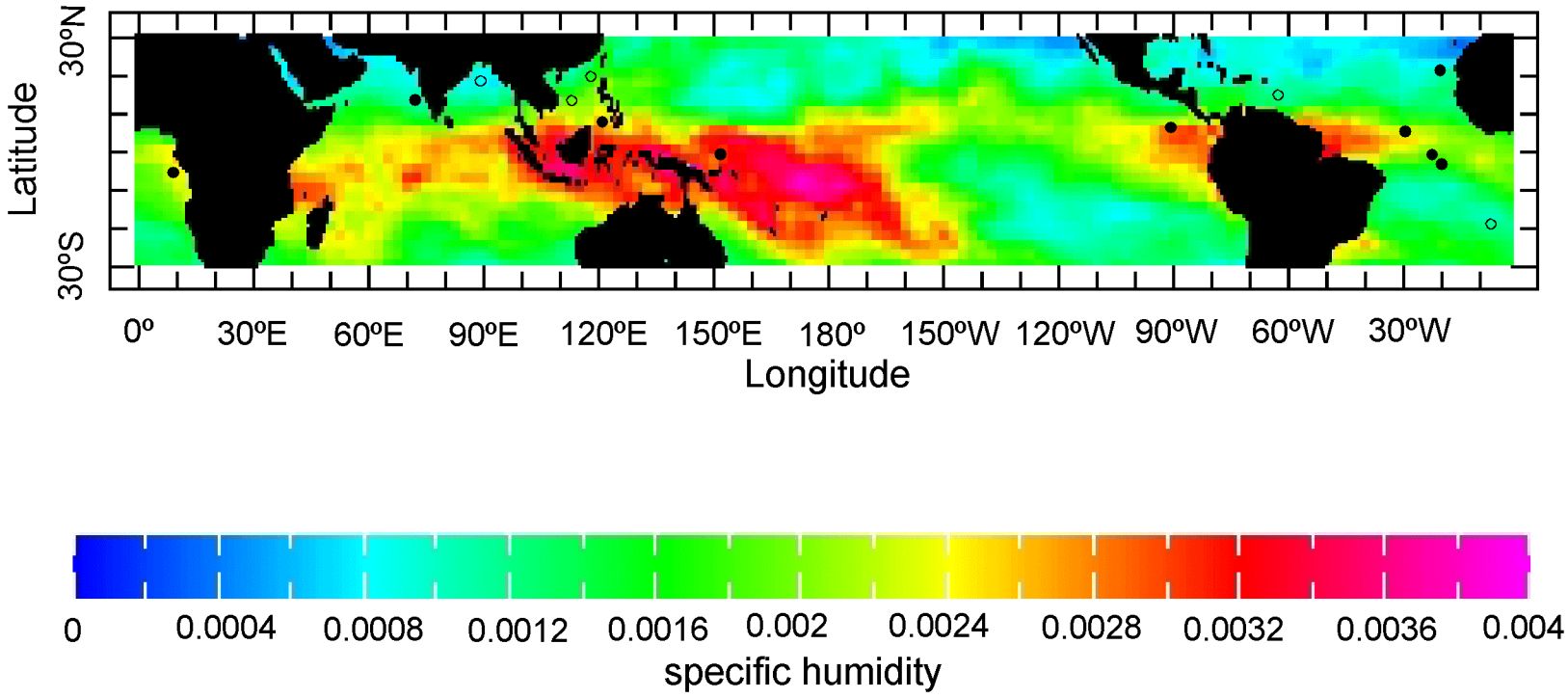

Figure 4.7: Water vapor concentration in the mid troposphere during January, 1989, a strong La Niña month. Data are taken from the European Center for Medium Range Weather Forecasts. In a La Niña year, moist air is found predominantly in the Western Pacific. Solid circles indicate SST leads the $\delta^{18}O$ record, whereas open circles indicate synchronous SST - $\delta^{18}O$ records, during the Last Glacial Maximum.

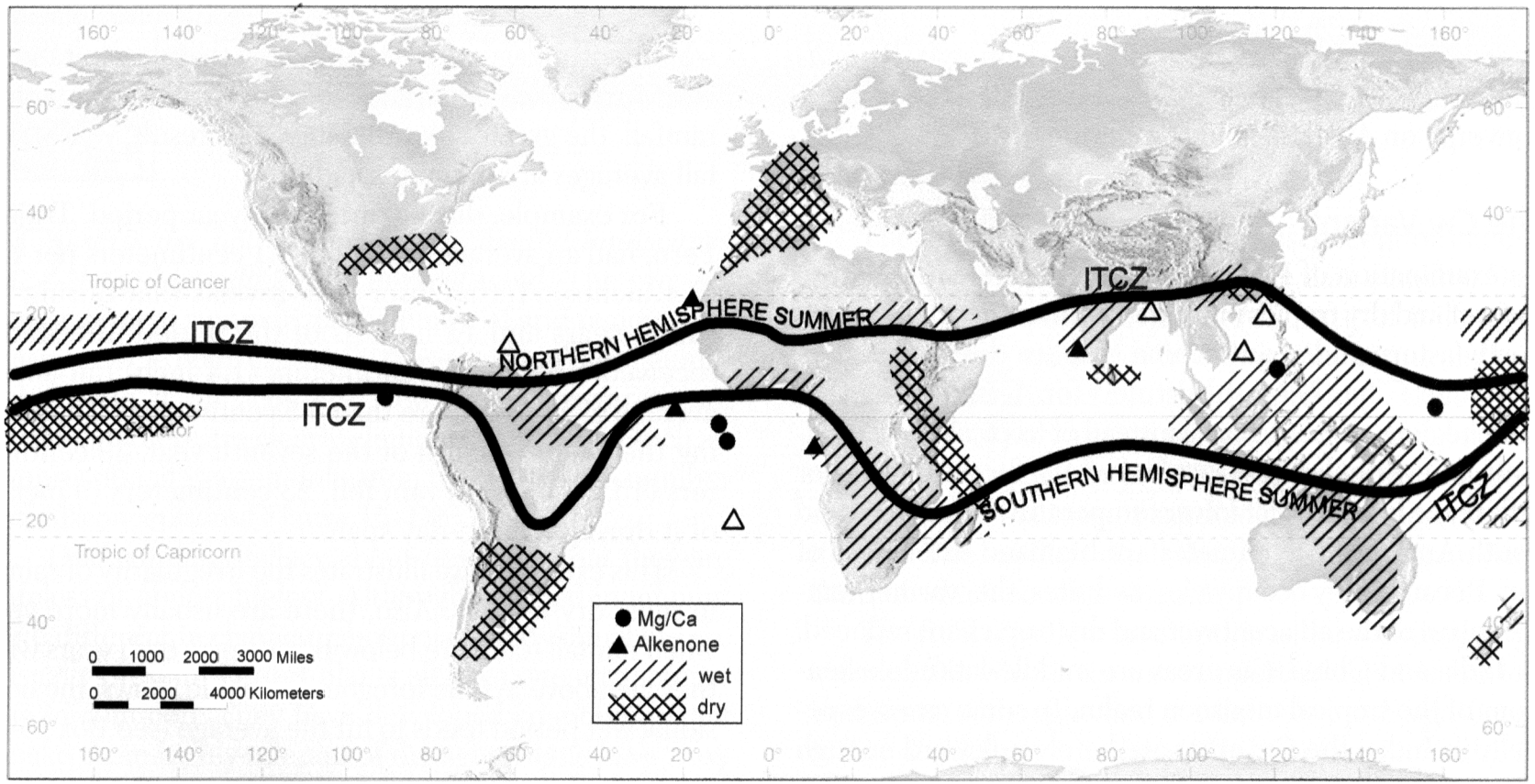

Figure 4.8: Schematics of the spatial and temporal responses of global hydro-climatological variables during a strong La Niña phase [modified from *Halbert and Ropelewski*, 1992]. Location of ocean sediment cores used to examine glacial-interglacial sea surface temperature and salinity changes by means of Mg/Ca (circle) and alkenones (triangle) analyses. Solid symbols indicate SST leads the $\delta^{18}O$ record, whereas open symbols indicate synchronous SST - $\delta^{18}O$ during the Last Glacial Maximum.

It is difficult to determine presently whether the effect on ENSO is related to the impact on tropical atmospheric circulation and the strength of the Asian Monsoon system [*Liu et al.*, 2000; *Otto-Bliesner*, 1999]. As pointed out by *Clement et al*., [2000] longer modeling experiments are needed to investigate the changes in tropical Pacific. The results of the study highlight the need of more high resolution data from this area.

4.6 Conclusions

I have compiled published planktonic foraminiferal oxygen isotope values and SST data based on Mg/Ca and alkenone analysis from the tropical and subtropical Atlantic and Pacific for the last 20,000 years. This compilation suggests that during the LGM precipitation minus evaporation must have been greater in cores where SST is leading the planktonic foraminiferal oxygen isotopic record by approximately 3,000 years, whereas in cores with no lead/lag relationship between SST and foraminiferal $\delta^{18}O$ data colder and drier conditions are indicated. Additionally, cores where SST is leading the $\delta^{18}O$ record are preferentially located in areas influenced by greater water vapor content during times of La Niña assuming that an ENSO system existed during glacial times.

REFERENCES

Anderson, R.Y., Linsley, B.K., Gardner, J.V., **1990**, Expression of seasonal and ENSO forcing in climatic variability at lower than ENSO frequencies: Evidence from Pleistocene marine varves of California. In Benson, LV., and Meyers, P.A. (eds), Paleoclimates: The record from Lakes, Ocean, and Land. *Palaeogeography, Palaeoclimato!ogy, Palaeoecology*., v. 78, p. 287-300.

Baker, P. A., Rigsby, C. A., Seltzer, G. O., Fritz, S. C., Lowenstein, T. K., Bacher, N. P., and Veliz, C., **2001**, Tropical climate changes at millennial and orbital timescales on the South American Altiplano. *Nature*, v. 409, p. 698-701.

Bard, E., Arnold, M., Fairbanks, R.G., and Hamelin, B., **1993**, ^{230}Th-^{234}U and ^{14}C ages obtained by mass spectrometry on coral. *Radiocarbon*, v. 35, no. 1, p. 191-199.

Bé, A.W.H., **1960**, Ecology of recent planktonic Foraminifera, Part 2. Bathymetric and season distributions in the Sargasso Sea off Bermuda. *Micro-paleontology*, v. 6, p. 144-151.

Berger, A., and Loutre, M.F., **1991**, Insolation values for the climate of the last 10 million years. *Quaternary Science Reviews*, v. 10, p. 297-317.

Berger, W.H., Killingley, J.S., and Vincent, E., **1978**. Stable isotopes in deep-sea carbonates: box cores ERDC-92, west equatorial Pacific. *Oceanol. Acta*, v. 1, p. 203-216.

Blunier T., and Brooks, E.J., **2001**, Timing of Millennial-Scale Climate Change in Antarctica and Greenland During the Last Glacial Period. *Science*, v. 291, p. 109-112.

Blunier, T., Chappellaz, J., Schwander, J., Dällenbach, A., Stauffer, B., Stocker, T.F., Raynaud, D., Jouzel, J., Clausen, H.B., Hammer, C.U., and Johnson, S.J., **1998**, Asynchrony of Antarctic and Greenland climate change during the last glacial period. *Nature*, v. 394, p. 739-743.

Broecker, W.S., and Denton, G.H., **1989**, The role of ocean-atmosphere reorganizations in glacial cycles. *Geochimica et Cosmochimica Acta*, v. 53 p. 2,465-2,501.

Brown, S.J., and Elderfield, H., **1996**, Variations in Mg/Ca and Sr/Ca ratios of planktonic foraminifera caused by postdepositional dissolution: Evidence of shallow Mg-dependent dissolution. *Paleoceanography*, v. 11, No. 4, p. 543-551.

Cane, M.A., **1998**, A Role for the Tropical Pacific. *Science*, v. 282, p.59-61.

Cane, M., and Clement, A.C, **1999**, A Role for the Tropical Pacific Coupled Ocean-Atmosphere System on Milankovitch and Millennial Timescales Part II: Global Impacts. *In*: Clark, P.U., Webb, R.S., and Keigwin, L.D. (editors) Mechanisms of global climate change at millennial time scales, *Geophysical Monograph*, v. 112, p. 373-384.

Causse, C., Gasse, F., Gibert, E., Kassir, A., Conrad, G., and Fontes, J.-C., **1988**, The last Pleistocene humid phase in the western Sahara, dated to about 80-100 ka. *Comptes Rendus - Academie des Sciences*, vol. 306, No.20, p. 1459-1464.

Chaisson, W.P., and Ravelo, A.C., **1997**, Changes in upper water-column structure at site 925, Late Miocene-Pleistocene: Planktonic Foraminifer assemblage and Isotopic Evidence. *In*: Shackleton, N.J., Curry, W.B., Richter, C., and Bralower, I.J., (Eds.), 1997, *Proceedings of the Ocean Drilling Program, Scientific Results*, v. 154, p. 255-268.

Chapman, M.R.; Shackleton, N.J.; Zhao, M., and Eglinton, G, **1996**,: Faunal and alkenone reconstructions of subtropical North Atlantic surface hydrography and paleotemperature over the last 28 kyr, *Paleoceanography*, v. 11, p. 343-357.

Chappell, J., Omura, A., Esat, T., McCulloch, M., Pandolfi, J., Ota, Y. and Pillans, B., **1996**, Reconciliation of late Quaternary sea levels derived from coral terraces at Huon Peninsula with deep sea oxygen isotope records. *Earth and Planetary Science Letters*, v. 141, p. 227-236.

Chappell, J., and Polach, H., **1991**, Post-glacial sea-level rise from a coral record at Huon Peninsula, Papua New Guinea. *Nature*, v. 349, p. 147-149.

Charles, C. D., Lynch-Stieglitz, J., Ninnemann, U. S., and Fairbanks, R. G., **1996**, Climate connections between the hemisphere revealed by deep sea sediment core/ice core correlations, *Earth and Planetary Science Letters*, v. 142, No. 1-2, p. 19-27.

Chen, F.H., Bloemendal, J., Wang, J.M., Li, J.J., and Oldfield, F., **1997**, High-resolution multi-proxy climate records from Chinese loess: evidence for rapid climatic changes over the last 75kyr. *Palaeogeography, Palaeoclimatology, Palaeoecology*, v. 130, p. 323-335.

Chen L., and Wu R., 2000, The role of the Asian/Australian monsoons and the Southern/Northern oscillation in the ENSO cycle. *Theoretical and Applied Climatology*, v. 65, no. 1-2, P. 37-47.

Clark, P.U., Alley, R.B., and Pollard, D., **1999**, Northern hemisphere ice-sheet influences on global climate change. *Science*, v. 286, p. 1104-1111.

Clement, A.C., Seager, R., and Cane, M.A., **2000**, Suppression of El Niño during the mid-Holocene by changes in the Earth's orbit. *Paleoceanography*, v. 15, No.6, p. 731-737.

Clement, A.C., and Cane, M., **1999**, A Role for the Pacific Coupled Ocean-Atmosphere System on Milankovitch and Millennial Timescales Part I: A Modeling Study of Tropical Pacific Variability. *In*: Clark, P.U., Webb, R.S., and Keigwin, L.D. (editors), **1999**, Mechanisms of global climate change at millennial time scales, *Geophysical Monograph*, v. 112, p.363-372.

Clement, A.C., Seager, R., and Cane, M.A., **1999**, Orbital controls on the El Niño/Southern Oscillation and the tropical climate, *Paleoceanography*, v. 14, No. 4, p. 441-456.

CLIMAP, **1981**, Seasonal reconstruction of the Earth's surface at the last glacial maximum. *Geological Society of America, Map and Chart Series*, v. C36.

Conkright, M., Levitus, S., O'Brien, T., Boyer, T., Antonov, J., and Stephens, C., **1998**, World Ocean Atlas 1998 CD-ROM Data Set Documentation. *Tech. Rep. 15, NODC Internal Report*, 16 pp.

Conrad, G., **1969**, L**'**évolution continentale post-hercynienne du Sahara algérien (Saoura, Erg, Chech, Tanezrouft, Ahnet-Mouydir*). Publication du Centre de Recherche sur les Zones arides CNRS sér Géol*, v. 10, pp. 527.

Curry, W.B., Thunell, R.C., and Honjo, S., **1983**, Seasonal changes in the isotopic composition of planktonic foraminifera collected in Panama Basin sediment traps. *Earth and Planetary Science Letters*, v. 64, p. 33-43.

deGaridel-Thoron, T., Beaufort, L., Linsely, B., and Dannenmann, S., **in press**, Millennial-scale dynamics of the East Asian winter monsoon during the last 200,000 years. *Paleoceanography*.

Duplessy, J.C., Be, A.W.H., Blank, P.L., **1981**, Oxygen and carbon isotopic composition and biogeographic distribution of planktonic foraminifera in the Indian Ocean. *Paleogeography, Paleoclimatology, Paleoecology*, v. 33, p. 9-46.

Edwards, R.L., et al, **1993**, A large drop in atmospheric $^{14}C/^{12}C$ and reduced melting in the Younger Dryas documented with Th-230 ages of corals. *Science*, v. 260, p. 962-968.

Elderfieid, H., and Gansen, G., **2000**, Past temperature and $\delta^{18}O$ surface ocean waters inferred from foraminiferal Mg/Ca ratios. *Nature*, v. 405, p.442-445.

Emiliani, C., **1954**, Depth habitats of some species of pelagic Foraminifera as indicated by oxygen isotope ratios. *American Journal of Science*, v. 252, No. 3, p. 149-158.

Epstein, S., Buchsbaum, R., Lowenstam, H.A., and Urey, H.C., **1953**, Revised carbonate-water isotopic temperature scale. *Bulletin of the Geological Society of America*, v. 64, p.1315-1326.

Erez, J., and Honjo, S., **1981**, Comparison of isotopic composition of planktonic foraminifera in plankton tows, sediment traps and sediments. *Palaeogeography, Palaeoclimatology, Palaeoecology*, v. 33, No. 1-3, p. 129-156.

Erez, J., and Luz, B., **1983**, Experimental paleotemperature equation for planktonic foraminifera. *Geochimica et Cosmochimica Acta*, v. 74, p. 1025-1031.

Exon, N. F., Haake, F. W., Hartmann, M., Koegler, F. C., Mueller, P. J., and Whiticar, M. J., **1981**, Morphology, water characteristics and sedimentation in the silled Sulu Sea, Southeast Asia, *Marine Geology*, v. 39, No. 3-4, p. 165-195.

Fairbanks, R.G., **1989**, A 17,000-year glacio-eustatic sea level record: influence of glacial melting rates on the Younger Dryas event and deep-ocean circulation. *Nature*, v. 342, p. -637-642.

Fairbanks, R.G., **1990**, The origin of the Younger Dryas climate event in Greenland ice cores. *Paleoceanography*, v. 6, p. 937-948.

Fairbanks, R. G., and Wiebe, P. H., **1980**, Foraminifera and chlorophyll maximum; vertical distribution, seasonal succession, and paleoceanographic significance. *Science*, v. 209, No. 4464, p. 1524-1526.

Fairbanks, R.G., Sverdlove, M., Free, R., Wiebe, P.H., and Bé, A.W.H., **1982**, Vertical distribution and isotopic fraction of living planktonic foraminifera from the Panama Basin. *Nature*, v. 298, p. 841-844.

Fairbanks, R.G., Wiebe, P.H., and Bé, A.W.H., **1980**, Vertical distribution and isotopic composition of living planktonic foraminifera in the western North Atlantic. *Science*, v. 207, p. 61-63.

Farrera, I., Harrison, S. P., Prentice, I. C., Ramstein, G., Guiot, J., and Bartlein, P. J., **1999**, Tropical climates at the last glacial maximum; a new synthesis of terrestrial palaeoclimate data; 1, Vegetation, lake-levels and geochemistry. *Climate Dynamics*, v. 15, No. 11, p. 823-856.

Guilderson, T.P., Burckle, L., Hemming, S., and Peltier, W.R., **2000**, Late Pleistocene sea level variations derived from the Argentine Shelf. *Geochemistry, Geophysics, Geosystems*, v. 1, Paper number 2000GC000098. (Available at http://www.g-cubed.org)

Guilderson, T.P., Fairbanks, R.G., and Rubenstone, J.L., **1994**, Tropical Temperature Variations Since 20,000 Years Ago: Modulating Interhemispheric Climate Change. *Science*, v. 263, p. 663-665.

Hanebuth T., Stattegger, K., and Grootes, P.M., **2000**, Rapid flooding of the Sunda Shelf: A late-glacial sea-level record. *Science*, p. 1033-1035.

Halpert, M.S., and Ropelewski, C.F., **1992**, Surface temperature patterns associated with the Southern Oscillation. *Journal of Climate*, v. 5, p. 577-593.

Harrison, S.P., and Digerfeldt, G., **1993**, European lakes as palaeohydrological and palaeoclimatic indicators. *Quaternary Science Review*, v. 12, p. 233**-**248.

Hastings, D.W., Russell, A.D., and Emerson, S.R., **1998**, Foraminiferal magnesium in *Globeriginoides sacculifer* as a paleotemperature proxy. *Paleoceanography*, v. 13, No. 2, p. 150-169.

Hemleben, C., Spindler, M., Anderson, O.R., **1989**, Modern Planktonic Foraminifera. Springer-Verlag, New York, pp. 370.

Herbert, T.D., **2001**, Review of alkenone calibrations (culture, water column, and sediments). *Geochem. Geophys. Geosys*., vol. 2, Paper number 2000GC000055. (Available at http://www.g-cubed.org)

Hostetler, S. T., and Clark, P.U., **2000**, Tropical Climate at the Last Glacial Maximum Inferred from Glacier Mass-Balance Modeling. Science, v. 290, p. 1747-1750.

Kienast, M., Steineke, S., Stattegger, K., Calvert, S.E., **2001**, Synchronous tropical South China Sea SST changes and Greenland warming during deglaciation. *Science*, v. 291, p. 2,132-2,134.

Kudrass, H.R., Erlenkeuser, H., Vollbrecht, R., and Weiss, W., **1991**, Global nature of the Younger Dryas cooling event inferred from oxygen isotope data from Sulu Sea cores. *Nature*, v. 349, p. 406- 409.

Kudrass, H. R., Hofmann, A., Doose, H., Emeis, K., and Erlenkeuser, H., **2001**, Modulation and amplification of climatic changes in the Northern Hemisphere by the Indian summer monsoon during the past 80 k.y., *Geology* , v. 29, No. 1, p. 63-66.

Kuehl, S.A., Fuglseth, T.J., and Thunell, R.C., **1993**, Sediment mixing and accumulation rates in the Sulu and South China Seas: Implications for organic carbon preservation in deep-sea environments. *Marine Geology*, v. 111, p. 15-35.

Kutzbach, G., **1987**, Monsoons, Eds. Fein, J.S., and Stephens, P.L.. Wiley-Interscience Publications. John Wiley and sons.

Lea, D. W., Pak, D. K., Spero, H. J., **2000,** Climate impact of late Quaternary Equatorial Pacific sea surface temperature variations, *Science* , v. 289, No. 5485, p. 1719-1724.

Levitus, S., Burgett, R., and Boyer, T.P., **1994**, World Ocean Atlas 1994, Volume 3: Nutrients. *NOAA Atlas NESDIS 3*, U.S. Department of Commerce, Washington D.C., pp. 117.

Li, C. Y., **1989**, Frequent activities of stronger aerotroughts in East Asia in wintertime and the occurrence of the El Niño event. *Science in China (Series B),* v. 32, no. 8, p. 976-985.

Linsley, B.K., **1996**, Oxygen-isotope record of sea level and climate variations in the Sulu Sea over the past 150,000 years. *Nature*, v. 380, p. 234-237.

Linsley, B.K., and Thunell, R.C., **1990**, The record of deglaciation in the Sulu Sea: Evidence for the Younger Dryas event in the tropical Western Pacific. *Paleoceanography*, v. 5, No. 6, p. 1025-1039.

Linsley, B. K., Thunell, R. C., Morgan, C., Williams, D. F., **1985**, Oxygen minimum expansion in the Sulu Sea, western Equatorial Pacific, during the last glacial low stand of sea level. *Marine Micropaleontology*, v. 9, No. 5, p. 395-418.

Liu, Z., Kutzbach, J., and Wu, L., **2000**, Modeling climate shift of El Niño variability in the Holocene. *Geophysical Research Letters* , v. 27, p. 15, p. 2265-2268.

Lohman, G.P., **1995**, A model for variation in the chemistry of planktonic foraminifera due to secondary calcification and selective dissolution. *Paleoceanography*, v. 10, No. 3, p. 445-457.

Manabe, S., and Stauffer, R.J., **1988**, Two stable equilibria of a coupled ocean-atmosphere model. *Journal of Climate*, v. 1., p. 841-866.

Martinson, D.G., Pisias, N.G., Hays, J.D., Imbrie, J., Moore, T.C., and Shackelton, N.H., **1987**, Age dating and the orbital theory of the Ice Ages: Development of a high-resolution 0 to 300,000-year chronostratigraphy. *Quaternary Research*, v. 27, p. 1-29.

Miao, Q., Thunell, R.C., and Anderson, D.M., **1994**, Glacial-Holocene carbonate dissolution and sea surface temperature in the South China and Sulu seas. *Paleoceanography*, v. 9, No. 2, p. 269-290.

Mix, A.C., Bard, E., and Schneider, R., **2001**, Environmental processes of the ice age: land, oceans, glaciers (EPILOG). *Quaternary Science Reviews*, v. 20, p. 627-657.

Müller, P.J., Kirst, G., Ruhland, G., Storch, I.V., and Rosell-Mele, A., **1998**, Calibration of the Alkenone paleotemperature index $U^{k'}_{37}$ based on core-tops from the eastern South Atlantic and the global ocean 60°N-60°S. *Geochim. Cosmochim. Acta*, v. 62. No. 10, p. 1757-1772.

Nikolaev, S.D., Oskina, N.S., Blyum, N.S., and Bubenshckikova, N.V., **1998**, Neogene-Quaternary variations of the 'Pole-Equator' temperature gradient of the surface oceanic waters in the North Atlantic and North Pacific. *Global and Planetary Change*, v. 18, p. 85-111.

Norris, R.D., Corfield, R.M., and Cartlidge, J.E., **1993**. Evolution of depth ecology in the planktic foraminifera lineage *Globorotalia (Fohsella). Geology*, v.21, p. 975-978.

Norris, R. D., **1994**. Evolutionary ecology of *Globorotalia (Globoconella)* (planktic foraminifera). *Marine Micropaleontol*., v. 23, p. 121-145.

Nozaki, Y., Alibo, D.-S., Amakawa, H., Gamo, T., Hasumoto, H., **1999**, Dissolved rare earth elements and hydrography in the Sulu Sea. *Geochimica et Cosmochimica Acta*, v. 63, No. 15, p. 2171-2181.

Nurnberg, D., Bjima, J., and Hemleben, C., **1996a**, Assessing the reliability of magnesium in foraminiferal calcite as a proxy for water mass temperatures. *Geochimica et Cosmochimica Acta*, v. 60, no. 5, p. 803-814.

Nurnberg, D., Bjima, J., and Hemleben, C., **1996b**, Assessing the reliability of magnesium in foraminiferal calcite as a proxy for water mass temperatures Erratum. *Geochimica et Cosmochimica Acta*, v. 60, no. 13, p. 2483-2484.

Nürnberg, D., Müller, A., and Schneider, R.R., **2000**, Paleo-sea surface temperature calculations in the equatorial east Atlantic from Mg/Ca ratios in planktic foraminifera: A comparison to sea surface temperature estimates from $U^{K'}_{37}$, oxygen isotopes, and foraminiferal transfer function. *Paleoceanography*, v. 15, No. 1, p. 124-134.

Otto-Bliesner, B. L., **1999,** ENSO and NAO; present and 6000 years before present as simulated by the NCAR Climate System Model (CSM). *In:* Karl, Thomas R. (chairperson), The ENSO Experiment research activities; exploring the linkages between the El Niño-Southern Oscillation (ENSO) and human health, *Symposium on Global Change Studies* , v. 10 , p. 313-316.

Pelejero, C., Grimalt, J.O., Sarnthein, M., Wang, L., and Flores, J.-A., **1999**, Molecular biomarker record of sea surface temperature and climatic change in the South China Sea during the last 140,000 years. *Marine Geology*, v. 156, p. 109-121.

Pierrehumbert, R. T., **2000**, Climate change and the tropical Pacific: The sleeping dragon wakes. *PNAS*, vol. 97, No. 4, p. 1355-1358.

Pierrehumbert, R. T., **1999**, Huascaran $\delta^{18}O$ as an indicator of tropical climate during the Last Glacial Maximum. *Geophysical Research Letters*, v. 26, p. 1345-1348.

Pinot, S., Ramstein, G., Harrison, S. P., Prentice, I. C., Guiot, J., Stute, M., Joussaume, S., **1999**, Tropical paleoclimates at the last glacial maximum; comparison of Paleoclimate Modeling Intercomparison Project (PMIP) simulations and paleodata. *Climate Dynamics* , v. 15, No.11, p. 857-874.

Porter, S.C., and Zhisheng, A., **1995**, Correlation between climate events in the North Atlantic and China during the last glaciation, *Nature*, vol. 375, p. 305-308.

Prahl, F.G., Muelhausen, L.A., and Zahnle, D.L., **1988**, Further evaluation of long-chain alkenones as indicators of paleoceanographic conditions. *Geochim. Cosmochim. Acta*, v. 52, p. 2303-2310.

Prentice, I. C., Guiot, J., Harrison, S. P., **1992**, Mediterranean vegetation, lake levels and palaeoclimate at the last glacial maximum, *Nature*, v. 360, No. 6405, p. 658-660.

Qu, T. ; Mitsudera, H. ; Yamagata, T., **2000**, Intrusion of the North Pacific waters into the South China Sea. *Journal of Geophysical Research*, v. 105 , No. C3 , p. 6415-6424.

Rahmstorf, S., **1994**, Rapid climate transitions in a coupled ocean-atmosphere model, Nature, v. 372, No. 6501, p. 82-85.

Rasmusson, E.M., and Arkin, P.A., **1993**, A global view of large-scale precipitation variability. *Journal of Climate*, v. 6, No.8, p. 1495-1522.

Rasmusson, E.M., and Carpenter, T.H., **1983**, Variations in tropical sea surface temperature and surface wind fields associated with the Southern Oscillations/ El Niño. *Monthly Weather Review*, v. 110, p. 354-384.

Ravelo, A.C., and Fairbanks, R.G., **1992**, Oxygen isotopic composition of multiple species of planktonic foraminifera: records of the modern photic zone temperature gradient. *Paleoceanography*, v. 7, No. 6, p. 815-831.

Rind, D., and Peteet, D., **1986**, Terrestrial Conditions at the Last Glacial Maximum and CLIMAP Sea- Surface Temperature Estimates: Are They Consistent? *Quaternary Research*, v.24, p. 1-22.

Rind, D., Peteet, D., Broecker, W., McIntyre, A., and Ruddiman, W.R., **1986**, The impact of cold North Atlantic sea surface temperature on climate: implication for Younger Dryas cooling (11-10k). Climate Dynamics, v. 1, p. 3-33.

Roberts, N., and Wright, Jr H.E., **1993**, Vegetational, Lake-Level, and Climatic History of the Near East and Southwest Asia. In: Wright, H.E., Kutzbach, J.E., Webb III, T., Ruddiman, W.F., Street- Perrott, F.A., Bartlein, P.J. (eds) *Global Climates since the Last Glacial Maximum*. University of Minnesota Press, Minneapolis- London, p. 194-220.

Rosenthal, Y., Field, M. P., and Sherrell, R.M, **1999**, Precise Determination of Element/Calcium Ratios in Calcareous Samples Using Sector Field Inductively Coupled Plasma Mass Spectrometry. *Analytical Chemistry*, v.71, No.15, p. 3248-3253.

Rosenthal, Y., Lohmann, G.P., Lohmann, K.C., and Sherrell, R.M., **2000**, Incorporation and preservation of Mg in *Globigerinoides sacculifer*: Implications for reconstructing the temperature and $^{18}O/^{16}O$ of seawater. *Paleoceanography*, v. 15, No. 1, p. 135-145.

Rosenthal, Y., Oppo, D. W., Dannenmann, S., and Linsley, B. K., **in prep.**, Millennial-scale variations in western equatorial Pacific sea surface temperature during glacial and Holocene climates.

Rühlemann, C., Mulitza, S., Müller, P.J., Wefer, G., and Zahn, R., **1999**, Warming of the tropical Atlantic Ocean and slowdown of thermohaline circulation during the last deglaciation. *Nature*, v. 402, p. 511-514.

Schneider, R.R., Müller, P.J., and Ruhland, G., **1995**, Late Quaternary surface circulation in the east-equatorial South Atlantic: evidence from alkenone sea surface temperatures. *Paleoceanography*, v. 10, p. 197-219.

Schneider, R.R., Müller, P.J., Ruhland, G., Meinecke, G., Schmidt, H., and Wefer, G., **1996**, Late Quarternary surface temperatures and productivity in the east-equatorial South Atlantic: response to changes in trade/monsoon wind forcing and surface water advection, *In*: Wefer, G., Berger, W.H., Siedler, G., and Webb, D. (eds.), *The South Atlantic: Present and Past Circulation*, Springer-Verlag, p. 527-551.

Schrag, D.P., Hampt, G., and Murray, D.W., **1996**, Pore fluid constraints on the temperature and oxygen isotopic composition of the glacial ocean. *Science*, v. 272, p. 1930-1932.

Shackleton, N. J., and Vincent, E., **1978**, Oxygen and carbon isotope studies in Recent foraminifera from the Southwest Indian Ocean. *Marine Micropaleontology*, v. 3, No. 1, p. 1-13.

Shaw, P.-T., Chao, S.-Y., Liu, K.-K., Pai, S.-C., and Liu, C.-T., **1996**, Winter upwelling off Luzon in the northeastern South China Sea. *Journal of Geophysical Research*, v. 101, No. C7, p. 16,435-16,448.

Shaw, P.-T., and Chao, S.-Y., **1994**, Surface circulation in the South China Sea. *Deep-Sea Research I*, v. 41, No. 11-12, p. 1663-1683.

Sikes, E.L., and Keigwin, L.D., **1994**, Equatorial Atlantic sea surface temperature for the last 30 kyr: A comparison of Uk37, $\delta^{18}O$ and foraminiferal assemblage temperature estimates. *Paleoceanography*, v. 9, p. 31-45.

Sirocko, D. Leuscher, M. Staubwasser, J. Maley, L. Heusser, **1999**, High-frequency Oscillations of the Last 70,000 years in the Tropical/Subtropical and Polar Climates. *In*: Clark, P.U., Webb, R.S., and Keigwin, L.D. (editors), **1999**, Mechanisms of global climate change at millennial time scales, *Geophysical Monograph*, v. 112, p.113-126.

Sonzogni, C., Bard, E., and Rostek, F., **1998**, Tropical sea-surface temperature during the last glacial period: a view based on alkenones in Indian Ocean sediments. *Quaternary Science Reviews*, v. 17, p. 1185-1201.

Stuiver, M., and Braziunas T. F.,**1993**, Modeling atmospheric ^{14}C influences and ^{14}C ages of marine samples back to 10,000 BC. *Radiocarbon*, 35, 137-189.

Stuiver, M., Reimer, P. J., Bard, E., Beck, J. W., Burr, G. S., Hughen, K. A., Kromer, B., McCormac, G., van der Plicht, J., and Spurk, M., **1998a,** INTCAL98 radiocarbon age calibration, 24,000-0 cal BP. *Radiocarbon*, v. 40, No. 3, p. 1041-1083.

Stuiver, M., Reimer, P. J., Braziunas, T. F., **1998b**, High-precision radiocarbon age calibration for terrestrial and marine samples, *Radiocarbon*, v. 40, No. 3, p. 1127-1151.

Stute, M., Forster, M., Frischkorn, H., Serejo, A., Clark, J.F., Schlosser, P., Broecker, W.S., and Bonani,G., **1995**, Cooling of tropical Brazil (5°C) during the last glacial maximum. *Science*, v. 269, p. 46-50.

Talley, L.D, **1999**, Some aspects of ocean heat transport by the shallow, intermediate and deep overturning circulations. *In*: Clark, P.U., Webb, R.S., and Keigwin, L.D. (editors), **1999**, Mechanisms of global climate change at millennial time scales, *Geophysical Monograph*, v. 112, p.1-22.

Thompson, L. G., Mosley-Thompson, E., and Henderson, K. A., **2000,** Ice-core paleoclimate records in tropical South America since the Last Glacial Maximum. J. Quat. Sci., v. 15, 377-394.

Thompson, L.G., Davis, M.E., Thompson, E.M., Sowers, T.A., Henderson, K.A., Zagorodnov, V.S., Lin, P.N., Mikhalenko, V.N., Campen, R.K., Bolzan, J.F., Cole-Dai, J., and Francou, B., **1998**, A 25,000 year tropical climate history from Bolivian ice cores. *Science*, v. 282, No. 5295, p.1858-1864.

Trenberth, K.,E., and Shea, D.J., **1987**, On the evolution of the Southern Oscillation. *Monthly Weather Review*, v. 115, p. 3,078-3,096.

Tudhope, A.W., Chilcott, C.P., McCulloch, M.T., Cook, E.R., Chappell, J., Ellam, R.M., Lea, D.W., Lough, J.M., and Shimmield, G.B., **2001**, Variability in the El Niño-Southern Oscillation through a glacial-interglacial cycle. *Science*, v. 291, p. 1511-1517.

Van der Kaars, S., Wang, X., Kershaw, P., Guichard, F., Setiabudi, D.A., **2000**, A late Quaternary palaeoecological record from the Banda Sea, Indonesia: patterns of vegetation, climate and biomass burning in Indonesia and northern Australia. *Palaeogeography, Palaeoclimatology, Palaeoecology*, v. 155, p. 135-153.

Walker, G.T., **1923**, Correlation in seasonal variations of weather. III: A preliminary study of world weather. *Memoir of the Indian Meteorological Department*, v. 24, p. 75-131.

Walker, G.T., **1924**, Correlation in seasonal variations of weather. IV: A further study of world weather. *Memoir of the Indian Meteorological Department*, v. 24, p. 275-332.

Walker, G.T., **1928**, World weather. III: *Memoir of Royal Meteorological Society*, v.2, p. 97-106.

Walker, G.T., and, Bliss, E.W.,**1932**, World weather. V: *Memoir of Royal Meteorological Society*, v. 4, p. 53-84.

Wang, L., Sarnthein, M. , Erlenkeuser, H., Grimalt, J., Grootes, P., Heilig, S., Ivanova, E., Kienast, M., Pelejero, C., and Pflaumann, U., **1999**, East Asian monsoon climate during the Late Pleistocene: high-resolution sediment records from the South China Sea. *Marine Geology*, v.156, No.1-4, pp. 245-284.

Webster, P.J., and Yang, S., **1992**, Monsoon and ENSO: selectively interactive systems. *Quaternary Journal of Research of the Meteorological Society*, v. 118, p. 877-926.

Wyrtki, K., **1961**, Scientific results of marine investigations of the South China Sea and the Gulf of Thailand, physical oceanography of the Southeast Asian water. *Univer. of Calif., Scripps Inst. of Oceanogr., La Jolla, Calif.,* pp. 195.

Wyrtki, K., **1975**, El Niño - The dynamic response of the equatorial Pacific Ocean to atmospheric forcing. *Journal of Physical Oceanography*, v. 5, p. 572-584.

Yuan, X. J., and Martinson, D.G., **2000,** Antarctic Sea Ice Extent Variability and Its Global Connectivity. *Journal of Climate*, v. 13, p.1697-1717.

NOTE: The tables of this appendix were reconstructed by Bill Kidd to digital form using Omnipage Pro X OCR software on scans of the pages from the printed dissertation. Although visual editing inspection removed a few obvious recognition errors, some may remain undetected. For critical uses, check numbers with the original printed pages.

APPENDIX I

IMAGES core MD97-2141: $\delta^{18}O$ and $\delta^{13}C$ data from *Globigerinoides ruber*

Depth (cm)	Age[$] (kyr)	$\delta^{18}O$ (G.rub)[‡] (‰)	$\delta^{13}C$ (G.rub)[‡] (‰)	Depth (cm)	Age[$] (kyr)	$\delta^{18}O$ (G.rub)[‡] (‰)	$\delta^{13}C$ (G.rub)[‡] (‰)
0	4.29	-2.531	1.368	46	6.00	-2.666	1.221
1	4.33	-2.462	0.992	47	6.03	-2.653	0.868
2	4.38	-2.579	1.133	48	6.06	-2.528	1.044
3	4.43	-2.629	1.142	49	6.10	-2.613	1.149
4	4.48	-2.624	0.936	50	6.13	-2.638	1.296
5	4.53	-2.581	0.863	51	6.16	-2.481	1.104
6	4.58	-2.483	0.982	52	6.19	-2.629	1.051
7	4.62	-2.509	0.974	53	6.23	-2.605	1.047
8	4.67	-2.677	0.920	54	6.26	-2.525	1.219
9	4.72	-2.546	1.078	55	6.29	-2.644	1.143
10	4.77	-2.484	1.124	56	6.32	-2.587	0.966
11	4.82	-2.490	0.894	57	6.36	-2.702	1.029
12	4.87	-2.467	0.903	58	6.39	-2.635	0.965
13	4.91	-2.736	0.888	59	6.42	-2.604	0.933
14	4.96	-2.789	0.929	60	6.48	-2.621	1.278
15	4.99	-2.668	1.163	61	6.54	-2.694	0.912
16	5.03	-2.479	0.958	62	6.60	-2.577	1.042
17	5.06	-2.529	1.146	63	6.66	-2.643	1.132
18	5.09	-2.628	1.124	64	6.73	-2.611	1.138
19	5.12	-2.632	1.077	65	6.79	-2.535	1.089
20	5.16	-2.580	1.037	66	6.85	-2.655	1.097
21	5.19	-2.740	1.036	67	6.91	-2.773	1.192
22	5.22	-2.591	0.942	68	6.97	-2.640	1.035
23	5.25	-2.529	0.985	69	7.03	-2.651	0.987
24	5.29	-2.471	0.957	70	7.09	-2.612	1.040
25	5.32	-2.524	0.985	71	7.15	-2.711	1.038
26	5.35	-2.590	0.965	72	7.21	-2.576	0.981
27	5.38	-2.559	0.927	73	7.27	-2.469	1.109
28	5.42	-2.462	0.869	74	7.33	-2.448	1.064
29	5.45	-2.411	1.136	75	7.39	-2.534	1.064
30	5.48	-2.627	1.158	76	7.45	-2.577	1.118
31	5.51	-2.552	1.279	77	7.51	-2.511	1.068
32	5.55	-2.675	0.960	78	7.56	-2.483	0.905
33	5.58	-2.575	0.955	79	7.62	-2.549	1.189
34	5.61	-2.590	1.086	80	7.68	-2.497	1.112
35	5.64	-2.568	1.070	81	7.74	-2.619	0.964
36	5.67	-2.479	0.836	82	7.80	-2.458	0.972
37	5.71	-2.582	0.941	83	7.85	-2.370	0.954
38	5.74	-2.669	1.042	84	7.91	-2.520	0.947
39	5.77	-2.466	0.947	85	7.97	-2.577	1.013
40	5.80	-2.686	1.139	86	8.03	-2.314	0.904
41	5.84	-2.738	1.118	87	8.09	-2.539	0.977
42	5.87	-2.592	1.069	88	8.14	-2.423	0.985
43	5.90	-2.545	1.022	89	8.20	-2.503	0.888
44	5.93	-2.751	0.974	90	8.26	-2.357	0.942
45	5.97	-2.610	1.065	91	8.32	-2.491	0.964

Depth (cm)	Age[$] (kyr)	$\delta^{18}O$ (G.rub)[‡] (‰)	$\delta^{13}C$ (G.rub)[‡] (‰)	Depth (cm)	Age[$] (kyr)	$\delta^{18}O$ (G.rub)[‡] (‰)	$\delta^{13}C$ (G.rub)[‡] (‰)
92	8.38	-2.414	0.725	138	10.63	-2.394	0.473
93	8.43	-2.338	0.715	139	10.66	-2.331	0.459
94	8.49	-2.249	0.790	140	10.70	-2.594	0.586
95	8.55	-2.505	1.073	141	10.73	-2.395	0.554
96	8.61	-2.568	0.961	142	10.77	-2.318	0.504
97	8.67	-2.603	0.797	143	10.80	-2.393	0.625
98	8.72	-2.384	0.897	144	10.84	-2.171	0.653
99	8.78	-2.138	0.601	145	10.87	-2.298	0.555
100	8.84	-2.561	0.792	146	10.91	-2.408	0.612
101	8.90	-2.344	0.738	147	10.94	-2.386	0.392
102	8.96	-2.574	0.698	148	10.98	-2.486	0.427
103	9.01	-2.510	0.807	149	11.01	-2.460	0.586
104	9.07	-2.391	0.846	150	11.05	-2.432	0.462
105	9.13	-2.606	0.790	151	11.06	-2.474	0.532
106	9.19	-2.516	0.807	152	11.07	-2.226	0.601
107	9.25	-2.405	0.704	153	11.09	-2.431	0.549
108	9.30	-2.562	0.787	154	11.10	-2.129	0.721
109	9.36	-2.435	0.736	155	11.11	-2.210	0.355
110	9.42	-2.528	0.707	156	11.13	-2.035	0.568
111	9.48	-2.506	0.592	157	11.14	-1.891	0.512
112	9.54	-2.367	0.718	158	11.15	-2.306	0.575
113	9.59	-2.642	0.772	159	11.20	-2.063	0.674
114	9.65	-2.565	0.802	160	11.24	-1.928	0.572
115	9.71	-2.516	0.556	161	11.29	-1.804	0.641
116	9.77	-2.553	0.680	162	11.33	-1.664	0.572
117	9.83	-2.665	0.466	163	11.37	-1.841	0.573
118	9.88	-2.525	0.700	164	11.42	-2.038	0.498
119	9.94	-2.581	0.759	165	11.46	-2.060	0.638
120	10.00	-2.363	0.603	166	11.51	-1.852	0.513
121	10.04	-2.641	0.707	167	11.55	-1.957	0.535
122	10.07	-2.648	0.889	168	11.60	-2.011	0.604
123	10.11	-2.574	0.564	169	11.64	-1.918	0.502
124	10.14	-2.566	0.673	170	11.68	-1.928	0.566
125	10.18	-2.562	0.405	171	11.73	-1.940	0.646
126	10.21	-2.350	0.549	172	11.77	-1.943	0.654
127	10.24	-2.469	0.386	173	11.82	-1.883	0.658
128	10.28	-2.482	0.848	174	11.86	-1.892	0.568
129	10.31	-2.463	0.793	175	11.91	-1.918	0.577
130	10.35	-2.516	0.647	176	11.95	-1.903	0.491
131	10.38	-2.499	0.580	177	12.00	-1.868	0.615
132	10.42	-2.568	0.562	178	12.04	-1.702	0.628
133	10.45	-2.609	0.436	179	12.08	-1.902	0.371
134	10.49	-2.519	0.388	180	12.13	-1.962	0.558
135	10.52	-2.595	0.501	181	12.17	-1.809	0.394
136	10.56	-2.469	0.497	182	12.22	-2.074	0.476
137	10.59	-2.397	0.414	183	12.26	-1.948	0.587

Depth (cm)	Age[$] (kyr)	$\delta^{18}O$ (G.rub)[‡] (‰)	$\delta^{13}C$ (G.rub)[‡] (‰)
184	12.31	-1.924	0.447
185	12.35	-1.896	0.396
186	12.39	-1.775	0.665
187	12.44	-1.919	0.584
188	12.48	-2.065	0.399
189	12.53	-2.064	0.545
190	12.57	-1.899	0.370
191	12.62	-2.124	0.583
192	12.66	-1.934	0.573
193	12.70	-1.842	0.491
194	12.75	-2.039	0.599
195	12.79	-1.875	0.503
196	12.84	-1.912	0.547
197	12.88	-2.048	0.438
198	12.93	-2.137	0.603
199	12.97	-1.983	0.735
200	13.01	-2.157	0.440
201	13.06	-2.103	0.546
202	13.10	-2.028	0.516
203	13.15	-2.084	0.663
204	13.19	-2.028	0.739
205	13.24	-2.118	0.657
206	13.31	-2.158	0.577
207	13.41	-2.045	0.483
208	13.52	-2.048	0.567
209	13.62	-1.869	0.427
210	13.72	-2.117	0.555
211	13.83	-1.877	0.735
212	13.93	-1.715	0.680
213	13.99	-1.818	0.653
214	14.05	-1.766	0.470
215	14.11	-1.961	0.474
216	14.17	-1.910	0.627
217	14.23	-1.923	0.509
218	14.29	-1.824	0.547
219	14.35	-1.842	0.387
220	14.41	-1.683	0.629
221	14.47	-1.829	0.607
222	14.53	-1.842	0.662
223	14.59	-1.576	0.543
224	14.65	-1.507	0.585
225	14.71	-1.438	0.630
226	14.77	-1.595	0.564
227	14.84	-1.276	0.547
228	14.94	-1.457	0.635
229	15.03	-1.568	0.621
230	15.12	-1.394	0.626
231	15.21	-1.544	0.573
232	15.31	-1.746	0.639
233	15.40	-1.610	0.514
234	15.49	-1.651	0.364
235	15.59	-1.377	0.348
236	15.68	-1.381	0.574
237	15.77	-1.470	0.492
238	15.86	-1.378	0.510
239	15.96	-1.372	0.482
240	16.05	-1.360	0.520
241	16.14	-1.334	0.511
242	16.24	-1.262	0.496
243	16.33	-1.225	0.695
244	16.42	-1.171	0.509
245	16.45	-1.320	0.619
246	16.48	-1.313	0.575
247	16.52	-1.364	0.641
248	16.55	-1.512	0.489
249	16.58	-1.581	0.780
250	16.61	-1.413	0.557
251	16.64	-1.420	0.574
252	16.67	-1.427	0.742
253	sample mixed with other sample		
254	16.73	-1.470	0.784
255	16.76	-1.565	0.753
256	16.80	-1.590	0.735
257	16.83	-1.581	0.793
258	16.86	-1.447	0.766
259	16.89	-1.365	0.624
260	16.92	-1.484	0.628
261	16.95	-1.319	0.647
262	16.98	-1.520	0.755
263	17.01	-1.400	0.651
264	17.04	-1.493	0.693
265	17.08	-1.343	0.809
266	17.11	-1.488	0.772
267	17.14	-1.401	0.736
268	17.17	-1.347	0.715
269	17.20	-1.264	0.786
270	17.23	-1.458	0.672
271	17.26	-1.363	0.738
272	17.29	-1.376	0.553
273	17.32	-1.406	0.626
274	17.35	-1.480	0.779
275	17.38	-1.507	0.625

Depth (cm)	Age[$] (kyr)	$\delta^{18}O$ (G.rub)[‡] (‰)	$\delta^{13}C$ (G.rub)[‡] (‰)	Depth (cm)	Age[$] (kyr)	$\delta^{18}O$ (G.rub)[‡] (‰)	$\delta^{13}C$ (G.rub)[‡] (‰)
276	17.41	-1.445	0.826	322	19.11	-1.529	0.822
277	17.44	-1.428	0.656	323	19.14	-1.348	0.610
278	17.47	-1.357	0.638	324	19.18	-1.834	0.939
279	17.50	-1.510	0.769	325	19.22	-1.472	0.668
280	17.53	-1.473	0.610	326	19.26	-1.451	0.752
281	17.56	-1.409	0.653	327	19.29	-1.802	0.856
282	17.59	-1.542	0.649	328	19.33	-1.585	0.658
283	17.63	-1.363	0.641	329	19.37	-1.528	0.901
284	17.67	-1.631	0.754	330	19.41	-1.716	0.848
285	17.70	-1.406	0.570	331	19.45	-1.510	0.811
286	17.74	-1.323	0.586	332	19.48	-1.652	0.781
287	17.78	-1.501	0.750	333	19.52	-1.567	0.795
288	17.82	-1.425	0.720	334	19.56	-1.737	0.845
289	17.86	-1.551	0.851	335	19.60	-1.798	0.573
290	17.89	-1.449	0.813	336	19.64	-1.581	0.624
291	17.93	-1.404	0.573	337	19.67	-1.762	0.941
292	17.97	-1.599	0.807	338	19.71	-1.467	0.701
293	18.01	-1.508	0.659	339	19.75	-1.520	0.774
294	18.05	-1.551	0.853	340	19.77	-1.535	0.656
295	18.08	-1.540	0.682	341	19.80	-1.516	0.629
296	18.12	-1.573	0.769	342	19.82	-1.546	0.738
297	18.16	-1.517	0.730	343	19.84	-1.505	0.682
298	18.20	-1.382	0.704	344	19.87	-1.380	0.577
299	18.23	-1.563	0.587	345	19.89	-1.531	0.751
300	18.27	-1.577	0.796	346	19.91	-1.554	0.536
301	18.31	-1.642	0.774	347	19.94	-1.603	0.657
302	18.35	-1.404	0.716	348	19.96	-1.659	0.728
303	18.39	-1.542	0.697	349	19.98	-1.545	0.904
304	18.42	-1.669	0.584	350	20.01	-1.640	0.742
305	18.46	-1.511	0.647	351	20.03	-1.523	0.652
306	18.50	-1.627	0.822	352	20.05	-1.545	0.624
307	18.54	-1.437	0.548	353	20.08	-1.482	0.448
308	18.58	-1.400	0.693	354	20.10	-1.610	0.714
309	18.61	-1.594	0.757	355	20.13	-1.620	0.711
310	18.65	-1.431	0.687	356	20.15	-1.519	0.689
311	18.69	-1.736	0.865	357	20.17	-1.634	0.698
312	18.73	-1.629	0.666	358	20.20	-1.585	0.734
313	18.76	-1.573	0.694	359	20.22	-1.452	0.665
314	18.80	-1.478	0.736	360	20.24	-1.534	0.724
315	18.84	-1.551	0.737	361	20.27	-1.551	0.748
316	18.88	-1.440	0.695	362	20.29	-1.738	0.612
317	18.92	-1.775	0.857	363	20.31	-1.680	0.795
318	18.95	-1.470	0.724	364	20.34	-1.707	0.571
319	18.99	-1.633	0.782	365	20.36	-1.734	0.860
320	19.03	-1.756	0.798	366	20.38	-1.574	0.637
321	19.07	-1.406	0.819	367	20.41	-1.518	0.674

Depth (cm)	Age[$] (kyr)	$\delta^{18}O$ (G.rub)[‡] (‰)	$\delta^{13}C$ (G.rub)[‡] (‰)
368	20.43	-1.507	0.759
369	20.47	-1.619	0.717
370	sample mixed with other sample		
371	20.56	-1.720	0.725
372	20.61	-1.510	0.677
373	20.65	-1.639	0.614
374	20.70	-1.602	0.697
375	20.74	-1.396	0.849
376	20.79	-1.387	0.678
377	20.83	-1.719	0.640
378	20.87	-1.568	0.673
379	20.92	-1.458	0.604
380	20.96	-1.672	0.492
381	21.01	-1.485	0.634
382	21.05	-1.699	0.693
383	21.10	-1.617	0.770
384	21.14	-1.557	0.905
385	21.18	-1.562	0.785
386	21.23	-1.643	0.703
387	21.27	-1.632	0.914
388	21.32	-1.578	0.757
389	21.36	-1.513	0.808
390	21.41	-1.677	0.547
391	21.45	-1.765	0.867
392	21.50	-1.725	0.816
393	21.54	-1.931	0.708
394	21.58	-1.730	0.712
395	21.63	-1.580	0.711
396	21.67	-1.740	0.743
397	21.72	-1.542	0.806
398	21.76	-1.570	0.706
399	21.81	-1.672	0.785
400	21.85	-1.643	0.499
401	hiatus	-1.436	0.743
402	hiatus	-1.589	0.840
403	hiatus	-1.597	0.761
404	hiatus	-1.701	0.700
405	hiatus	-1.696	0.759
406	hiatus	-1.398	0.720
407	hiatus	-1.766	0.647
408	hiatus	-1.702	0.628
409	hiatus	-1.675	0.568
410	hiatus	-2.018	0.635
411	hiatus	-1.757	0.946
412	hiatus	-1.910	0.713
413	hiatus	-2.003	0.580
414	hiatus	-1.733	0.745
415	hiatus	-1.900	0.821
416	hiatus	-1.880	0.879
417	hiatus	-2.017	0.708
418	hiatus	-1.943	0.731
419	hiatus	-1.997	0.779
420	hiatus	-1.940	0.729
421	27.23	-1.776	0.751
422	27.49	-1.873	0.821
423	27.74	-2.181	0.800
424	28.00	-2.111	0.777
425	28.26	-1.861	0.643
426	28.51	-2.106	0.697
427	28.77	-1.724	0.711
428	29.03	-2.002	0.690
429	29.28	-1.959	0.771
430	29.54	-1.878	0.836
431	29.79	-1.916	0.788
432	30.05	-2.037	0.881
433	30.31	-2.052	0.926
434	30.56	-1.983	0.931
435	30.82	-1.780	0.762
436	31.08	-1.775	0.775
437	31.33	-1.919	0.734
438	31.59	-1.829	0.866
439	31.84	-1.969	0.818
440	32.10	-1.941	0.964
441	32.16	-1.881	0.771
442	32.23	-2.036	1.132
443	32.29	-1.699	0.590
444	32.36	-1.875	0.719
445	32.42	-1.885	0.746
446	32.49	-1.920	0.806
447	32.55	-2.016	0.815
448	32.62	-2.045	0.936
449	32.68	-1.906	0.915
450	32.75	-1.935	0.788
451	32.81	-2.162	0.724
452	32.88	-1.884	0.775
453	32.94	-2.215	0.954
454	33.01	-2.019	0.796
455	33.07	-2.134	0.655
456	33.14	-2.116	0.890
457	33.20	-2.174	0.758
458	33.27	-2.084	0.769
459	33.33	-1.860	0.803

Depth (cm)	Age[$] (kyr)	$\delta^{18}O$ (G.rub)[‡] (‰)	$\delta^{13}C$ (G.rub)[‡] (‰)
460	33.40	-1.988	0.938
461	33.46	-2.219	0.613
462	33.53	-2.228	0.867
463	33.59	-2.025	0.702
464	33.66	-2.329	0.858
465	33.72	-2.066	0.645
466	33.79	-2.081	0.878
467	33.85	-1.781	0.703
468	33.92	-2.037	0.904
469	33.98	-2.057	0.890
470	34.05	-1.944	0.934
471	34.11	-2.186	0.856
472	34.18	-2.020	0.792
473	34.24	-2.043	0.681
474	34.31	-1.975	0.841
475	34.37	-2.000	0.809
476	34.44	-1.855	0.721
477	34.50	-1.857	0.779
478	34.57	-2.024	0.651
479	34.63	-2.169	0.833
480	34.70	-1.862	0.764
481	34.76	-1.847	0.793
482	34.83	-1.925	0.702
483	34.89	-1.922	0.803
484	34.96	-2.128	0.882
485	35.02	-2.026	0.902
486	35.09	-1.922	0.873
487	35.15	-2.019	0.848
488	35.26	-2.083	0.718
489	35.37	-2.220	0.787
490	35.48	-1.884	0.870
491	35.59	-2.011	0.749
492	35.70	-2.144	0.610
493	35.81	-2.040	0.607
494	35.92	-2.021	0.894
495	36.03	-1.942	0.800
496	36.14	-2.209	0.739
497	36.25	-2.033	0.748
498	36.36	-1.896	0.834
499	36.47	-2.069	0.471
500	36.58	-1.814	0.673
501	36.69	-1.780	0.534
502	36.80	-2.041	0.683
503	36.91	-1.889	0.738
504	37.02	-2.076	0.842
505	37.13	-2.072	0.789
506	37.24	-2.203	0.766
507	37.30	-2.292	0.785
508	37.31	-2.181	0.758
509	37.33	-1.916	0.700
510	37.35	-1.884	0.680
511	37.36	-2.000	0.791
512	37.38	-2.207	0.779
513	37.40	-2.009	0.794
514	37.41	-1.881	0.763
515	37.43	-2.083	0.996
516	37.45	-1.912	0.841
517	37.46	-1.954	0.861
518	37.48	-1.802	0.788
519	37.50	-1.883	0.850
520	37.51	-1.959	0.767
521	37.53	-1.711	0.854
522	37.55	-1.709	0.884
523	37.56	-1.798	0.654
524	37.58	-1.812	0.961
525	37.60	-1.842	0.587
526	37.61	-1.480	0.703
527	37.63	-1.635	0.851
528	37.65	-1.735	0.785
529	37.66	-1.481	0.853
530	37.68	-1.809	0.864
531	37.69	-1.510	0.764
532	37.71	-1.515	0.856
533	37.73	-1.735	0.922
534	37.74	-1.538	0.672
535	37.76	-1.636	0.754
536	37.78	-1.546	0.785
537	37.79	-1.738	0.798
538	37.81	-1.452	0.691
539	37.83	-1.495	0.593
540	37.84	-1.632	0.842
541	37.86	-1.705	0.647
542	37.88	-1.471	0.830
543	37.89	-1.467	0.761
544	37.98	-1.486	0.776
545	38.07	-1.615	0.956
546	38.16	-1.678	0.821
547	38.25	-1.912	0.927
548	38.34	-1.638	0.877
549	38.43	-1.765	0.633
550	38.52	-1.822	1.065
551	38.61	-1.808	0.714

Depth (cm)	Age[$] (kyr)	$\delta^{18}O$ (G.rub)[‡] (‰)	$\delta^{13}C$ (G.rub)[‡] (‰)	Depth (cm)	Age[$] (kyr)	$\delta^{18}O$ (G.rub)[‡] (‰)	$\delta^{13}C$ (G.rub)[‡] (‰)
552	38.70	-1.986	0.836	598	41.36	-1.675	0.716
553	38.79	-2.146	0.706	599	41.42	-2.259	0.964
554	38.85	-1.908	0.721	600	41.48	-1.947	0.946
555	38.90	-1.887	0.898	601	41.54	-2.075	0.888
556	38.96	-2.017	0.870	602	41.59	-2.146	0.914
557	39.02	-1.842	0.900	603	41.65	-2.024	0.843
558	39.08	-2.062	0.853	604	41.71	-2.001	0.789
559	39.13	-1.978	0.894	605	41.77	-2.028	0.685
560	39.19	-2.086	0.831	606	41.82	-2.229	0.902
561	39.25	-1.826	0.861	607	41.88	-1.916	0.579
562	39.30	-1.960	0.753	608	41.94	-1.895	0.689
563	39.36	-1.896	0.822	609	42.00	-2.035	0.859
564	39.42	-1.922	0.752	610	42.05	-1.940	0.880
565	39.48	-1.897	0.780	611	42.11	-2.060	0.963
566	39.53	-1.863	0.709	612	42.17	-2.077	0.797
567	39.59	-1.864	0.870	613	42.23	-2.166	0.797
568	39.65	-1.924	0.978	614	42.28	-2.301	0.847
569	39.70	-1.981	0.878	615	42.34	-2.061	0.906
570	39.76	-2.197	0.926	616	42.40	-2.079	0.930
571	39.82	-1.900	0.830	617	42.46	-1.855	0.663
572	39.88	-1.898	0.811	618	42.51	-2.055	0.813
573	39.93	-1.983	0.999	619	42.57	-1.980	1.006
574	39.99	-1.755	0.844	620	42.63	-1.990	0.779
575	40.05	-1.945	0.914	621	42.69	-1.793	0.603
576	40.10	-1.979	0.873	622	42.74	-1.932	0.843
577	40.16	-1.957	1.140	623	42.80	-1.903	0.833
578	40.22	-2.100	0.937	624	42.86	-2.025	0.814
579	40.28	-2.150	0.770	625	42.92	-1.995	0.880
580	40.33	-1.986	0.795	626	42.97	-1.886	0.867
581	40.39	-1.878	0.917	627	43.03	-1.791	0.885
582	40.45	-1.986	0.892	628	43.09	-1.727	0.586
583	40.51	-1.814	0.921	629	43.15	-1.757	0.855
584	40.56	-1.939	0.871	630	43.20	-1.812	0.775
585	40.62	-1.924	0.861	631	43.26	-1.991	0.750
586	40.68	-1.900	0.762	632	43.32	-1.801	0.677
587	40.73	-2.085	0.704	633	43.37	-1.938	0.759
588	40.79	-2.033	0.951	634	43.43	-1.888	0.858
589	40.85	-1.899	0.506	635	43.49	-2.025	0.796
590	40.91	-1.871	0.842	636	43.55	-1.940	0.838
591	40.96	-2.029	0.916	637	43.60	-1.990	0.732
592	41.02	-1.899	0.865	638	43.66	-1.864	0.894
593	41.08	-1.818	0.928	639	43.72	-1.947	0.803
594	41.13	-1.715	0.661	640	43.78	-1.933	0.842
595	41.19	-1.883	0.949	641	43.83	-1.937	0.910
596	41.25	-2.038	0.831	642	43.89	-1.995	0.445
597	41.31	-2.034	0.963	643	43.95	-1.945	0.770

Depth (cm)	Age[$] (kyr)	$\delta^{18}O$ (G.rub)[‡] (‰)	$\delta^{13}C$ (G.rub)[‡] (‰)
644	44.01	-1.963	0.906
645	44.06	-1.924	0.837
646	44.12	-2.258	0.888
647	44.18	-2.029	0.719
648	44.24	-2.062	0.794
649	44.29	-2.054	0.591
650	44.35	-2.137	0.857
651	44.41	-2.148	0.684
652	44.47	-1.927	0.669
653	44.52	-2.166	0.946
654	44.58	-1.973	0.642
655	44.64	-2.186	0.835
656	44.70	-2.355	0.636
657	44.75	-2.336	0.896
658	44.81	-2.167	0.673
659	44.87	-1.970	0.839
660	44.93	-2.135	0.772
661	44.98	-2.210	0.617
673	45.04	-2.272	0.816
674	45.10	-2.278	0.809
675	45.16	-2.041	0.684
676	45.21	-2.284	0.878
677	45.27	-2.310	0.610
678	45.33	-2.286	0.751
679	45.39	-2.092	0.687
680	45.44	-2.193	0.799
681	45.50	-2.303	0.901
682	45.56	-2.030	0.755
683	45.62	-2.166	0.722
684	45.67	-2.251	0.754
685	45.73	-2.273	0.666
686	45.79	-2.346	0.728
687	45.85	-2.241	0.944
688	45.90	-2.100	0.848
689	45.96	-2.069	0.796
690	46.02	-1.963	0.739
691	46.08	-2.107	0.748
692	46.13	-1.913	0.939
693	46.19	-1.934	0.754
694	46.25	-1.778	0.616
695	46.31	-2.276	0.827
696	46.36	-1.957	0.714
697	46.42	-1.997	0.751
698	46.48	-1.821	0.739
699	46.54	-2.060	0.690
700	46.59	-2.107	0.706
701	46.65	-2.077	0.776
702	46.71	-1.757	0.867
703	46.76	-1.866	0.627
704	46.82	-1.865	0.692
705	46.88	-1.845	0.982
706	46.94	-1.919	0.898
707	46.99	-2.018	0.819
708	47.05	-1.849	0.794
709	47.11	-2.023	0.679
710	47.17	-1.677	0.756
711	47.22	-1.838	0.567
712	47.28	-2.048	0.713
713	47.34	-2.012	0.973
714	47.40	-1.896	0.593
715	47.45	-1.995	0.775
716	47.51	-1.997	0.882
717	47.57	-1.783	0.734
718	47.63	-1.726	0.690
719	47.68	-1.940	1.014
720	47.74	-1.992	0.903
721	47.80	-2.146	0.906
722	47.86	-2.062	0.651
723	47.91	-2.118	0.651
724	47.97	-2.189	0.886
725	48.03	-1.958	0.893
726	48.09	-1.963	0.624
727	48.14	-2.005	0.816
728	48.20	-1.933	0.774
729	48.26	-2.158	0.822
730	48.32	-2.016	0.839
731	48.37	-1.984	0.748
732	48.43	-1.862	0.689
733	48.49	-2.077	0.853
734	48.55	-2.291	0.814
735	48.60	-1.899	0.684
736	48.66	-2.153	0.824
737	48.72	-1.969	0.641
738	48.78	-2.329	0.778
739	48.83	-2.177	0.688
740	48.89	-2.143	0.831
741	48.95	-2.097	0.757
742	49.01	-2.172	0.869
743	49.06	-2.237	0.790
744	49.12	-2.284	0.771
745	49.18	-2.223	0.631
746	49.24	-2.268	0.827

Depth (cm)	Age[$] (kyr)	$\delta^{18}O$ (G.rub)[‡] (‰)	$\delta^{13}C$ (G.rub)[‡] (‰)	Depth (cm)	Age[$] (kyr)	$\delta^{18}O$ (G.rub)[‡] (‰)	$\delta^{13}C$ (G.rub)[‡] (‰)
747	49.29	-2.275	0.827	793	51.94	-2.303	0.652
748	49.35	-2.289	0.834	794	51.99	-2.185	0.490
749	49.41	-2.036	0.773	795	52.05	-1.870	0.572
750	49.47	-2.029	0.765	796	52.11	-2.269	0.583
751	49.52	-2.152	0.682	797	52.17	-2.352	0.652
752	49.58	-2.041	0.743	798	52.22	-2.092	0.612
753	49.64	-2.334	0.566	799	52.28	-2.196	0.613
754	49.70	-2.057	0.808	800	52.34	-2.050	0.566
755	49.75	-2.462	0.715	801	52.40	-1.893	0.440
756	49.81	-2.476	0.800	802	52.45	-2.316	0.437
757	49.87	-2.250	0.714	803	52.51	-2.347	0.638
758	49.93	-2.241	0.718	804	52.57	-2.372	0.578
759	49.98	-2.394	0.708	805	52.63	-1.907	0.478
760	50.04	-2.110	0.696	806	52.68	-1.912	0.378
761	50.10	-2.153	0.729	807	52.74	-2.217	0.547
762	50.15	-2.205	0.766	808	52.80	-2.332	0.314
763	50.21	-2.238	0.677	809	52.86	-1.947	0.440
764	50.27	-2.412	0.718	810	52.91	-1.884	0.423
765	50.33	-2.274	0.830	811	52.97	-1.843	0.501
766	50.38	-2.143	0.700	812	53.03	-1.968	0.464
767	50.44	-2.217	0.690	813	53.09	-1.795	0.343
768	50.50	-2.067	0.649	814	53.14	-1.795	0.389
769	50.56	-2.209	0.858	815	53.20	-1.638	0.194
770	50.61	-2.172	0.481	816	53.26	-1.533	0.439
771	50.67	-2.429	0.533	817	53.32	-2.147	0.482
772	50.73	-2.223	0.697	818	53.37	-1.999	0.565
773	50.79	-2.307	0.832	819	53.43	-1.666	0.339
774	50.84	-2.400	0.868	820	53.49	-1.978	0.312
775	50.90	-2.059	0.822	821	53.55	-1.981	0.463
776	50.96	-2.279	0.764	822	53.60	-1.807	0.592
777	51.02	-2.440	0.766	823	53.66	-1.796	0.381
778	51.07	-2.304	0.800	824	53.72	-1.659	0.306
779	51.13	-2.348	0.755	825	53.77	-1.689	0.478
780	51.19	-2.311	0.575	826	53.83	-1.797	0.195
781	51.25	-2.234	0.704	827	53.89	-1.653	0.371
782	51.30	-2.251	0.743	828	53.95	-1.846	0.299
783	51.36	-2.405	0.578	829	54.00	-1.980	0.553
784	51.42	-1.948	0.584	830	54.06	-1.710	0.406
785	51.48	-2.114	0.702	831	54.12	-1.769	0.290
786	51.53	-2.009	0.560	832	54.18	-1.861	0.446
787	51.59	-2.092	0.415	833	54.23	-1.721	0.321
788	51.65	-2.088	0.815	834	54.29	-1.897	0.524
789	51.71	-2.217	0.686	835	54.35	-1.757	0.367
790	51.76	-2.118	0.560	836	54.41	-1.815	0.431
791	51.82	-2.081	0.561	837	54.46	-1.877	0.530
792	51.88	-2.213	0.419	838	54.52	-1.741	0.482

Depth (cm)	Age[$] (kyr)	$\delta^{18}O$ (G.rub)[‡] (‰)	$\delta^{13}C$ (G.rub)[‡] (‰)	Depth (cm)	Age[$] (kyr)	$\delta^{18}O$ (G.rub)[‡] (‰)	$\delta^{13}C$ (G.rub)[‡] (‰)
839	54.58	-2.229	0.728	885	57.22	-2.179	0.428
840	54.64	-2.131	0.374	886	57.28	-2.042	0.658
841	54.69	-2.185	0.415	887	57.34	-2.080	0.161
842	54.75	-2.541	0.760	888	57.39	-2.143	0.553
843	54.81	-2.402	0.637	889	57.45	-2.160	0.490
844	54.87	-2.389	0.618	890	57.51	-1.991	0.516
845	54.92	-2.182	0.541	891	57.57	-2.244	0.646
846	54.98	-2.437	0.650	892	57.62	-2.456	0.394
847	55.04	-2.400	0.637	893	57.68	-2.409	0.482
848	55.10	-2.550	0.470	894	57.74	-2.221	0.337
849	55.15	-2.472	0.569	895	57.80	-2.215	0.604
850	55.21	-2.201	0.606	896	57.85	-2.028	0.481
851	55.27	-2.402	0.624	897	57.91	-2.195	0.520
852	55.33	-2.298	0.443	898	57.97	-2.381	0.527
853	55.38	-2.242	0.497	899	58.03	-2.306	0.532
854	55.44	-2.455	0.577	900	58.08	-2.227	0.500
855	55.50	-2.551	0.743	901	58.14	-2.468	0.476
856	55.56	-2.273	0.566	902	58.20	-2.209	0.388
857	55.61	-2.337	0.802	903	58.26	-2.277	0.361
858	55.67	-2.295	0.472	904	58.31	-2.205	0.571
859	55.73	-2.082	0.662	905	58.37	-2.315	0.516
860	55.79	-1.941	0.679	906	58.43	-2.402	0.350
861	55.84	-2.432	0.456	907	58.49	-2.165	0.310
862	55.90	-2.251	0.928	908	58.54	-2.099	0.594
863	55.96	-2.167	0.650	909	58.60	-2.223	0.335
864	56.02	-2.392	0.720	910	58.66	-2.253	0.473
865	56.07	-2.159	0.445	911	58.72	-2.367	0.495
866	56.13	-2.141	0.560	912	58.77	-2.313	0.556
867	56.19	-2.202	0.482	913	58.83	-2.054	0.561
868	56.25	-1.973	0.742	914	58.89	-2.249	0.564
869	56.30	-1.959	0.752	915	58.95	-2.201	0.432
870	56.36	-1.980	0.693	916	59.00	-2.028	0.490
871	56.42	-2.257	0.512	917	59.06	-2.129	0.365
872	56.48	-1.982	0.606	918	59.12	-2.104	0.489
873	56.53	-2.179	0.258	919	59.18	-1.816	0.425
874	56.59	-2.179	0.589	920	59.23	-1.922	0.392
875	56.65	-2.112	0.649	921	59.29	-2.291	0.555
876	56.71	-2.031	0.645	922	59.35	-2.113	0.510
877	56.76	-2.044	0.545	923	59.41	-2.011	0.427
878	56.82	-1.913	0.476	924	59.46	-2.268	0.451
879	56.88	-2.008	0.664	925	59.52	-2.347	0.389
880	56.94	-2.032	0.585	926	59.58	-2.439	0.453
881	56.99	-1.868	0.699	927	59.64	-2.184	0.425
882	57.05	-1.955	0.404	928	59.69	-2.061	0.510
883	57.11	-2.055	0.451	929	59.75	-2.225	0.513
884	57.16	-2.151	0.510	930	59.81	-2.053	0.391

Depth (cm)	Age[$] (kyr)	$\delta^{18}O$ (G.rub)[‡] (‰)	$\delta^{13}C$ (G.rub)[‡] (‰)
931	59.87	-2.037	0.656
932	59.92	-2.180	0.540
936	60.15	-1.940	0.435
940	60.38	-1.818	0.271
941	60.44	-1.909	0.387
942	60.58	-1.882	0.336
943	60.73	-1.986	0.618
944	60.87	-1.885	0.468
945	61.01	-1.536	0.360
946	61.15	-1.627	0.457
947	61.30	-1.540	0.345
948	61.44	-1.495	0.334
949	61.58	-1.644	0.447
950	61.72	-1.686	0.388
951	61.87	-1.495	0.382
952	62.01	-1.593	0.451
953	62.15	-1.429	0.305
954	62.29	-1.558	0.513
955	62.44	-1.790	0.087
956	62.58	-1.758	0.409
957	62.72	-1.926	0.442
958	62.86	-1.651	0.363
959	63.01	-1.850	0.526
960	63.15	-1.772	0.374
961	63.29	-1.825	0.558
962	63.43	-1.659	0.369
963	63.58	-1.672	0.691
964	63.72	-1.683	0.355
965	63.86	-1.754	0.436
966	64.00	-1.621	0.739
967	64.15	-1.834	0.545
968	64.29	-1.535	0.613
969	64.43	-1.588	0.438
970	64.57	-1.692	0.516
971	64.72	-1.604	0.405
972	64.86	-1.864	0.558
973	65.00	-1.675	0.518
974	65.20	-1.738	0.563
975	65.40	-1.712	0.519
976	65.60	-1.698	0.314
977	65.80	-1.520	0.646
978	66.00	-1.810	0.654
979	66.20	-1.659	0.388
980	66.40	-1.818	0.563
981	66.60	-1.863	0.533
982	66.80	-1.904	0.641
983	67.00	-1.777	0.640
984	67.20	-1.784	0.609
985	67.40	-1.600	0.656
986	67.60	-1.760	0.441
987	67.80	-1.816	0.472
988	68.00	-1.782	0.664
989	68.20	-1.788	0.649
990	68.40	-1.987	0.621
991	68.60	-1.805	0.627
992	68.80	-1.789	0.671
993	69.00	-1.708	0.479
994	69.20	-1.612	0.760
995	69.40	-1.762	0.632
996	69.60	-1.571	0.676
997	69.80	-1.599	0.760
998	70.00	-1.831	0.459
999	70.20	-1.830	0.545
1000	70.40	-1.769	0.685
1001	70.60	-1.757	0.639
1002	70.80	-1.560	0.650
1003	71.00	-1.654	0.631
1004	71.20	-1.469	0.851
1005	71.40	-1.701	0.375
1006	71.60	-2.053	0.643
1007	71.80	-1.776	0.797
1008	72.00	-1.977	0.493
1009	72.20	-1.864	0.691
1010	72.40	-1.851	0.452
1011	72.60	-1.830	0.609
1012	72.80	-1.669	0.801
1013	73.00	-1.942	0.642
1014	73.20	-1.741	0.583
1015	73.40	-1.710	0.446
1016	73.60	-1.815	0.460
1017	73.80	-1.888	0.687
1018	74.00	-1.914	0.741
1019	74.20	-2.194	0.576
1020	74.40	-1.930	0.512
1021	74.60	-1.807	0.648
1022	74.80	-2.147	0.865
1023	75.00	-1.999	1.016
1024	75.20	-2.142	0.651
1025	75.40	-2.273	0.906
1026	75.60	-2.153	0.956
1027	75.80	-2.206	0.790
1028	76.00	-2.192	0.832

Depth (cm)	Age[$] (kyr)	$\delta^{18}O$ (G.rub)[‡] (‰)	$\delta^{13}C$ (G.rub)[‡] (‰)
1029	76.20	-1.899	0.661
1030	76.40	-1.920	0.699
1031	76.60	-2.220	0.937
1032	76.80	-2.022	1.156
1033	77.00	-2.111	1.067
1034	77.20	-2.052	0.869
1035	77.40	-2.715	0.841
1036	77.60	-2.545	0.662
1037	77.80	-2.338	1.180
1038	78.00	-2.443	0.775
1039	78.10	-1.989	0.785
1040	78.21	-1.990	0.672
1041	78.31	-1.975	0.814
1042	78.42	-2.329	0.715
1043	78.52	-2.165	0.828
1044	78.62	-2.338	0.850
1045	78.73	-2.400	0.987
1046	78.83	-2.087	0.677
1047	78.94	-2.524	0.798
1048	79.04	-2.374	0.907
1049	79.14	-2.254	0.698
1050	79.25	-2.231	0.813
1051	79.35	-2.234	0.681
1052	79.46	-2.268	0.920
1053	79.56	-2.279	0.762
1054	79.66	-2.203	1.073
1055	79.77	-2.107	0.805
1056	79.87	-2.240	0.953
1057	79.98	-2.150	0.732
1058	80.08	-2.171	1.036
1059	80.18	-2.112	1.036
1060	80.29	-2.293	0.776
1061	80.39	-2.010	0.855
1062	80.50	-2.415	0.869
1063	80.60	-2.169	0.840
1064	80.70	-2.377	0.809
1065	80.81	-2.302	1.011
1066	80.91	-2.235	0.957
1067	81.01	-2.326	0.790
1068	81.12	-2.425	0.855
1069	81.22	-2.217	0.813
1070	81.33	-2.123	0.825
1071	81.43	-2.041	0.644
1072	81.53	-2.102	0.767
1073	81.64	-2.118	0.893
1074	81.74	-2.198	0.608
1075	81.85	-2.019	0.777
1076	81.95	-1.970	0.630
1077	82.05	-2.118	0.995
1078	82.16	-1.838	0.787
1079	82.26	-2.249	0.885
1080	82.37	-2.149	0.904
1081	82.47	-2.318	0.495
1082	82.57	-1.952	0.795
1083	82.68	-2.009	0.883
1084	82.78	-2.113	0.733
1085	82.89	-2.250	0.781
1086	82.99	-1.939	0.903
1087	83.09	-2.116	0.647
1088	83.20	-1.819	0.670
1089	83.30	-1.948	0.768
1090	83.41	-1.792	0.579
1091	83.51	-1.862	0.802
1092	83.61	-2.084	0.710
1093	83.72	-2.193	0.857
1094	83.82	-2.128	0.724
1095	83.93	-2.031	0.768
1096	84.03	-1.954	0.922
1097	84.13	-2.019	0.798
1098	84.24	-2.219	0.838
1099	84.34	-2.132	0.696
1100	84.45	-2.073	0.705
1101	84.55	-2.037	0.761
1102	84.65	-2.043	0.805
1103	84.76	-2.058	0.829
1104	84.86	-1.893	0.538
1105	84.97	-2.078	0.696
1106	85.07	-1.937	0.641
1107	85.17	-1.968	0.730
1108	85.28	-1.927	0.741
1109	85.38	-2.233	0.836
1110	85.49	-2.041	0.856
1111	85.59	-1.882	1.143
1112	85.69	-2.000	0.738
1113	85.80	-2.064	0.810
1114	85.90	-1.953	0.941
1115	86.00	-1.937	0.428
1116	86.11	-2.027	0.757
1117	86.21	-1.959	0.837
1118	86.32	-1.808	0.885
1119	86.42	-2.155	0.929
1120	86.52	-1.878	0.553

Depth (cm)	Age[$] (kyr)	$\delta^{18}O$ (G.rub)[‡] (‰)	$\delta^{13}C$ (G.rub)[‡] (‰)
1121	86.63	-2.128	0.737
1122	86.73	-1.782	0.758
1123	86.84	-1.996	0.834
1124	86.94	-1.943	0.717
1125	87.04	-1.913	0.870
1126	87.15	-2.015	0.663
1127	87.25	-1.952	0.895
1128	87.36	-1.913	0.842
1129	87.46	-1.970	0.726
1130	87.56	-2.127	0.858
1131	87.67	-2.094	0.843
1132	87.77	-2.064	0.773
1133	87.88	-2.168	0.927
1134	87.98	-1.891	0.799
1135	88.08	-2.134	0.872
1136	88.19	-1.950	0.814
1137	88.29	-2.025	0.873
1138	88.40	-1.980	0.942
1139	88.50	-2.321	1.000
1140	88.60	-2.055	0.795
1141	88.71	-2.130	0.787
1142	88.81	-2.149	0.899
1143	88.92	-1.867	0.782
1144	89.02	-1.834	0.906
1145	89.12	-1.953	0.742
1146	89.23	-2.065	0.798
1147	89.33	-2.112	0.667
1148	89.44	-2.256	0.634
1149	89.54	-2.098	0.662
1150	89.64	-2.119	0.726
1151	89.75	-1.895	0.711
1152	89.85	-2.022	0.761
1153	89.96	-1.872	0.745
1154	90.06	-1.975	0.819
1155	90.16	-2.081	0.693
1156	90.27	-2.360	0.785
1157	90.37	-1.811	0.596
1158	90.48	-2.172	0.823
1159	90.58	-2.442	0.705
1160	90.68	-2.336	0.735
1161	90.79	-2.256	0.591
1162	90.89	-1.969	0.918
1163	91.00	-2.219	0.889
1164	91.10	-2.321	0.784
1165	91.20	-2.038	0.259
1166	91.31	-2.134	0.950
1167	91.41	-1.914	0.767
1168	91.51	-2.046	0.714
1169	91.62	-1.925	0.737
1170	91.72	-2.150	0.687
1171	91.83	-2.140	0.921
1172	91.93	-2.125	0.862
1173	92.03	-1.734	0.909
1174	92.14	-1.827	0.878
1175	92.24	-1.945	0.865
1176	92.35	-1.918	0.896
1177	92.45	-2.178	0.814
1178	92.55	-2.001	0.685
1179	92.66	-1.876	0.618
1180	92.76	-2.314	0.809
1181	92.87	-2.060	0.758
1182	92.97	-2.131	0.857
1183	93.07	-2.404	0.903
1184	93.18	-2.441	0.706
1185	93.28	-2.134	0.782
1186	93.39	-2.031	0.716
1187	93.49	-2.065	0.570
1188	93.59	-2.512	0.772
1189	93.70	-2.239	0.679
1190	93.80	-2.648	0.916
1191	93.91	-2.443	0.514
1192	94.01	-2.317	0.853
1193	94.11	-2.270	0.803
1194	94.22	-2.262	0.822
1195	94.32	-2.178	0.811
1196	94.43	-1.991	0.644
1197	94.53	-2.027	0.800
1198	94.63	-1.908	0.809
1199	94.74	-2.032	0.774
1200	94.84	-1.619	0.750
1201	94.95	-1.680	0.549
1202	95.05	-1.672	0.676
1203	95.15	-1.637	0.739
1204	95.26	-1.415	1.016
1205	95.36	-1.980	0.849
1206	95.47	-1.346	0.959
1207	95.57	-1.195	1.204
1208	95.67	-1.702	0.581
1209	95.78	-1.917	0.773
1210	95.88	-2.189	0.987
1211	95.99	-2.130	0.907
1212	96.09	-2.178	1.036

Depth (cm)	Age[$] (kyr)	$\delta^{18}O$ (G.rub)[‡] (‰)	$\delta^{13}C$ (G.rub)[‡] (‰)
1213	96.19	-2.313	1.291
1214	96.30	-2.245	1.065
1215	96.40	-1.854	1.092
1216	96.50	-2.099	0.824
1217	96.61	-2.188	0.900
1218	96.71	-2.318	1.063
1219	96.82	-1.918	1.070
1220	96.92	-2.270	1.071
1221	97.02	-2.380	1.080
1222	97.13	-2.259	0.865
1223	97.23	-2.004	1.030
1224	97.34	-2.104	1.013
1225	97.44	-2.188	0.896
1254	97.54	-2.245	1.048
1255	97.65	-1.785	1.016
1256	97.75	-1.893	0.676
1257	97.86	-1.895	0.755
1258	97.96	-2.041	0.832
1259	98.06	-1.884	0.767
1260	98.17	-2.178	0.946
1261	98.27	-2.240	0.763
1262	98.38	-2.006	1.021
1263	98.48	-2.059	0.757
1264	98.58	-2.242	0.988
1265	98.69	-2.198	0.866
1266	98.79	-2.310	0.989
1267	98.90	-2.456	1.045
1268	99.00	-2.341	0.992
1269	99.08	-2.448	1.078
1270	99.17	-2.433	0.830
1271	99.25	-2.435	1.110
1272	99.33	-2.661	0.923
1273	99.41	-2.646	1.070
1274	99.50	-2.254	0.782
1275	99.58	-2.297	0.878
1276	99.66	-2.331	0.983
1277	99.74	-2.280	0.868
1278	99.83	-2.576	0.871
1279	99.91	-2.343	1.010
1280	99.99	-2.326	0.829
1281	100.07	-2.488	0.700
1282	100.16	-2.370	0.761
1283	100.24	-2.495	0.958
1284	100.32	-2.352	0.623
1285	100.40	-2.357	0.510
1286	100.49	-2.241	0.998
1287	100.57	-2.369	0.743
1288	100.65	-2.092	0.799
1289	100.74	-2.552	0.583
1290	100.82	-2.278	0.761
1291	100.90	-2.228	0.862
1292	100.98	-2.318	0.670
1293	101.07	-2.043	0.669
1294	101.15	-2.166	0.812
1295	101.23	-2.136	0.708
1296	101.31	-2.257	0.908
1297	101.40	-2.419	0.718
1298	101.48	-2.375	1.033
1299	101.56	-2.063	0.953
1300	101.64	-1.910	0.949
1301	101.73	-2.012	0.878
1302	101.81	-2.176	1.094
1303	101.89	-2.494	1.122
1304	101.97	-1.801	1.014
1305	102.06	-2.128	0.951
1306	102.14	-2.035	0.838
1307	102.22	-2.225	0.952
1308	102.30	-2.113	0.840
1309	102.39	-2.248	0.970
1310	102.47	-2.326	0.953
1311	102.55	-2.074	0.954
1312	102.64	-1.970	1.069
1313	102.72	-2.179	1.157
1314	102.80	-2.191	1.079
1315	102.88	-2.032	0.968
1316	102.97	-1.843	0.854
1317	103.05	-1.895	0.803
1318	103.13	-1.598	0.954
1319	103.21	-1.979	0.984
1320	103.30	-1.853	0.850
1321	103.38	-1.960	1.085
1322	103.46	-1.924	0.972
1323	103.54	-2.157	0.895
1324	103.63	-2.156	1.031
1325	103.71	-2.326	1.347
1326	103.79	-1.878	0.916
1327	103.87	-2.101	0.721
1328	103.96	-2.186	1.005
1329	104.04	-1.986	0.966
1330	104.12	-2.173	0.975
1331	104.21	-1.929	0.937
1332	104.29	-2.056	1.059

Depth (cm)	Age[$] (kyr)	$\delta^{18}O$ (G.rub)[‡] (‰)	$\delta^{13}C$ (G.rub)[‡] (‰)
1333	104.37	-2.063	0.822
1334	104.45	-1.986	0.997
1335	104.54	-2.038	0.752
1336	104.62	-2.068	0.975
1337	104.70	-1.940	1.077
1338	104.78	-2.229	1.078
1339	104.87	-2.331	0.905
1340	104.95	-2.152	0.834
1341	105.03	-2.248	0.998
1342	105.11	-2.299	1.015
1343	105.20	-2.396	0.845
1344	105.28	-2.045	0.725
1345	105.36	-2.402	1.084
1346	105.44	-2.429	0.931
1347	105.53	-2.503	0.955
1348	105.61	-2.525	1.107
1349	105.69	-2.108	0.885
1350	105.77	-2.263	0.807
1351	105.86	-1.936	1.013
1352	105.94	-2.376	0.946
1353	106.02	-2.290	0.865
1354	106.11	-2.184	1.011
1355	106.19	-2.071	0.776
1356	106.27	-2.022	0.644
1357	106.35	-2.055	0.622
1358	106.44	-1.974	0.783
1359	106.52	-2.242	0.856
1360	106.60	-2.227	0.845
1361	106.68	-2.014	0.767
1362	106.77	-2.088	0.648
1363	106.85	-1.931	0.858
1364	106.93	-2.205	0.733
1365	107.01	-1.980	1.026
1366	107.10	-2.164	0.697
1367	107.18	-2.200	0.777
1368	107.26	-2.173	0.860
1369	107.34	-2.254	0.865
1370	107.43	-2.325	0.783
1371	107.51	-1.963	0.732
1372	107.59	-2.095	0.878
1373	107.68	-2.177	0.792
1374	107.76	-2.253	0.950
1375	107.84	-2.215	0.900
1376	107.92	-2.345	0.863
1377	108.01	-2.122	0.763
1378	108.09	-2.254	0.999
1379	108.17	-2.243	0.608
1380	108.25	-2.349	1.023
1393	108.34	-2.115	0.744
1394	108.42	-2.143	0.735
1395	108.50	-2.392	0.933
1396	108.58	-2.353	0.746
1397	108.67	-2.188	0.847
1398	108.75	-1.928	0.863
1399	108.83	-2.352	0.995
1400	108.91	-2.392	0.710
1401	109.00	-2.448	0.816
1402	109.08	-2.160	0.992
1403	109.16	-2.124	0.849
1404	109.25	-2.340	0.672
1405	109.33	-2.258	0.985
1406	109.41	-2.280	0.823
1407	109.49	-2.336	0.805
1408	109.58	-2.165	0.886
1409	109.66	-2.266	1.083
1410	109.74	-2.340	0.805
1411	109.82	-2.329	0.725
1412	109.91	-2.195	0.839
1413	109.99	-2.298	0.793
1414	110.07	-2.264	0.960
1415	110.15	-2.075	0.866
1416	110.24	-2.335	0.886
1417	110.32	-2.122	1.143
1418	110.40	-2.329	0.992
1419	110.48	-2.161	1.040
1420	110.57	-1.964	0.919
1421	110.65	-2.060	0.885
1422	110.73	-2.149	0.951
1423	110.81	-2.212	0.997
1424	110.90	-2.190	1.208
1425	110.98	-2.240	0.787
1426	111.06	-2.322	0.849
1427	111.15	-2.229	0.823
1428	111.23	-2.117	0.818
1429	111.31	-1.945	0.820
1430	111.39	-2.287	0.632
1431	111.48	-1.972	0.821
1432	111.56	-2.387	0.638
1433	111.64	-2.315	0.739
1434	111.72	-2.184	0.661
1435	111.81	-1.950	0.670
1436	111.89	-2.108	0.925

Depth (cm)	Age[$] (kyr)	$\delta^{18}O$ (G.rub)[‡] (‰)	$\delta^{13}C$ (G.rub)[‡] (‰)
1437	111.97	-2.244	0.859
1438	112.05	-2.191	0.611
1439	112.14	-2.222	0.572
1440	112.22	-2.159	0.684
1441	112.30	-2.543	0.724
1442	112.38	-2.226	0.708
1443	112.47	-2.300	0.904
1444	112.55	-2.583	0.742
1445	112.63	-2.286	0.814
1446	112.72	-2.295	0.854
1447	112.80	-2.253	0.849
1448	112.88	-2.367	0.838
1449	112.96	-2.030	0.650
1450	113.05	-1.776	0.763
1451	113.13	-2.200	1.034
1452	113.21	-2.379	0.728
1453	113.29	-2.198	0.731
1454	113.38	-2.108	0.897
1455	113.46	-2.061	0.795
1456	113.54	-2.160	0.845
1457	113.62	-2.227	0.952
1458	113.71	-2.128	0.874
1459	113.79	-2.205	0.819
1460	113.87	-1.914	0.818
1461	113.95	-2.051	0.825
1462	114.04	-1.775	0.775
1463	114.12	-2.083	0.564
1464	114.20	-1.906	0.852
1465	114.28	-2.237	1.018
1466	114.37	-2.052	0.845
1467	114.45	-2.010	0.765
1468	114.53	-2.338	0.902
1469	114.62	-2.225	0.752
1470	114.70	-2.142	0.800
1471	114.78	-2.146	0.884
1472	114.86	-2.054	0.820
1473	114.95	-2.041	0.960
1474	115.03	-2.133	0.684
1475	115.11	-1.894	0.750
1476	115.19	-1.972	0.778
1477	115.28	-1.938	0.663
1478	115.36	-2.435	0.726
1479	115.44	-2.045	0.684
1480	115.52	-2.310	0.756
1481	115.61	-2.077	0.559
1482	115.69	-1.897	1.014
1483	115.77	-2.474	1.031
1484	115.85	-2.377	0.845
1485	115.94	-2.647	1.129
1486	116.02	-2.383	0.712
1487	116.10	-2.323	0.705
1488	116.19	-2.382	0.750
1489	116.27	-2.054	0.669
1490	116.35	-2.185	0.889
1491	116.43	-2.242	0.676
1492	116.52	-1.844	0.801
1493	116.60	-1.996	0.596
1494	116.68	-2.073	0.788
1495	116.76	-2.755	0.667
1498	117.01	-1.880	0.659
1499	117.09	-2.027	0.793
1500	117.18	-2.246	0.655
1501	117.26	-2.370	0.771
1502	117.34	-2.414	0.700
1503	117.42	-2.032	0.780
1504	117.51	-2.260	0.519
1505	117.59	-2.476	1.030
1506	117.67	-2.531	0.820
1507	117.75	-2.383	0.652
1508	117.84	-2.357	0.795
1510	118.00	-2.170	0.554
1511	118.09	-2.370	0.635
1516	118.50	-2.818	0.699
1519	118.75	-2.575	0.836
1520	118.83	-2.283	0.935
1521	118.91	-1.886	0.661
1522	118.99	-2.526	0.682
1523	119.08	-2.380	0.903
1524	119.16	-2.327	0.738
1525	119.24	-2.666	0.831
1526	119.32	-2.040	0.720
1527	119.41	-1.966	0.612
1528	119.49	-2.163	0.972
1529	--	not enough *G. ruber*	
1530	119.66	-2.215	0.870
1531	119.74	-2.042	0.710
1532	119.82	-2.157	0.818
1533	119.90	-2.560	0.724
1534	119.99	-2.273	0.675
1535	--	not enough *G. ruber*	
1536	--	-1.579	0.861
1537	120.23	-2.181	0.539

Depth (cm)	Age[$] (kyr)	$\delta^{18}O$ (G.rub)[‡] (‰)	$\delta^{13}C$ (G.rub)[‡] (‰)
1538	120.32	-1.965	0.473
1539	120.40	-2.127	0.684
1540	120.48	-2.475	0.635
1541	120.56	-2.169	0.696
1542	120.65	-2.439	0.840
1543	120.73	-2.553	0.730
1544	120.81	-2.459	0.969
1545	120.89	-2.469	0.628
1546	120.98	-2.311	0.790
1547	121.06	-2.304	0.698
1548	121.14	-2.294	0.991
1549	121.23	-2.168	1.094
1550	121.31	-2.605	0.842
1551	121.39	-2.234	0.761
1552	121.47	-2.361	1.020
1553	121.56	-2.667	0.891
1554	121.64	-2.741	0.728
1555	121.72	-2.794	0.869
1556	121.80	-2.721	0.802
1557	121.89	-2.660	0.991
1558	121.97	-2.654	0.999
1559	122.05	-2.819	0.888
1560	122.13	-2.622	0.837
1561	122.22	-2.641	0.865
1562	122.30	-2.596	1.022
1563	122.38	-2.637	0.698
1564	122.46	-2.743	0.983
1565	122.55	-2.740	0.925
1566	122.63	-2.698	0.937
1567	122.71	-2.727	0.765
1568	122.79	-2.735	0.888
1569	122.88	-2.754	0.876
1570	122.96	-2.696	0.597
1571	123.04	-2.704	0.985
1572	123.13	-2.679	0.919
1573	123.21	-2.752	1.004
1574	123.29	-2.700	0.883
1575	123.37	-2.546	0.984
1576	123.46	-2.789	0.944
1577	123.54	-2.625	1.037
1578	123.62	-2.665	0.556
1579	123.70	-2.716	0.621
1580	123.79	-2.633	0.582
1581	123.87	-2.517	0.780
1582	123.95	-2.729	0.772
1583	124.03	-2.752	0.752
1584	124.12	-2.765	0.785
1585	124.20	-3.019	0.877
1586	124.28	-2.865	0.707
1587	124.36	-2.646	0.579
1588	124.45	-2.650	0.691
1589	124.53	-2.416	0.676
1590	124.61	-2.734	0.693
1591	124.70	-2.734	0.690
1592	124.78	-2.695	0.828
1593	124.86	-2.916	0.783
1594	124.94	-2.678	0.773
1595	125.03	-2.789	0.548
1596	125.11	-2.776	0.689
1597	125.19	-2.773	0.561
1598	125.27	-2.785	0.620
1599	125.36	-2.807	0.487
1600	125.44	-2.630	0.545
1601	125.52	-2.782	0.662
1602	125.60	-2.386	0.422
1603	125.69	-2.647	0.586
1604	125.77	-2.663	0.724
1605	125.85	-2.587	0.725
1606	125.93	-2.607	0.608
1607	126.02	-2.480	0.140
1608	126.10	-2.467	0.426
1609	126.18	-2.436	0.479
1610	126.26	-2.586	0.432
1611	126.35	-2.480	0.513
1612	126.43	-2.319	0.495
1613	126.51	-2.123	0.423
1614	126.60	-2.252	0.252
1615	126.68	-2.129	0.478
1616	126.76	-2.276	0.335
1617	126.84	-2.182	0.400
1618	126.93	-2.203	0.461
1619	127.01	-2.204	0.298
1620	127.09	-2.227	0.334
1621	127.17	-2.204	0.248
1622	127.26	-2.129	0.294
1623	127.34	-2.127	0.245
1624	127.42	-2.298	0.094
1625	127.50	-2.338	0.554
1626	127.59	-2.474	0.115
1627	127.67	-2.341	0.224
1628	127.75	-2.373	0.368
1629	127.83	-2.269	0.265

Depth (cm)	Age[$] (kyr)	$\delta^{18}O$ (G.rub)[‡] (‰)	$\delta^{13}C$ (G.rub)[‡] (‰)
1630	127.92	-2.425	0.407
1631	128.00	-2.370	0.354
1632	128.11	-2.292	0.278
1633	128.22	-2.315	0.290
1634	128.33	-2.415	0.280
1635	128.44	-2.663	0.513
1636	128.55	-2.459	0.536
1637	128.66	-2.338	0.319
1638	128.77	-2.167	0.304
1639	128.88	-2.101	0.352
1640	128.99	-1.812	0.222
1642	129.21	-1.646	0.080
1643	129.32	-1.541	0.330
1644	129.42	-1.546	0.300
1645	129.53	-1.637	0.199
1646	129.64	-1.996	0.547
1647	129.75	-1.572	0.282
1648	129.86	-1.661	0.334
1649	129.97	-1.709	0.357
1650	130.08	-1.747	0.300
1651	130.19	-1.705	0.191
1652	130.30	-1.700	0.327
1653	130.41	-1.483	0.421
1654	130.52	-1.551	0.359
1655	130.63	-1.569	0.160
1656	130.74	-1.587	0.190
1657	130.85	-1.662	0.186
1658	130.96	-1.586	0.171
1659	131.07	-1.297	0.093
1660	131.18	-1.532	0.236
1661	131.29	-1.308	0.413
1662	131.40	-1.629	0.016
1663	131.51	-1.412	0.236
1664	131.62	-1.623	0.234
1665	131.73	-1.745	0.373
1666	131.84	-1.629	0.453
1667	131.95	-1.573	0.251
1668	132.05	-1.584	0.327
1669	132.16	-1.590	0.588
1670	132.27	-1.505	0.167
1671	132.38	-1.678	0.411
1672	132.49	-1.528	0.433
1673	132.60	-1.650	0.125
1674	132.71	-1.403	0.277
1675	132.82	-1.464	0.295
1676	132.93	-1.654	0.292
1677	133.04	-1.579	0.296
1678	133.15	-1.417	0.150
1679	133.26	-1.537	0.496
1680	133.37	-1.538	0.385
1681	133.48	-1.401	0.243
1682	133.59	-1.532	0.447
1683	133.70	-1.519	0.390
1684	133.81	-1.367	0.264
1685	133.92	-1.637	0.478
1686	134.03	-1.622	0.403
1687	134.14	-1.627	0.511
1688	134.25	-1.562	0.309
1689	134.36	-1.420	0.366
1690	134.47	-1.321	0.332
1691	134.58	-1.471	0.077
1692	134.68	-1.457	0.280
1693	134.79	-1.491	0.299
1694	134.90	-1.628	0.504
1695	135.01	-1.507	0.166
1696	135.12	-1.670	0.350
1697	135.23	-1.376	0.149
1698	135.34	-1.460	0.384
1699	135.45	-1.462	0.365
1700	135.56	-1.627	0.543
1701	135.67	-1.470	0.129
1702	135.78	-1.379	0.581
1703	135.89	-1.764	0.301
1704	136.00	-1.577	0.380
1705	136.11	-1.466	0.464
1706	136.22	-1.654	0.484
1707	136.33	-1.311	0.269
1708	136.44	-1.321	0.251
1709	136.55	-1.677	0.357
1710	136.66	-1.512	0.406
1711	136.77	-1.653	0.527
1712	136.88	-1.688	0.428
1713	136.99	-1.547	0.526
1714	137.10	-1.732	0.478
1715	137.21	-1.557	0.514
1716	137.32	-1.745	0.378
1717	137.42	-1.954	0.490
1718	137.53	-1.930	0.447
1719	137.64	-1.731	0.526
1720	137.75	-1.647	0.412
1721	137.86	-1.721	0.446
1722	137.97	-1.537	0.354

Depth (cm)	Age[$] (kyr)	$\delta^{18}O$ (G.rub)[‡] (‰)	$\delta^{13}C$ (G.rub)[‡] (‰)
1723	138.08	-1.739	361.000
1724	138.19	-1.722	0.267
1725	138.30	-1.686	0.362
1726	138.41	-1.634	0.331
1727	138.52	-1.792	0.403
1728	138.63	-1.520	0.463
1729	138.74	-1.767	0.466
1730	138.85	-1.630	0.411
1731	138.96	-1.440	0.273
1732	139.07	-1.459	0.345
1733	139.18	-1.312	0.277
1734	139.29	-1.584	0.397
1735	139.40	-1.661	0.439
1736	139.51	-1.490	0.360
1737	139.62	-1.670	0.206
1738	139.73	-1.525	0.238
1739	139.84	-1.445	0.222
1740	139.95	-1.273	0.286
1741	140.05	-1.251	0.115
1742	140.16	-1.426	0.438
1743	140.27	-1.397	0.353
1744	140.38	-1.156	0.454
1745	140.49	-1.461	0.387
1746	140.60	-1.534	0.674
1747	140.71	-1.706	0.459
1748	140.82	-1.558	0.486
1749	140.93	-1.619	0.483
1750	141.04	-1.714	0.440
1751	141.15	-1.672	0.456
1752	141.26	-1.520	0.425
1753	141.37	-1.235	0.549
1754	141.48	-1.517	0.363
1755	141.59	-1.387	0.378
1756	141.70	-1.514	0.609
1757	141.81	-1.165	0.631
1758	141.92	-1.311	0.531
1759	142.03	-1.090	0.437
1760	142.14	-1.293	0.457
1761	142.25	-1.285	0.438
1762	142.36	-1.095	0.280
1763	142.47	-1.276	0.489
1764	142.58	-1.267	0.445
1765	142.68	-1.469	0.279
1766	142.79	-1.328	0.317
1767	142.90	-1.611	0.394
1768	143.01	-1.861	0.605
1769	143.12	-1.697	0.456
1770	143.23	-1.614	0.369
1771	143.34	-1.381	0.365
1772	143.45	-1.575	0.400
1773	143.56	-1.641	0.455
1774	143.67	-1.683	0.371
1775	143.78	-1.492	0.440
1776	143.89	-1.608	0.536
1777	144.00	-1.761	0.559
1778	144.11	-1.753	0.486
1779	144.21	-1.841	0.705
1780	144.32	-1.660	0.338
1781	144.42	-1.427	0.555
1782	144.53	-1.681	0.579
1783	144.64	-1.757	0.368
1784	144.74	-1.245	0.482
1785	144.85	-1.680	0.407
1786	144.95	-1.824	0.802
1787	145.06	-1.650	0.438
1788	145.17	-1.809	0.529
1789	145.27	-1.741	0.427
1790	145.38	-1.962	0.493
1791	145.48	-2.062	0.560
1792	145.59	-1.510	0.292
1793	145.70	-1.599	0.379
1794	145.80	-1.413	0.409
1795	145.91	-1.585	0.778
1796	146.01	-1.637	0.386
1797	146.12	-1.685	0.429
1798	146.23	-1.892	0.390
1799	146.33	-1.743	0.413
1800	146.44	-1.784	0.147

Note:

[$] see Table 1 for age model

[‡] *G. rub* = Globigerinoides ruber (215-250 µm)

samples 662-672,1226-1253, 1381-1392 are voids in original core

samples: 370, 933-935, 937-939,1509, and 1641 are lost in mail

APPENDIX II

IMAGES core MD97-2141: Mg/Ca and Sr/Ca data from *Globigerinoides ruber*

Sample (depth, cm)	Age[$] (kyr)	average shell mass (µg)	Mg/Ca (mmol/mol)	Sr/Ca (mmol/mol)	SST[†] (ºC)	$\delta 18O_{seawater}$ [a] (‰)
421	27.23	7.10	3.656	1.437	28.09	0.64
423	27.74	6.60	3.694	1.430	28.21	0.26
427	28.77	6.30	3.559	1.430	27.79	0.63
430	29.54	6.60	3.806	1.425	28.55	0.64
433	30.31	6.90	3.780	1.440	28.47	0.45
436	31.08	6.40	3.698	1.431	28.22	0.67
439	31.84	6.40	3.663	1.429	28.12	0.46
441	32.16	6.40	3.653	1.423	28.08	0.53
443	32.29	7.30	3.691	1.433	28.20	0.74
445	32.42	6.40	3.669	1.435	28.13	0.54
450	32.75	6.60	3.471	1.438	27.51	0.36
453	32.94	6.80	3.557	1.431	27.79	0.14
455	33.07	6.70	3.685	1.446	28.18	0.30
459	33.33	6.60	3.561	1.432	27.80	0.49
462	33.53	6.30	3.834	1.444	28.63	0.31
464	33.66	6.80	3.733	1.434	28.33	0.14
469	33.98	6.40	3.813	1.438	28.57	0.47
471	34.11	6.30	3.563	1.435	27.80	0.17
474	34.31	7.20	3.690	1.431	28.20	0.47
477	34.50	7.00	3.700	1.442	28.23	0.59
479	34.63	7.00	3.838	1.441	28.64	0.37
481	34.76	7.10	3.698	1.442	28.22	0.60
484	34.96	7.90	3.728	1.436	28.31	0.34
486	35.09	7.30	3.650	1.443	28.08	0.49
489	35.26	7.40	3.845	1.437	28.66	0.32
492	35.43	7.40	3.565	1.428	27.81	0.21
494	35.54	7.80	3.799	1.441	28.52	0.49
496	35.65	6.80	3.632	1.425	28.02	0.19
498	35.76	7.10	3.821	1.444	28.59	0.63
500	35.87	7.10	3.704	1.451	28.24	0.64
505	36.14	7.00	3.848	1.440	28.67	0.47
508	36.31	7.30	3.871	1.433	28.74	0.38
510	36.42	7.30	3.812	1.441	28.56	0.64
511	36.47	7.70	3.874	1.440	28.74	0.56
512	36.53	7.60	3.712	1.421	28.26	0.25
514	36.64	7.50	3.843	1.434	28.65	0.66
515	36.69	7.00	3.611	1.432	27.95	0.30
518	36.86	6.00	3.744	1.433	28.36	0.67
520	36.97	7.20	3.841	1.443	28.65	0.58
522	37.08	7.00	3.808	1.435	28.55	0.81
525	37.25	7.10	3.634	1.433	28.03	0.56
527	37.36	7.50	3.682	1.429	28.17	0.80
529	37.47	7.00	3.621	1.432	27.99	0.91
531	37.58	7.30	3.632	1.416	28.02	0.89
533	37.69	7.50	3.809	1.433	28.55	0.78
535	37.80	7.30	3.640	1.426	28.04	0.77
540	38.07	7.40	3.896	1.425	28.81	0.94

Sample (depth, cm)	Age[$] (kyr)	average shell mass (µg)	Mg/Ca (mmol/mol)	Sr/Ca (mmol/mol)	SST[†] (ºC)	$\delta 18O_{seawater}$ [a] (‰)
541	38.13	7.70	3.446	1.426	27.43	0.57
544	38.29	7.40	3.599	1.419	27.92	0.89
545	38.35	7.10	3.600	1.410	27.92	0.77
546	38.40	7.10	3.607	1.433	27.94	0.71
547	38.46	7.60	3.876	1.430	28.75	0.65
550	38.62	7.30	3.673	1.428	28.15	0.61
552	38.73	7.10	3.648	1.440	28.07	0.43
555	38.90	7.30	3.643	1.420	28.05	0.52
556	38.96	6.60	3.574	1.422	27.84	0.35
557	39.02	7.10	3.734	1.420	28.33	0.63
560	39.19	6.70	3.868	1.419	28.73	0.47
563	39.36	7.20	3.599	1.429	27.92	0.48
566	39.53	8.50	3.547	1.411	27.75	0.48
568	39.65	6.60	3.435	1.414	27.39	0.34
570	39.76	8.50	3.702	1.421	28.23	0.25
575	40.05	7.60	3.577	1.413	27.85	0.42
579	40.27	7.90	3.847	1.423	28.67	0.39
581	40.39	7.90	3.605	1.425	27.94	0.51
586	40.67	7.10	3.556	1.444	27.78	0.45
588	40.79	8.00	3.548	1.436	27.76	0.31
590	40.90	7.30	3.752	1.430	28.38	0.61
591	40.96	7.60	3.749	1.440	28.38	0.45
593	41.07	7.10	3.526	1.439	27.69	0.51
597	41.24	7.40	3.876	1.428	28.75	0.52
600	41.47	7.70	3.943	1.438	28.94	0.66
602	41.59	7.00	3.929	1.434	28.90	0.45
604	41.70	7.10	3.992	1.431	29.08	0.63
610	42.05	7.80	3.903	1.425	28.83	0.64
614	42.28	7.90	3.861	1.439	28.71	0.25
616	42.39	8.20	3.760	1.440	28.41	0.41
618	42.51	8.20	3.777	1.428	28.46	0.44
620	42.62	7.70	3.986	1.429	29.06	0.64
622	42.74	8.50	3.692	1.428	28.20	0.51
624	42.85	7.50	3.787	1.418	28.49	0.48
628	43.08	6.90	3.490	1.410	27.57	0.58
636	43.54	6.80	3.480	1.430	27.54	0.36
640	43.77	7.50	3.750	1.420	28.38	0.55
644	44.00	7.60	3.590	1.410	27.89	0.41
650	44.35	6.50	3.820	1.410	28.59	0.39
654	44.58	7.00	3.840	1.410	28.65	0.57
656	44.69	7.00	3.630	1.420	28.01	0.05
658	44.81	7.20	3.750	1.430	28.38	0.31
660	44.92	7.20	3.770	1.430	28.44	0.36
675	45.15	6.80	3.740	1.430	28.35	0.43
677	45.27	7.50	3.860	1.420	28.70	0.24
681	45.50	6.80	3.890	1.440	28.79	0.27
684	45.67	7.40	3.840	1.421	28.65	0.29

Sample (depth, cm)	Age[$] (kyr)	average shell mass (µg)	Mg/Ca (mmol/mol)	Sr/Ca (mmol/mol)	SST[†] (ºC)	$\delta 18O_{seawater}$ [a] (‰)
688	45.90	7.10	4.090	1.414	29.35	0.59
689	45.96	7.50	3.750	1.440	28.38	0.41
690	46.01	7.30	4.098	1.421	29.38	0.74
694	46.24	7.90	4.070	1.420	29.30	0.90
697	46.42	7.00	3.810	1.430	28.56	0.52
700	46.59	7.50	3.740	1.420	28.35	0.37
703	46.76	7.80	3.660	1.440	28.11	0.56
709	47.11	8.20	3.770	1.440	28.44	0.47
710	47.16	7.30	4.049	1.435	29.24	0.99
713	47.34	7.60	3.809	1.420	28.55	0.51
716	47.51	7.40	4.049	1.423	29.24	0.67
718	47.62	8.00	3.899	1.416	28.82	0.85
721	47.80	7.30	3.709	1.421	28.26	0.31
724	47.97	7.10	3.991	1.405	29.08	0.44
729	48.26	7.30	3.990	1.405	29.08	0.48
732	48.43	7.70	4.040	1.417	29.22	0.80
734	48.54	7.60	3.732	1.407	28.32	0.18
738	48.77	8.20	3.673	1.414	28.15	0.10
741	48.95	7.90	3.695	1.417	28.21	0.35
743	49.06	7.00	3.695	1.423	28.21	0.21
746	49.23	7.30	3.845	1.417	28.66	0.27
748	49.35	7.80	3.653	1.412	28.08	0.13
750	49.46	7.90	3.783	1.415	28.48	0.47
753	49.64	7.20	3.940	1.426	28.93	0.27
756	49.81	7.30	3.684	1.422	28.18	-0.04
758	49.92	7.70	3.610	1.404	27.95	0.15
761	50.10	8.00	3.586	1.403	27.88	0.22
764	50.27	8.10	3.704	1.420	28.24	0.04
768	50.50	8.10	3.562	1.401	27.80	0.29
771	50.67	7.50	3.634	1.399	28.03	-0.02
775	50.90	7.00	4.100	1.404	29.38	0.64
777	51.01	8.00	3.787	1.417	28.49	0.06
781	51.24	6.30	3.926	1.415	28.89	0.36
783	51.36	7.10	4.334	1.416	30.01	0.43
784	51.42	7.10	4.101	1.432	29.38	0.75
787	51.59	7.10	3.916	1.431	28.87	0.50
791	51.82	7.10	4.080	1.422	29.33	0.61
793	51.93	7.50	3.850	1.421	28.67	0.24
795	52.05	8.40	4.158	1.423	29.54	0.86
797	52.16	7.40	3.801	1.415	28.53	0.16
799	52.28	7.90	3.928	1.442	28.90	0.40
801	52.39	7.40	4.308	1.426	29.94	0.93
804	52.57	8.40	4.071	1.424	29.30	0.31
806	52.68	8.60	4.076	1.412	29.32	0.77
808	52.80	7.80	4.130	1.443	29.46	0.38
809	52.85	7.10	4.011	1.426	29.13	0.70
811	52.97	8.90	3.771	1.429	28.44	0.65

Sample (depth, cm)	Age[$] (kyr)	average shell mass (µg)	Mg/Ca (mmol/mol)	Sr/Ca (mmol/mol)	SST[†] (ºC)	$\delta 18O_{seawater}$ [a] (‰)
813	53.08	6.30	3.962	1.418	29.00	0.82
816	53.26	7.90	3.904	1.419	28.83	1.05
817	53.31	7.50	4.056	1.429	29.26	0.53
818	53.37	8.00	3.805	1.440	28.54	0.52
821	53.54	8.20	3.956	1.434	28.98	0.63
825	53.77	7.00	3.840	1.426	28.65	0.85
829	54.00	7.80	4.031	1.426	29.19	0.68
831	54.12	6.40	3.770	1.421	28.44	0.72
836	54.41	5.90	3.870	1.427	28.73	0.74
838	54.52	5.90	3.827	1.422	28.61	0.79
840	54.64	7.10	4.064	1.422	29.28	0.55
842	54.75	7.20	4.178	1.434	29.59	0.20
844	54.87	6.50	3.667	1.423	28.13	0.04
847	55.04	6.60	3.610	1.426	27.95	-0.01
848	55.10	7.50	3.908	1.446	28.84	0.03
850	55.21	8.00	4.170	1.431	29.57	0.54
853	55.38	7.30	3.886	1.416	28.78	0.33
855	55.50	6.30	3.394	1.405	27.26	-0.31
857	55.61	8.80	3.757	1.427	28.40	0.15
859	55.73	8.20	3.586	1.418	27.88	0.29
860	55.78	6.60	3.905	1.427	28.83	0.64
861	55.84	8.80	3.673	1.438	28.15	0.00
863	55.96	7.70	3.812	1.426	28.56	0.35
866	56.13	6.40	3.885	1.443	28.78	0.43
869	56.30	7.90	3.666	1.449	28.12	0.47
871	56.42	6.10	3.647	1.453	28.07	0.16
874	56.59	7.90	3.687	1.459	28.19	0.26
876	56.70	7.90	3.788	1.436	28.49	0.47
880	56.93	8.10	3.523	1.411	27.68	0.30
881	56.99	7.70	3.801	1.427	28.53	0.65
883	57.11	8.20	3.795	1.430	28.51	0.45
884	57.16	6.90	3.574	1.425	27.84	0.21
887	57.34	8.30	3.773	1.427	28.45	0.42
890	57.51	8.00	3.665	1.428	28.12	0.43
891	57.57	8.10	3.678	1.416	28.16	0.19
892	57.62	8.30	3.900	1.433	28.82	0.12
894	57.74	7.30	3.842	1.438	28.65	0.32
896	57.85	8.10	3.886	1.424	28.78	0.54
898	57.97	7.90	3.676	1.430	28.16	0.05
902	58.20	8.20	3.994	1.430	29.09	0.43
906	58.43	7.70	3.785	1.433	28.48	0.10
911	58.72	6.40	4.113	1.427	29.42	0.34
913	58.83	8.90	3.930	1.427	28.91	0.54
915	58.95	7.20	3.883	1.438	28.77	0.36
917	59.06	7.00	4.025	1.435	29.17	0.52
919	59.18	7.60	3.895	1.434	28.81	0.76
920	59.23	7.40	3.718	1.431	28.28	0.54

Sample (depth, cm)	Age[$] (kyr)	average shell mass (µg)	Mg/Ca (mmol/mol)	Sr/Ca (mmol/mol)	SST[†] (ºC)	$\delta^{18}O_{seawater}$ [a] (‰)
921	59.29	7.60	3.862	1.435	28.71	0.26
923	59.41	7.30	3.923	1.421	28.89	0.58
925	59.52	7.60	4.031	1.436	29.19	0.31
926	59.58	8.20	3.767	1.427	28.43	0.05
928	59.69	7.40	3.925	1.436	28.89	0.53
931	59.87	8.00	4.021	1.426	29.16	0.61
936	60.15	9.10	4.195	1.430	29.64	0.82
941	60.44	7.70	4.171	1.421	29.57	0.83
945	60.81	7.10	3.868	1.435	28.73	1.02
948	61.10	10.31	3.889	1.414	28.79	1.08

Note:

[$] see Table 1 for age model

[†] SST = sea surface temperature based on equation by Lea et al., [2000]

[a] $\delta^{18}O_{seawater}$ = based on Erez and Luz [1983]

APPENDIX III

IMAGES core MD97-2141: $\delta^{18}O$ and $\delta^{13}C$ data from *Globigerinoides sacculifer*

Sample (depth, cm)	Age[$] (kyr)	$\delta^{18}O$ (G.sacc[‡]) (‰)	$\delta^{13}C$ (G.sacc[‡]) (‰)
0	4.29	-2.234	1.993
10	4.77	-2.204	1.743
20	5.16	-2.149	1.813
30	5.48	-2.366	1.947
40	5.80	-2.276	1.865
50	6.13	-2.374	1.810
60	6.48	-2.327	1.663
70	7.09	-2.290	1.931
80	7.68	-2.504	1.949
90	8.26	-2.018	1.700
100	8.84	-2.177	1.694
110	9.42	-2.162	1.449
120	10.00	-2.264	1.418
130	10.35	-2.251	1.419
140	10.70	-1.933	1.334
150	11.05	-2.306	1.162
160	11.24	-1.473	1.226
170	11.68	-1.685	1.260
180	12.13	-1.467	1.246
190	12.57	-1.317	1.023
200	13.01	-1.290	0.905
210	13.72	-1.422	1.094
220	14.41	-1.017	1.081
230	15.12	-0.923	1.370
240	16.05	-0.941	1.155
250	16.61	-1.004	1.142
260	16.92	-1.001	1.176
270	17.23	-1.077	1.260
280	17.53	-0.755	1.192
290	17.89	-0.980	1.130
300	18.27	-1.320	1.398
310	18.65	-1.117	1.241
320	19.03	-1.097	1.367
330	19.41	-1.234	1.281
340	19.77	-1.317	1.241
350	20.01	-1.036	1.262
360	20.24	-1.136	1.126
371	20.56	-1.280	1.309
380	20.96	-1.071	1.472
390	21.41	-1.086	1.383
400	21.85	-1.195	1.416
410	hiatus	-1.519	1.422
420	hiatus	-1.684	1.512
430	29.54	-1.592	1.487
440	32.10	-1.676	1.496
450	32.75	-1.690	1.532
460	33.40	-1.508	1.464
470	34.05	-1.546	1.467
480	34.70		1.497
490	35.48	-1.573	1.498
500	36.58	-1.577	1.504
510	37.35	-1.519	1.335
520	37.51	-1.415	1.525
530	37.68	-1.212	1.367
540	37.84	-1.311	1.431
550	38.52	-1.567	1.419
560	39.19	-1.439	1.534
570	39.76	-1.435	1.421
580	40.33	-1.577	1.557
590	40.91	-1.603	1.470
600	41.48	-1.573	1.330
610	42.05	-1.492	1.301
620	42.63	-1.466	1.480
630	43.20	-1.492	1.570
640	43.78	-1.709	1.481
650	44.35	-1.678	1.434
660	44.93	-1.752	1.257
673	45.04	-1.926	1.261
680	45.44	-1.793	1.408
690	46.02	-1.642	1.280
700	46.59	-1.329	1.219
710	47.17	-1.800	1.256
720	47.74	-1.672	1.386
730	48.32	-1.600	1.247
740	48.89	-1.729	1.380
750	49.47	-1.733	1.419
760	50.04	-1.499	1.312
770	50.61	-1.797	1.298
780	51.19	-1.598	1.215
790	51.76	-1.768	1.212
800	52.34	-1.593	1.161
810	52.91	-1.596	1.065
820	53.49	-1.354	1.129
830	54.06	-1.481	1.039
840	54.64	-1.948	1.305
850	55.21	-1.616	1.192
860	55.79	-1.724	1.474
870	56.36	-1.659	1.320
880	56.94	-1.635	1.301
890	57.51	-1.652	1.168
900	58.08	-1.225	1.109
910	58.66	-1.652	0.814
920	59.23	-1.707	1.230
930	59.81	-1.558	0.896

Sample (depth, cm)	Age[$] (kyr)	$\delta^{18}O$ (G.sacc[‡]) (‰)	$\delta^{13}C$ (G.sacc[‡]) (‰)
940	60.38	-1.287	0.880
950	61.72	-1.288	1.101
960	63.15	-1.172	0.946
970	64.57	-1.154	0.895
980	66.40	-1.129	0.932
990	68.40	-1.259	1.274
1000	70.40	-0.971	1.246
1010	72.40	-1.515	1.300
1020	74.40	-1.424	1.235
1030	76.40	-2.034	1.808
1040	78.21	-1.612	1.590
1050	79.25	-2.058	1.661
1060	80.29	-1.850	1.559
1070	81.33	-1.648	1.632
1080	82.37	-1.798	1.535
1090	83.41	-1.261	1.389
1100	84.45	-1.407	1.362
1110	85.49	-1.614	1.325
1120	86.52	-1.377	1.453
1130	87.56	-1.628	1.254
1140	88.60	-1.861	1.638
1150	89.64	-1.796	1.662
1160	90.68	-1.823	1.406
1170	91.72	-1.735	1.523
1180	92.76	-1.843	1.852
1190	93.80	-2.056	1.781
1200	94.84	-1.919	1.703
1210	95.88	-1.906	1.900
1220	96.92	-1.721	2.118
1260	98.17	-1.850	1.848
1270	99.17	-2.099	1.553
1280	99.99	-1.809	1.531
1290	100.82	-1.884	1.551
1300	101.64	-1.794	1.784
1310	102.47	-1.713	1.801
1320	103.30	-1.931	1.770
1330	104.12	-1.939	1.789
1340	104.95	-2.055	1.857
1350	105.77	-1.946	1.763
1360	106.60	-1.962	1.676
1370	107.43	-1.820	1.455
1380	108.25	-1.731	1.565
1400	108.91	-2.098	1.299
1410	109.74	-1.803	1.659
1420	110.57	-1.763	1.714
1430	111.39	-2.102	1.580
1440	112.22	-2.157	1.695
1450	113.05	-2.036	1.415
1460	113.87	-1.907	1.823
1470	114.70	-1.764	1.709
1480	115.52	-2.100	1.600
1490	116.35	-2.110	1.507
1500	117.18	-2.214	1.725
1510	118.00	-2.111	1.421
1520	118.83	-1.664	1.570
1530	119.66	-1.897	1.428
1540	120.48	-2.155	1.601
1550	121.31	-2.269	1.481
1560	122.13	-2.344	1.253
1570	122.96	-2.282	1.507
1580	123.79	-2.392	1.455
1590	124.61	-2.336	1.422
1600	125.44	-2.161	1.202
1610	126.26	-2.202	0.992
1620	127.09	-1.884	0.907
1630	127.92	-2.088	0.762
1640	128.99	-1.549	0.787
1650	130.08	-1.234	0.720
1660	131.18	-1.078	0.743
1670	132.27	-0.984	0.803
1680	133.37	-0.984	0.803
1690	134.47	-1.007	0.980
1700	135.56	-1.114	0.907
1710	136.66	-1.002	0.754
1720	137.75	-1.082	0.945
1730	138.85	-1.265	0.971
1740	139.95	-1.236	0.982
1750	141.04	-1.083	0.943
1760	142.14	-1.384	1.088
1770	143.23	-1.036	0.950
1780	144.32	-1.167	0.989
1790	145.38	-1.312	1.052
1800	146.44	-1.170	0.985

Note:

[$] see Table 1 for age model

[‡] G. sacc = Globigerinoides sacculifer (300-355 μm)

APPENDIX IV

IMAGES core MD97-2141: $\delta^{18}O$ and $\delta^{13}C$ data from *Neogloboquadrina dutertrei*

Sample (depth, cm)	Age[$] (kyr)	$\delta^{18}O$ (N.dut[‡]) (‰)	$\delta^{13}C$ (N.dut[‡]) (‰)
508	36.31	-0.529	0.600
510	36.42	-0.451	0.491
511	36.47	-0.346	0.600
512	36.53	-0.580	0.827
514	36.64	-0.277	0.791
515	36.69	-0.567	0.669
518	36.86	-0.401	0.626
520	36.97	-0.283	0.683
522	37.08	-0.250	0.673
525	37.25	-0.258	0.668
527	37.36	-0.273	0.807
529	37.47	-0.271	0.833
531	37.58	-0.339	0.665
533	37.69	-0.209	0.788
535	37.80	-0.241	0.731
538	37.96	-0.497	0.986
540	38.07	-0.538	0.648
541	38.13	-0.205	0.693
544	38.29	-0.211	0.772
545	38.35	-0.448	0.779
546	38.40	-0.187	0.623
547	38.46	-0.521	0.669
549	38.57	-0.281	0.652
550	38.62	-0.308	0.790
552	38.73	-0.400	0.804
556	38.96	-0.382	0.829
557	39.02	-0.262	0.930
560	39.19	-0.248	0.612
563	39.36	-0.312	1.020
566	39.53	-0.324	0.827
568	39.65	-0.313	0.832
570	39.76	-0.228	0.687
575	40.05	-0.549	0.812
581	40.39	-0.441	0.748
590	40.91	-0.219	0.795
593	41.08	-0.165	0.666
600	41.48	-0.540	0.792
608	41.94	-0.493	0.549
610	42.05	-0.515	0.670
614	42.28	-0.418	0.770
618	42.51	-0.328	0.823
624	42.86	-0.702	0.920
626	42.97	-0.263	0.838
628	43.09	-0.259	0.758
636	43.55	-0.399	0.618
640	43.78	-0.646	0.950
644	44.01	-0.507	0.508
650	44.35	-0.388	0.655
653	44.52	-0.402	0.815
654	44.58	-0.534	0.663
656	44.70	-0.956	0.474
657	44.75	-0.748	0.698
658	44.81	-0.723	0.610
659	44.87	-0.558	0.626
661	44.98	-0.793	0.675
673	45.04	-0.480	0.535
674	45.10	-0.665	0.591
675	45.16	-0.545	0.978
677	45.27	-0.659	0.844
679	45.39	-0.647	0.620
681	45.50	-0.561	0.758
683	45.62	-0.453	0.610
686	45.79	-0.717	0.655
689	45.96	-0.469	0.629
691	46.08	-0.658	0.692
694	46.25	-0.443	0.761
700	46.59	-0.516	0.734
703	46.76	-0.294	0.900
709	47.11	-0.333	0.826
710	47.17	-0.456	0.660
713	47.34	-0.339	0.753
716	47.51	-0.363	0.859
718	47.63	-0.393	0.693
721	47.80	-0.376	0.731
724	47.97	-0.820	0.688
729	48.26	-0.643	0.835
734	48.55	-0.545	0.956
738	48.78	-0.643	0.879
741	48.95	-0.538	0.874
746	49.24	-0.474	0.714
748	49.35	-0.680	0.676
753	49.64	-0.630	0.699
756	49.81	-0.840	0.609
758	49.93	-0.732	0.751
761	50.10	-0.525	0.609
764	50.27	-0.565	0.753
768	50.50	-0.831	0.658
771	50.67	-0.582	0.454
774	50.84	-0.739	0.395
775	50.90	-0.591	0.646
777	51.02	-0.742	0.627
783	51.36	-0.716	0.520
787	51.59	-0.484	0.582
793	51.94	-0.612	0.564

Sample (depth, cm)	Age[$] (kyr)	$\delta^{18}O$ (N.dut[‡]) (‰)	$\delta^{13}C$ (N.dut[‡]) (‰)
799	52.28	-0.593	0.515
804	52.57	-0.701	0.491
809	52.86	-0.630	0.710
813	53.09	-0.619	0.374
818	53.37	-0.351	0.406
825	53.77	-0.548	0.333
829	54.00	-0.156	0.422
831	54.12	-0.310	0.209
836	54.41	-0.239	0.597
838	54.52	-0.482	0.301
839	54.58	-0.662	0.588
840	54.64	-0.940	0.584
842	54.75	-0.330	0.371
844	54.87	-0.787	0.633
847	55.04	-0.775	0.571

[$] see Table 1 for age model

[‡] *N. dut* = *Neogloboquadrina dutertrei* (250-300 μm)

APPENDIX V

IMAGES core MD97-2141: $\delta^{18}O$ and $\delta^{13}C$ data from *Globorotalia crassaformis*

Sample (depth, cm)	Age[$] (kyr)	$\delta^{18}O$ (G.cras[‡]) (‰)	$\delta^{13}C$ (G.cras[‡]) (‰)
510	36.42	0.648	0.750
511	36.47	0.659	0.654
512	36.53	0.490	0.484
514	36.64	0.670	0.698
515	36.69	0.859	0.545
518	36.86	0.571	0.737
520	36.97	0.967	0.816
522	37.08	0.737	0.673
525	37.25	0.659	0.684
527	37.36	0.898	0.775
529	37.47	0.681	0.762
531	37.58	0.819	0.712
533	37.69	0.800	0.737
535	37.80	0.699	0.753
538	37.96	0.652	0.703
540	38.07	0.741	0.895
541	38.13	0.892	0.903
544	38.29	0.936	0.833
545	38.35	0.784	0.733
546	38.40	0.757	0.726
547	38.46	0.864	0.844
549	38.57	0.424	0.589
550	38.62	0.919	0.871
552	38.73	0.776	0.763
556	38.96	0.799	0.848
557	39.02	0.917	0.909
560	39.19	0.725	0.763
563	39.36	0.813	0.754
566	39.53	0.716	0.743
568	39.65	0.629	0.783
570	39.76	0.833	0.715
575	40.05	0.519	0.576
579	40.28	0.818	0.643
581	40.39	0.768	0.610
590	40.91	0.829	0.745
593	41.08	0.047	0.620
600	41.48	0.578	0.535
608	41.94	0.318	0.596
610	42.05	0.469	0.426
614	42.28	0.449	0.579
618	42.51	0.539	0.599
624	42.86	0.816	0.758
626	42.97	0.291	0.533
628	43.09	0.387	0.388
636	43.55	0.634	0.670
640	43.78	0.652	0.707
644	44.01	0.327	0.483
650	44.35	0.165	0.395
653	44.52	0.661	0.439
654	44.58	0.391	0.493
655	44.64	0.464	0.664
657	44.75	0.724	0.465
658	44.81	0.475	0.365
659	44.87	0.930	0.759
660	44.93	0.350	0.488
661	44.98	0.783	0.568
673	45.04	0.642	0.513
674	45.10	1.090	0.720
677	45.27	0.670	0.545
681	45.50	0.349	0.370
686	45.79	0.016	0.536
689	45.96	0.114	0.485
691	46.08	0.456	0.543
697	46.42	0.682	0.599
700	46.59	0.647	0.537
703	46.76	0.696	0.578
709	47.11	0.682	0.526
710	47.17	0.848	0.645
713	47.34	0.759	0.589
716	47.51	0.931	0.714
718	47.63	0.607	0.828
721	47.80	0.632	0.598
724	47.97	0.539	0.599
729	48.26	0.634	0.567
734	48.55	0.754	0.699
738	48.78	0.641	0.646
741	48.95	0.692	0.641
746	49.24	0.755	0.652
748	49.35	0.866	0.580
753	49.64	0.531	0.558
756	49.81	0.877	0.678
758	49.93	0.810	0.698
761	50.10	0.518	0.620
764	50.27	0.656	0.608
768	50.50	0.806	0.543
771	50.67	0.752	0.615
774	50.84	0.563	0.509
775	50.90	0.369	0.543
777	51.02	0.738	0.594
783	51.36	0.923	0.520
787	51.59	0.704	0.589
793	51.94	0.496	0.547
799	52.28	0.861	0.491
804	52.57	0.619	0.446

Sample (depth, cm)	Age[$] (kyr)	$\delta^{18}O$ (G.cras[‡]) (‰)	$\delta^{13}C$ (G.cras[‡]) (‰)
809	52.86	0.246	0.630
813	53.09	0.775	0.586
818	53.37	0.842	0.491
825	53.77	0.731	0.543
829	54.00	0.659	0.462
831	54.12	0.836	0.469
836	54.41	0.687	0.556
838	54.52	0.741	0.570
839	54.58	0.574	0.438
840	54.64	0.440	0.606
842	54.75	0.506	0.468
844	54.87	0.309	0.482
847	55.04	0.561	0.562

[$] see Table 1 for age model

[‡] G. *cras* = *Globorotalia crassaformis* (300-355 µm)

APPENDIX VI

IMAGES core MD97-2141: Relative abundance of planktonic foraminifera between 35-60 kyr

Sample (depth, cm)	*O. uni*	*G. congl*	*G. rub* (white)	*G. tene*	*G. sac* w/out sac	*G. sac* w/ sac	*G. sac* total	*G. aequi*	*G. calid*	*G. bull*	*G. falc*	*G. digit*	*G. rubes*	*N. pachy* (right)	*N. duter*	*P. obliq*	*G. inflat*	*G. trunc* (right)	*G. crass*	*G. scit*	*G. men*	*G. turn*	*G. glut*	*G. uvula*	other	total
500	9	0	73	14	5	2	7	11	23	42	0	0	8	13	66	5	0	0	2	3	3	22	55	0	0	356
507	8	9	84	17	7	3	10	10	28	36	1	1	7	1	59	2	0	0	2	2	0	19	88	2	0	364
515	18	0	85	13	11	1	12	26	28	81	11	7	15	8	103	4	0	0	10	0	1	31	86	0	1	538
520	5	0	88	17	11	2	13	11	28	69	1	1	9	8	66	2	0	0	3	0	2	22	72	0	0	397
533	8	0	68	11	21	2	23	18	34	62	2	3	11	5	66	1	0	0	5	0	2	20	74	0	0	413
538	13	0	91	9	10	3	13	21	25	42	0	1	5	12	80	3	0	0	5	8	1	29	57	2	3	418
543	4	0	34	5	8	6	14	8	9	31	8	1	6	4	45	4	0	0	9	18	0	15	41	1	3	258
547	3	0	37	19	16	9	25	13	27	51	1	1	10	14	85	0	0	0	7	5	2	14	84	0	1	359
553	5	0	48	8	11	6	17	13	19	33	2	0	4	12	71	2	0	0	18	2	0	24	82	1	2	343
560	4	1	43	6	15	2	17	11	36	50	4	1	8	16	73	2	0	0	19	4	4	21	49	0	1	370
570	5	0	65	8	7	1	8	30	49	47	2	0	18	18	60	8	0	0	8	6	2	32	65	0	1	432
800	14	0	79	8	3	2	5	14	21	62	2	1	5	10	43	6	0	0	2	5	2	26	87	0	0	390
608	12	1	59	8	8	2	10	9	20	52	0	0	5	15	42	5	0	0	4	3	1	29	43	0	0	318
618	9	0	81	12	35	3	38	20	15	19	2	0	3	11	58	5	0	0	5	1	7	19	42	1	1	329
628	1	1	47	13	18	2	20	32	24	18	3	1	13	12	89	1	0	0	5	0	2	18	26	2	6	314
640	8	0	69	20	25	13	38	18	26	27	7	0	9	8	82	6	0	0	10	0	2	18	34	8	2	392
650	11	0	48	7	13	3	16	40	4	30	17	3	12	2	66	8	0	0	2	0	0	25	47	14	2	352
660	8	2	76	14	13	2	15	32	28	25	10	0	8	8	62	4	2	0	0	1	3	27	55	1	3	384
877	6	0	50	12	7	7	14	10	26	24	13	0	11	5	31	2	0	0	1	0	0	23	42	10	7	287
681	9	0	100	27	17	5	22	18	17	60	32	2	24	3	47	3	0	0	3	1	0	16	73	1	3	461
686	1	0	68	30	9	2	11	6	22	43	11	1	26	7	32	2	0	0	1	0	0	7	48	12	0	328
691	5	0	104	21	16	8	22	14	42	53	29	0	51	4	65	5	0	0	2	2	0	22	88	0	7	536
697	13	0	48	19	15	9	24	16	24	21	7	3	20	9	74	1	0	0	3	0	0	28	45	3	5	361
703	4	1	77	22	16	3	19	17	21	16	18	2	40	12	46	1	0	0	3	0	0	13	84	1	11	388
727	7	2	56	10	9	2	11	17	17	71	4	2	9	1	50	1	0	0	0	1	5	28	85	0	3	380
748	4	0	48	11	15	3	18	11	22	39	3	1	12	3	37	2	0	0	2	8	1	19	43	0	3	287
788	8	0	82	10	15	1	16	21	29	43	13	1	38	7	50	4	0	0	4	21	0	24	78	2	0	451
774	10	0	99	10	8	1	9	17	31	53	9	1	19	12	44	6	0	0	6	3	0	32	70	0	3	434
777	5	0	87	10	11	2	13	14	35	48	1	1	19	10	36	7	0	0	2	5	2	11	70	0	0	356
783	1	0	57	8	17	0	17	11	29	41	4	0	17	6	71	8	0	0	4	9	0	12	50	0	0	343
804	5	0	79	5	8	0	6	11	18	59	4	0	10	9	50	8	0	9	6	4	2	32	52	0	0	369
825	7	1	116	24	7	1	8	25	20	79	6	1	21	20	62	8	0	0	1	64	3	26	105	1	3	601
847	0	0	76	10	6	5	11	17	29	70	6	1	19	1	31	5	0	0	6	11	2	11	57	0	0	363
896	1	0	55	11	10	6	16	8	15	46	4	3	10	12	49	7	0	0	0	19	8	18	40	0	0	320
919	2	1	85	19	6	3	9	23	36	88	5	3	22	12	53	8	0	0	3	13	1	17	73	0	0	473

APPENDIX VII

IMAGES core MD97-2141: Sample weight and occurrence of pteropods and ash layers

Sample (depth, cm)	Sample weight	weight >63µm	weight >63<150µm	weight >150µm	Pteropods	Ash	Comments
0	1.306	0.261	0.095	0.165		√	speckled forams: ash?
1	0.798	0.134	0.040	0.088		√	speckled forams: ash?
2	2.182	0.342	0.106	0.232		√	speckled forams: ash?
3	1.624	0.260	0.086	0.170		√	
4	3.582	0.592	0.220	0.372		√	
5	1.182	0.274	0.122	0.152		√	
6	2.442	0.688	0.492	0.192		√	ash
7	2.584	0.646	0.420	0.226		√	
8	2.122	0.480	0.214	0.266		√	
9	2.828	0.690	0.438	0.250		√	? ash
10	0.811	0.177	0.058	0.111		√	
11	1.750	0.298	0.176	0.122		√	
12	1.048	0.202	0.120	0.086		√	
13	1.628	0.340	0.210	0.130		√	? ash
14	2.224	0.338	0.150	0.186		√	
15	1.124	0.196	0.062	0.134		√	
16	1.456	0.254	0.070	0.182		√	
17	1.592	0.276	0.070	0.202		√	
18	2.054	0.310	0.090	0.220		√	
19	1.412	0.228	0.082	0.144		√	
20	1.115	0.218	0.062	0.149		√	
21	2.144	0.370	0.102	0.262		√	
22	1.810	0.336	0.070	0.262			
23	2.538	0.292	0.070	0.218			
24	3.012	0.292	0.070	0.222			glass shards
25	2.986	0.270	0.076	0.198			
26	2.098	0.208	0.052	0.156			
27	2.784	0.264	0.066	0.198			
28	2.148	0.138	0.036	0.100			
29	3.182	0.258	0.068	0.190			
30	2.291	0.365	0.082	0.276			
31	1.550	0.246	0.056	0.192			
32	1.892	0.306	0.086	0.220			
33	2.922	0.272	0.068	0.204			
34	3.228	0.354	0.082	0.272			
35	1.752	0.290	0.072	0.218			
36	1.614	0.285	0.074	0.210			
37	1.686	0.290	0.070	0.220			
38	2.632	0.466	0.110	0.356			
39	1.806	0.508	0.100	0.408			
40	1.551	0.374	0.071	0.300			glass shards
41	2.556	0.538	0.114	0.420			
42	1.718	0.372	0.076	0.296			glass shards
43	2.128	0.410	0.080	0.330			
44	3.066	0.556	0.104	0.450			
45	2.674	0.468	0.098	0.370			
46	2.498	0.434	0.084	0.350			
47	2.180	0.452	0.104	0.348			

Sample (depth, cm)	Sample weight	weight >63µm	weight >63<150µm	weight >150µm	Pteropods	Ash	Comments
48	2.172	0.382	0.086	0.296			
49	2.190	0.472	0.090	0.380			
50	1.366	0.317	0.059	0.251			
51	1.696	0.360	0.286	0.068		√	? ash
52	2.178	0.474	0.096	0.372			
53	1.824	0.390	0.084	0.300			
54	1.642	0.376	0.070	0.298			
55	1.446	0.264	0.060	0.204			
56	1.392	0.350	0.070	0.280			
57	1.348	0.292	0.052	0.238			
58	1.304	0.326	0.060	0.252			
59	1.710	0.426	0.078	0.344			
60	1.079	0.267	0.066	0.196			
61	1.420	0.352	0.066	0.280			
62	1.440	0.380	0.074	0.300			
63	1.640	0.488	0.090	0.396			
64	2.052	0.522	0.104	0.410			
65	2.242	0.422	0.098	0.320			
66	1.592	0.316	0.068	0.246			
67	1.424	0.204	0.046	0.156			
68	1.764	0.424	0.098	0.322			
69	1.436	0.322	0.074	0.246			
70	1.439	0.397	0.087	0.300			
71	1.550	0.380	0.060	0.316			3 mm thick black/brown flat elongated 1-2 cm long pieces; glassy at some parts: ash?
72	1.502	0.238	0.040	0.196			
73	2.194	0.396	0.052	0.336			
74	1.652	0.400	0.052	0.340			3 mm thick black/brown flat elongated 1-2 cm long pieces; glassy at some parts: ash?
75	1.316	0.328	0.036	0.288			3 mm thick black/brown flat elongated 1-2 cm long pieces; glassy at some parts: ash?
76	1.416	0.258	0.040	0.212			
77	1.716	0.338	0.058	0.274			
78	1.776	0.294	0.054	0.240			
79	1.946	0.388	0.066	0.322			
80	1.410	0.453	0.104	0.344			
81	1.412	0.320	0.056	0.268			3 mm thick black/brown flat elongated 1-2 cm long pieces; glassy at some parts: ash?

Sample (depth, cm)	Sample weight	weight >63µm	weight >63<150µm	weight >150µm	Pteropods	Ash	Comments
82	1.794	0.364	0.070	0.296			3 mm thick black/brown flat elongated 1-2 cm long pieces; glassy at some parts: ash?
83	2.946	0.580	0.118	0.460			
84	1.226	0.218	0.056	0.164			
85	2.060	0.384	0.074	0.308			
86	1.844	0.364	0.066	0.286			
87	1.566	0.320	0.060	0.258			glass shards
88	2.398	0.440	0.084	0.348			
89	1.502	0.274	0.050	0.220			
90	1.440	0.409	0.130	0.270			
91	1.408	0.312	0.052	0.248			
92	1.646	0.364	0.062	0.294			
93	2.252	0.470	0.090	0.378			
94	2.192	0.454	0.084	0.360			
95	2.098	0.392	0.070	0.314			
96	1.744	0.420	0.068	0.340			
97	2.952	0.718	0.112	0.590			
98	3.082	0.652	0.112	0.532			
99	1.958	0.486	0.072	0.414			
100	0.928	0.377	0.071	0.292			
101	0.638	0.142	0.026	0.110			
102	1.948	0.496	0.080	0.404			glass shards; 3 mm thick black/brown flat elongated<1 cm long pieces; glassy at some parts: ash?
103	3.182	0.832	0.132	0.698			
104	1.992	0.478	0.088	0.390			
105	1.380	0.372	0.060	0.314			
106	2.310	0.598	0.096	0.492			glass shards
107	1.246	0.388	0.062	0.326			
108	1.976	0.504	0.080	0.376			
109	0.938	0.242	0.038	0.198			
110	1.169	0.358	0.103	0.250			
111	0.934	0.220	0.046	0.168			
112	1.196	0.302	0.058	0.234			
113	1.746	0.452	0.082	0.360			
114	1.680	0.434	0.096	0.326			
115	1.362	0.360	0.076	0.284			
116	1.224	0.338	0.062	0.266			
117	2.222	0.594	0.102	0.484			
118	2.084	0.558	0.112	0.438			
119	2.496	0.620	0.118	0.496			
120	1.127	0.366	0.134	0.221			
121	1.008	0.209	0.042	0.154			
122	1.194	0.276	0.058	0.212			
123	1.488	0.404	0.078	0.320			

Sample (depth, cm)	Sample weight	weight >63µm	weight >63<150µm	weight >150µm	Pteropods	Ash	Comments
124	1.144	0.290	0.056	0.226			
125	1.154	0.260	0.058	0.198			
126	1.422	0.378	0.078	0.300			
127	2.028	0.416	0.084	0.328			
128	2.336	0.580	0.112	0.464			glass shards
129	1.486	0.360	0.062	0.286			
130	1.209	0.360	0.100	0.253			
131	1.516	0.346	0.066	0.276			
132	1.494	0.316	0.060	0.252			
133	1.578	0.322	0.064	0.252			
134	2.406	0.504	0.094	0.400			
135	1.496	0.310	0.082	0.228			
136	2.414	0.458	0.090	0.360			
137	1.946	0.376	0.072	0.296			
138	2.308	0.342	0.080	0.250			
139	1.966	0.376	0.082	0.286			
140	1.412	0.334	0.102	0.223			
141	2.244	0.372	0.074	0.292			
142	2.256	0.346	0.072	0.264			
143	2.116	0.350	0.068	0.276			
144	2.194	0.348	0.074	0.266			
145	0.918	0.126	0.024	0.096			
146	1.382	0.226	0.044	0.176			
147	1.936	0.346	0.060	0.284			
148	2.164	0.320	0.060	0.254			
149	1.926	0.300	0.054	0.236			
150	1.298	0.356	0.118	0.229			
151	2.036	0.396	0.068	0.316			
152	2.228	0.424	0.074	0.344			
153	1.993	0.388	0.060	0.316			
154	2.426	0.314	0.048	0.258			
155	1.686	0.280	0.048	0.222			
156	0.852	0.192	0.030	0.156			
157	1.246	0.240	0.042	0.192			
158	1.558	0.286	0.050	0.226			
159	1.246	0.232	0.044	0.176			
160	0.887	0.231	0.068	0.158			
161	1.646	0.358	0.054	0.298			
162	1.636	0.382	0.056	0.306			
163	1.416	0.266	0.044	0.214			
164	1.242	0.274	0.042	0.222			
165	1.860	0.502	0.084	0.416			
166	1.692	0.414	0.072	0.338			
167	1.264	0.298	0.042	0.246			
168	2.046	0.480	0.074	0.404			
169	1.552	0.364	0.054	0.300			
170	1.209	0.295	0.062	0.229			
171	1.106	0.256	0.046	0.206			

Sample (depth, cm)	Sample weight	weight >63µm	weight >63<150µm	weight >150µm	Pteropods	Ash	Comments
172	1.216	0.292	0.050	0.234			
173	1.472	0.288	0.054	0.226			
174	1.914	0.504	0.084	0.420			
175	1.560	0.320	0.054	0.260			
176	1.440	0.302	0.052	0.242			
177	1.442	0.322	0.052	0.268			
178	1.678	0.368	0.066	0.302			
179	1.668	0.394	0.064	0.334			
180	1.361	0.350	0.085	0.264			
181	1.192	0.290	0.046	0.240			
182	2.096	0.570	0.104	0.458			
183	2.026	0.506	0.084	0.416			
184	2.242	0.604	0.110	0.484			
185	1.756	0.448	0.086	0.358			
186	0.762	0.204	0.040	0.160			
187	1.568	0.434	0.102	0.332			
188	1.620	0.386	0.078	0.304			
189	1.544	0.384	0.068	0.312			
190	0.923	0.269	0.059	0.209			
191	1.660	0.360	0.082	0.276			
192	1.218	0.348	0.076	0.268			
193	2.036	0.504	0.096	0.402			
194	2.722	0.724	0.148	0.570			
195	0.820	0.194	0.040	0.148			
196	1.662	0.458	0.112	0.342			
197	1.486	0.348	0.076	0.270			
198	2.280	0.346	0.088	0.252		√	
199	2.228	0.482	0.136	0.338		√	
200	1.573	0.419	0.117	0.301		√	ash
201	0.910	0.200	0.038	0.158	√		pteropods
202	1.070	0.256	0.060	0.192	√	√	pteropods
203	1.038	0.204	0.046	0.152		√	ash
204	2.284	0.432	0.116	0.308	√		pteropods
205	1.554	0.304	0.070	0.226		√	
206	1.690	0.292	0.098	0.192		√	
207	1.390	0.212	0.048	0.160			
208	2.008	0.348	0.070	0.270	√		pteropods
209	1.072	0.226	0.044	0.176	√		pteropods
210	0.869	0.326	0.092	0.233	√		pteropods
211	1.248	0.256	0.054	0.196	√		pteropods
212	1.736	0.450	0.088	0.352			
213	1.224	0.318	0.062	0.246	√		pteropods
214	0.862	0.202	0.044	0.156	√		pteropods
215	0.516	0.120	0.024	0.088	√		pteropods
216	0.868	0.230	0.040	0.180	√		pteropods
217	1.354	0.308	0.056	0.244	√		pteropods
218	1.362	0.382	0.066	0.312	√		pteropods
219	1.240	0.294	0.058	0.232	√	√	pteropods, ash

Sample (depth, cm)	Sample weight	weight >63µm	weight >63<150µm	weight >150µm	Pteropods	Ash	Comments
220	1.493	0.540	0.154	0.386	√	√	pteropods
221	1.430	0.304	0.076	0.220	√	√	pteropods
222	2.850	0.484	0.264	0.210	√	√	pteropods, ash
223	1.786	0.296	0.156	0.138	√	√	pteropods, ash
224	1.494	0.240	0.122	0.104	√	√	pteropods, ash
225	1.466	0.268	0.122	0.138	√	√	pteropods, ash
226	1.522	0.273	0.126	0.134		√	ash
227	1.256	0.220	0.104	0.106		√	ash
228	1.172	0.230	0.048	0.164		√	ash
229	1.390	0.292	0.062	0.214	√		pteropods
230	1.612	0.532	0.161	0.370	√		pteropods
231	1.426	0.306	0.076	0.224	√		pteropods
232	1.586	0.268	0.074	0.178	√		pteropods
233	1.308	0.240	0.064	0.168	√		pteropods
234	1.524	0.278	0.076	0.196	√		pteropods
235	1.382	0.174	0.048	0.116	√		pteropods
236	1.478	0.186	0.046	0.134	√		pteropods
237	1.306	0.190	0.052	0.130	√		pteropods
238	1.996	0.386	0.070	0.208	√		pteropods
239	1.658	0.302	0.074	0.216	√		pteropods
240	1.831	0.528	0.196	0.324	√		pteropods
241	1.866	0.312	0.080	0.224	√		pteropods
242	1.300	0.186	0.054	0.126	√		pteropods
243	1.960	0.284	0.084	0.190	√		pteropods
244	1.572	0.266	0.072	0.188			
245	2.124	0.362	0.096	0.252	√		pteropods
246	1.664	0.246	0.072	0.164	√		pteropods
247	1.702	0.262	0.074	0.182	√		pteropods
248	1.828	0.388	0.100	0.278	√		pteropods
249	0.872	0.038	0.004	0.034	√		lost most of sample, pteropods
250	1.689	0.574	0.205	0.360	√		pteropods
251	1.862	0.314	0.126	0.180	√	√	pteropods, ash
252	1.539	0.318	0.122	0.194	√		pteropods
253	2.368	0.496	0.186	0.294	√		pteropods
254	2.210	0.394	0.156	0.238	√		pteropods
255	2.556	0.458	0.162	0.292	√	√	pteropods, ash
256	3.018	0.510	0.184	0.324	√		pteropods
257	1.866	0.332	0.122	0.198	√	√	pteropods, ash
258	2.734	0.468	0.174	0.288	√		pteropods
259	3.382	0.614	0.250	0.358	√	√	pteropods, ash
260	1.353	0.361	0.133	0.210	√		pteropods
261	2.796	0.496	0.184	0.300	√		pteropods
262	2.666	0.584	0.206	0.372	√		pteropods
263	2.814	0.546	0.190	0.346	√		pteropods
264	2.466	0.548	0.166	0.360	√		pteropods
265	2.030	0.464	0.146	0.308	√		pteropods
266	2.706	0.568	0.180	0.382	√		pteropods

Sample (depth, cm)	Sample weight	weight >63µm	weight >63<150µm	weight >150µm	Pteropods	Ash	Comments
267	2.172	0.496	0.142	0.352	√		pteropods
268	1.644	0.446	0.142	0.300	√		pteropods
269	1.756	0.392	0.150	0.236	√		pteropods
270	1.320	0.412	0.143	0.257	√		pteropods
271	1.708	0.340	0.116	0.216	√		pteropods
272	1.710	0.296	0.120	0.176	√		pteropods
273	1.714	0.426	0.190	0.230	√		pteropods
274	3.106	0.784	0.344	0.432	√		pteropods
275	1.592	0.388	0.174	0.208	√		pteropods
276	2.090	0.506	0.232	0.260	√	√	pteropods, ash
277	1.938	0.548	0.236	0.306	√	√	pteropods, ash
278	2.924	0.794	0.450	0.334	√	√	pteropods, ash
279	3.888	1.180	0.728	0.442	√		pteropods
280	1.791	0.654	0.440	0.200	√	√	pteropods, ash
281	3.224	1.546	1.076	0.430	√	√	magnetite layer, pteropods
282	2.224	0.928	0.666	0.248	√	√	magnetite layer, pteropods
283	1.494	0.450	0.290	0.154	√	√	magnetite layer, pteropods
284	2.204	0.580	0.240	0.330	√	√	magnetite layer, pteropods
285	1.952	0.590	0.350	0.230	√		pteropods
286	1.402	0.364	0.140	0.214	√		pteropods
287	1.704	0.378	0.126	0.240	√		pteropods
288	3.230	0.738	0.272	0.458	√		pteropods
289	2.310	0.506	0.166	0.330	√		pteropods
290	1.561	0.448	0.164	0.272	√		pteropods
291	1.702	0.376	0.118	0.256	√		pteropods
292	2.076	0.376	0.108	0.266	√		pteropods
293	3.100	0.544	0.154	0.384	√		pteropods
294	2.526	0.386	0.106	0.270	√		pteropods
295	2.010	0.344	0.098	0.236	√		pteropods
296	2.192	0.376	0.102	0.264	√		pteropods
297	2.010	0.314	0.082	0.220	√		pteropods
298	1.608	0.254	0.070	0.182	√		pteropods
299	2.412	0.364	0.104	0.254	√		pteropods
300	1.803	0.448	0.126	0.318	√		pteropods
301	2.712	0.510	0.130	0.374	√		pteropods
302	1.446	0.208	0.066	0.140	√		pteropods
303	3.042	0.546	0.142	0.398	√		pteropods
304	2.040	0.376	0.100	0.274	√		pteropods
305	1.922	0.420	0.118	0.292	√		pteropods
306	1.300	0.268	0.070	0.192	√		pteropods
307	2.338	0.438	0.122	0.306	√		pteropods
308	2.626	0.558	0.158	0.394	√		pteropods
309	2.756	0.548	0.144	0.398	√		pteropods
310	1.312	0.381	0.123	0.233	√		pteropods
311	2.518	0.500	0.146	0.348	√		pteropods
312	2.076	0.454	0.120	0.324	√		pteropods
313	2.458	0.522	0.136	0.380	√		pteropods
314	2.262	0.442	0.128	0.308	√		pteropods

Sample (depth, cm)	Sample weight	weight >63µm	weight >63<150µm	weight >150µm	Pteropods	Ash	Comments
315	1.932	0.338	0.102	0.234	√		pteropods
316	1.022	0.184	0.058	0.118	√		pteropods
317	1.304	0.264	0.060	0.176	√		pteropods
318	1.708	0.364	0.104	0.256	√		pteropods
319	3.740	0.692	0.200	0.486	√		pteropods
320	1.542	0.306	0.097	0.199	√		pteropods
321	1.716	0.266	0.076	0.186	√		pteropods
322	1.048	0.178	0.048	0.124	√		pteropods
323	1.920	0.280	0.074	0.196	√		pteropods
324	2.746	0.716	0.118	0.310	√		pteropods
325	1.910	0.316	0.108	0.206	√		pteropods
326	2.018	0.294	0.090	0.198	√		pteropods
327	2.188	0.370	0.096	0.262	√		pteropods
328	2.504	0.488	0.132	0.344	√		pteropods
329	1.520	0.256	0.074	0.174	√		pteropods
330	1.951	0.310	0.102	0.202	√		pteropods
331	1.436	0.210	0.068	0.136	√		pteropods
332	1.490	0.164	0.054	0.108	√		pteropods
333	2.068	0.284	0.092	0.184	√		pteropods
334	3.490	0.462	0.152	0.302	√		pteropods
335	2.128	0.316	0.096	0.216	√		pteropods
336	1.600	0.276	0.084	0.186	√		pteropods
337	1.584	0.230	0.078	0.150	√		pteropods
338	3.350	0.358	0.150	0.202	√		pteropods
339	1.304	0.214	0.060	0.142	√		pteropods
340	1.329	0.238	0.082	0.146	√		pteropods
341	1.864	0.332	0.088	0.222	√		pteropods
342	0.930	0.330	0.092	0.228	√		pteropods
343	1.402	0.226	0.066	0.154	√		pteropods
344	1.874	0.340	0.098	0.230	√		pteropods
345	1.846	0.328	0.096	0.222	√		pteropods
346	2.260	0.422	0.136	0.278	√		pteropods
347	1.482	0.240	0.066	0.162	√		pteropods
348	1.564	0.246	0.076	0.158	√		pteropods
349	2.914	0.434	0.138	0.282	√		pteropods
350	1.820	0.329	0.105	0.210	√		pteropods
351	1.406	0.236	0.064	0.162	√		pteropods
352	1.756	0.272	0.082	0.182	√		pteropods
353	1.744	0.298	0.084	0.200	√		pteropods
354	1.844	0.268	0.076	0.176	√		pteropods
355	1.724	0.246	0.076	0.158	√		pteropods
356	1.180	0.208	0.070	0.144	√		pteropods
357	0.982	0.166	0.060	0.106	√		pteropods
358	1.658	0.268	0.094	0.174	√		pteropods
359	2.066	0.340	0.116	0.220	√		pteropods
360	0.878	0.139	0.035	0.095	√		pteropods
361	1.782	0.300	0.106	0.194	√		pteropods
362	2.494	0.398	0.144	0.252	√		pteropods

Sample (depth, cm)	Sample weight	weight >63µm	weight >63<150µm	weight >150µm	Pteropods	Ash	Comments
363	1.872	0.328	0.106	0.220	√		pteropods
364	1.672	0.254	0.084	0.170	√		pteropods
365	1.676	0.256	0.086	0.170	√		pteropods
366	2.226	0.278	0.088	0.186	√		pteropods
367	2.018	0.272	0.094	0.176	√		pteropods
368	2.669	0.416	0.132	0.286	√		pteropods
369	2.704	0.392	0.126	0.264	√		pteropods
370							missing
371	1.793	0.251	0.086	0.169	√		pteropods
372	1.568	0.176	0.058	0.116	√		pteropods
373	1.616	0.242	0.074	0.162	√		pteropods
374	2.856	0.494	0.148	0.344	√		pteropods
375	1.228	0.174	0.054	0.114	√		pteropocis
376	3.362	0.442	0.280	0.152	√	√	pteropods
377	1.964	0.328	0.220	0.096	√	√	pteropods, ash
378	2.424	0.400	0.124	0.264	√		pteropods
379	1.992	0.374	0.110	0.252	√		pteropods
380	1.515	0.269	0.065	0.185	√		Pteropods
381	1.658	0.290	0.082	0.198	√		pteropods
382	1.332	0.212	0.066	0.138	√		pteropods
383	1.426	0.240	0.070	0.164	√		pteropods
384	1.614	0.220	0.070	0.148	√	√	pteropods, ash
385	1.724	0.268	0.106	0.154	√		Pteropods
386	1.596	0.234	0.078	0.138	√		pteropods
387	0.738	0.126	0.042	0.076	√		pteropods
388	1.268	0.198	0.068	0.128	√		pteropods
389	1.082	0.174	0.060	0.106	√		pteropods
390	1.697	0.257	0.074	0.169	√		pteropods
391	1.084	0.156	0.054	0.096	√		pteropods
392	1.316	0.206	0.058	0.130	√		pteropods
393	1.082	0.176	0.050	0.120	√		pteropods
394	1.390			0.166	√		pteropods
395	1.278			0.124	√	√	pteropods, ash
396	1.302			0.146	√		pteropods
397	1.638			0.140	√		pteropods
398	2.010			0.214	√		pteropods
399	1.576			0.190	√		pteropods
400	2.315	0.407	0.103	0.294	√		pteropods
401	1.870			0.236	√		pteropods
402	2.574			0.280	√		pteropods
403	2.162			0.202	√		pteropods
404	3.056			0.356	√		pteropods
405	2.298			0.262	√		pteropods
406	2.398			0.304	√		pteropods
407	3.352			0.420	√		pteropods
408	3.576			0.396	√		pteropods
409	3.070			0.328	√		pteropods
410	1.806	0.428	0.127	0.288	√		pteropods

Sample (depth, cm)	Sample weight	weight >63µm	weight >63<150µm	weight >150µm	Pteropods	Ash	Comments
411	2.540			0.348	√		pteropods
412	2.466			0.304	√		pteropods
413	2.370			0.246	√		pteropods, ash(?)
414	2.116			0.232	√		pteropods, ash
415	1.946			0.256	√		pteropods, ash
416	2.386			0.208	√		pteropods, ash
417	2.150			0.238	√		pteropods, ash
418	2.334			0.234		√	ash
419	2.586			0.224	√		pteropods
420	1.402	0.262	0.047	0.210	√		pteropods
421	1.818			0.238	√	√	pteropods, ash
422	2.096			0.292	√	√	pteropods, ash
423	2.194			0.162	√		pteropods
424	1.038			0.024			
425	2.186			0.208			
426	1.548			0.152	√		pteropods
427	2.462			0.300	√		pteropods
428	1.554	0.178	0.048	0.130	√		pteropods
429	2.296	0.314	0.072	0.236	√		pteropods
430	2.083	0.328	0.066	0.254	√		pteropods
431	2.002	0.352	0.086	0.262	√		pteropods
432	2.498	0.200	0.048		√		pteropods
433	1.756	0.318	0.062	0.248	√		pteropods
434	1.488	0.220	0.050	0.164	√		pteropods
435	1.652	0.238	0.050	0.186	√		pteropods
436	2.160	0.386	0.076	0.306	√		pteropods
437	1.492	0.282	0.068	0.210			
438	1.218	0.386	0.088	0.290	√		pteropods
439	1.396	0.222	0.052	0.166	√		pteropods
440	1.662	0.231	0.041	0.180	√		pteropods
441	1.660	0.240	0.056	0.178	√		pteropods
442	1.970	0.274	0.070	0.194	√		pteropods
443	1.176	0.200	0.054	0.138	√		pteropods
444	2.204	0.290	0.082	0.202	√		pteropods
445	2.158	0.352	0.110	0.236	√		pteropods
446	1.572	0.218	0.050	0.162	√		pteropods
447	1.280	0.206	0.058	0.144	√		pteropods
448	1.716	0.270	0.078	0.184	√		pteropods
449	2.208	0.506	0.114	0.374	√		pteropods
450	2.798	0.467	0.078	0.383	√		pteropods
451	2.116	0.298	0.086	0.208			
452	2.712	0.412	0.108	0.304	√		pteropods
453	2.640	0.322	0.088	0.224	√		pteropods
454	2.186	0.326	0.082	0.240	√		pteropods
455	1.726	0.366	0.086	0.280	√		pteropods
456	1.424	0.262	0.066	0.194	√		pteropods
457	1.154	0.168	0.036	0.128	√		pteropods
458	1.736	0.274	0.070	0.202	√		pteropods

Sample (depth, cm)	Sample weight	weight >63µm	weight >63<150µm	weight >150µm	Pteropods	Ash	Comments
459	1.986	0.328	0.074	0.244	√		pteropods
460	1.613	0.279	0.048	0.223			
461	1.768	0.576	0.140	0.432	√		pteropods
462	1.740	0.286	0.062	0.218	√		pteropods
463	1.948	0.344	0.080	0.254	√		pteropods
464	2.032	0.186	0.040	0.146	√		pteropods
465	1.866	0.228	0.042	0.182	√		pteropods
466	1.974	0.282	0.042	0.232	√		pteropods
467	2.042	0.180	0.038	0.144	√		pteropods
468	2.086	0.338	0.060	0.270	√		pteropods
469	2.422	0.196	0.036	0.150	√		pteropods
470	2.382	0.327	0.050	0.269	√		pteropods
471	1.798	0.232	0.040	0.188	√		pteropods
472	1.798	0.228	0.044	0.180	√		pteropods
473	2.542	0.282	0.054	0.214	√		pteropods
474	1.980	0.202	0.034	0.162	√		pteropods
475	1.220	0.282	0.054	0.224	√		pteropods
476	2.408	0.220	0.040	0.170	√		pteropods
477	1.988	0.228	0.042	0.184	√		pteropods
478	1.844	0.200	0.038	0.158	√		pteropods
479	1.458	0.252	0.048	0.198	√		pteropods
480	1.341	0.178	0.042	0.133	√		pteropods
481	1.976	0.168	0.036	0.130	√		pteropods
482	2.860	0.250	0.052	0.192	√		pteropods
483	2.400	0.180	0.042	0.130	√		pteropods
484	3.042	0.152	0.036	0.118			
485	2.226	0.160	0.038	0.118	√		pteropods
486	2.792	0.166	0.038	0.124	√		pteropods
487	2.600	0.284	0.062	0.214	√		pteropods
488	2.468	0.218	0.050	0.162			
489	1.740	0.294	0.080	0.214			
490	1.496	0.208	0.062	0.139			
491	3.002	0.300	0.078	0.220			
492	2.402	0.264	0.072	0.188			
493	1.990	0.346	0.084	0.260			
494	1.876	0.236	0.052	0.180			
495	2.942	0.266	0.058	0.202			
496	2.684	0.122	0.024	0.088			
497	3.608	0.210	0.050	0.160			
498	2.422	0.188	0.044	0.134			
499	2.684	0.356	0.072	0.278			
500	1.809	0.475	0.171	0.285			
501	2.498	0.368	0.070	0.288			
502	3.014	0.308	0.066	0.234			
503	1.826	0.294	0.060	0.224			
504	2.244	0.234	0.048	0.182			
505	2.648	0.302	0.062	0.232			
506	2.770	0.254	0.050	0.188			

Sample (depth, cm)	Sample weight	weight >63µm	weight >63<150µm	weight >150µm	Pteropods	Ash	Comments
507	2.842	0.236	0.050	0.174			
508	2.960	0.222	0.040	0.170			
509	1.984	0.266	0.056	0.196			
510	1.156	0.205	0.056	0.133			
511	2.474	0.376	0.072	0.292			
512	2.604	0.238	0.044	0.176			
513	2.012	0.300	0.052	0.240			
514	2.590	0.272	0.066	0.192			
515	1.968	0.250	0.046	0.192			
516	1.874	0.262	0.050	0.204			
517	2.422	0.254	0.048	0.196			
518	2.860	0.190	0.038	0.144			
519	2.634	0.264	0.062	0.190			
520	1.907	0.287	0.084	0.200			
521	3.456	0.224	0.056	0.158			
522	2.880	0.164	0.040	0.122			
523	2.604	0.338	0.082	0.250			
524	1.884	0.232	0.054	0.176			
525	2.476	0.382	0.094	0.278			
526	2.688	0.188	0.046	0.132			
527	3.026	0.384	0.080	0.296			
528	1.974	0.228	0.056	0.162			
529	2.228	0.422	0.110	0.302			
530	2.396	0.339	0.089	0.249			
531	2.846	0.398	0.104	0.282			
532	2.704	0.256	0.064	0.182			
533	3.610	0.558	0.134	0.418			
534	2.384	0.374	0.100	0.268			
535	3.274	0.456	0.122	0.336			
536	2.328	0.356	0.088	0.264			
537	1.752	0.256	0.062	0.188			
538	2.690	0.426	0.106	0.312			
539	2.072	0.330	0.074	0.244			
540	2.905	0.417	0.114	0.298			
541	2.642	0.380	0.096	0.274			
542	1.628	0.282	0.076	0.202			
543	2.308	0.406	0.094	0.310			
544	2.818	0.470	0.116	0.344			
545	2.330	0.400	0.088	0.306			
546	1.896	0.290	0.060	0.222			
547	2.430	0.430	0.090	0.326			
548	1.782	0.296	0.058	0.222			
549	1.616	0.236	0.048	0.178			
550	2.475	0.405	0.088	0.311			
551	2.336	0.448	0.092	0.346			
552	1.994	0.390	0.086	0.252			
553	1.936	0.346	0.078	0.266			
554	2.676	0.466	0.088	0.368	√		pteropods?

Sample (depth, cm)	Sample weight	weight >63µm	weight >63<150µm	weight >150µm	Pteropods	Ash	Comments
555	1.982	0.290	0.056	0.222			
556	1.784	0.224	0.056	0.164	√		pteropods?
557	3.384	0.514	0.118	0.368			
558	2.382	0.338	0.084	0.214			
559	2.460	0.308	0.078	0.226			
560	2.153	0.404	0.094	0.209	√		pteropods
561	1.494	0.218	0.054	0.162	√		pteropods
562	2.872	0.450	0.104	0.340	√		pteropods
563	2.692	0.348	0.090	0.254	√		pteropods
564	3.434	0.478	0.118	0.350			
565	2.726	0.442	0.116	0.322			
566	3.346	0.544	0.118	0.416			
567	1.798	0.286	0.064	0.216			
568	2.170	0.346	0.078	0.260			
569	2.654	0.302	0.084	0.210			
570	2.097	0.298	0.073	0.223			
571	2.078	0.334	0.086	0.240			
572	2.232	0.370	0.084	0.274			
573	2.946	0.470	0.122	0.338			
574	3.728	0.540	0.138	0.394			
575	2.826	0.376	0.102	0.264			
576	2.808	0.422	0.112	0.298			ash (?)
577	2.118	0.296	0.074	0.210			
578	2.844	0.482	0.126	0.348			
579	2.450	0.354	0.100	0.246			
580	2.264	0.315	0.087	0.227			
581	2.152	0.292	0.080	0.208			
582	2.242	0.392	0.150	0.208			
583	2.196	0.294	0.070	0.212			
584	2.228	0.326	0.018	0.230			
585	2.258	0.346	0.084	0.254			
586	2.224	0.360	0.076	0.282			
587	2.212	0.324	0.078	0.240			
588	2.518	0.386	0.100	0.282			
589	2.194	0.290	0.082	0.194			
590	2.561	0.327	0.090	0.234			
591	2.022	0.302	0.070	0.220			
592	2.048	0.298	0.070	0.222			
593	2.770	0.454	0.130	0.312			
594	2.902	0.552	0.146	0.394			
595	2.288	0.488	0.146	0.326			
596	2.880	0.576	0.184	0.390			
597	2.076	0.404	0.128	0.264			ash (?)
598	2.918	0.590	0.204	0.380			ash (?)
599	1.528	0.296	0.120	0.166			
600	2.057	0.339	0.109	0.227			
601	2.120	0.332	0.112	0.212			
602	2.332	0.348	0.128	0.216		√	ash

Sample (depth, cm)	Sample weight	weight >63µm	weight >63<150µm	weight >150µm	Pteropods	Ash	Comments
603	2.702	0.438	0.114	0.304			
604	2.996	0.522	0.142	0.368			
605	2.188	0.368	0.102	0.264			
606	2.074	0.330	0.098	0.230			
607	1.970	0.322	0.086	0.230			
608	2.256	0.366	0.100	0.260			
609	1.810	0.324	0.076	0.240			
610	2.627	0.454	0.123	0.329			
611	2.256	0.426	0.106	0.306			
612	2.106	0.330	0.102	0.224			
613	1.976	0.302	0.054	0.240			
614	3.006	0.362	0.096	0.256			
615	1.752	0.268	0.068	0.196			
616	1.876	0.266	0.076	0.184			
617	1.572	0.248	0.066	0.176			
618	2.276	0.420	0.094	0.306			
619	1.936	0.290	0.072	0.214			
620	1.820	0.281	0.065	0.213			
621	2.526	0.502	0.118	0.382			
622	1.310	0.250	0.056	0.192			
623	2.804	0.444	0.094	0.340			
624	2.850	0.4.44	0.110	0.328			
625	1.788	0.324	0.074	0.246			
626	2.586	0.376	0.094	0.278			
627	2.164	0.292	0.078	0.210			
628	1.458	0.248	0.058	0.184			
629	2.008	0.294	0.080	0.208			
630	1.747	0.231	0.064	0.166			
631	3.182	0.424	0.110	0.310			
632	1.762	0.228	0.062	0.160			
633	1.774	0.270	0.026	0.234			
634	2.054	0.322	0.084	0.236			
635	1.776	0.274	0.042	0.228			
636	1.050	0.186	0.058	0.122			
637	1.616	0.260	0.060	0.194			
638	2.582	0.374	0.098	0.268			
639	1.286	0.214	0.066	0.146			
640	2.232	0.323	0.083	0.237			
641	2.064	0.366	0.090	0.268			
642	1.836	0.260	0.072	0.180			
643	2.254	0.304	0.088	0.210			
644	2.468	0.392	0.104	0.282			
645	2.082	0.326	0.082	0.232			
646	1.570	0.258	0.064	0.184			
647	2.368	0.396	0.112	0.270			
648	2.102	0.302	0.078	0.220			
649	1.810	0.266	0.076	0.184			
650	1.889	0.259	0.080	0.176			

Sample (depth, cm)	Sample weight	weight >63µm	weight >63<150µm	weight >150µm	Pteropods	Ash	Comments
651	1.812	0.294	0.074	0.206			
652	2.364	0.452	0.108	0.336			
653	2.250	0.398	0.100	0.292			
654	3.290	0.496	0.126	0.366			
655	1.236	0.218	0.054	0.162			
656	1.260	0.184	0.046	0.134			
657	1.146	0.168	0.044	0.122			
658	1.894	0.336	0.084	0.240			
659	1.164	0.204	0.058	0.141			
660	1.224	0.215	0.051	0.163			
661	1.744	0.292	0.076	0.210			
673	1.233	0.224	0.052	0.170			
674	1.404	0.296	0.076	0.214			
675	2.044	0.458	0.110	0.338			
676	1.424	0.300	0.076	0.218			
677	1.972	0.304	0.080	0.202			
678	2.316	0.414	0.144	0.262		√	ash
679	1.966	0.348	0.114	0.226		√	ash
680	2.076	0.308	0.119	0.187		√	ash
681	2.232	0.376	0.130	0.234		√	ash
682	1.686	0.374	0.142	0.222		√	ash
683	2.714	0.516	0.128	0.334		√	ash
684	2.096	0.356	0.102	0.252		√	ash
685	1.880	0.314	0.094	0.218		√	ash
686	2.094	0.250	0.126	0.122		√	ash
687	2.020	0.270	0.086	0.182		√	ash
688	3.898	0.592	0.170	0.416		√	ash
689	1.950	0.312	0.100	0.204		√	ash
690	1.995	0.298	0.073	0.201			
691	3.062	0.492	0.144	0.342			
692	2.420	0.458	0.118	0.334			
693	2.720	0.468	0.134	0.326			
694	1.966	0.348	0.094	0.244			
695	3.122	0.380	0.102	0.272			
696	2.174	0.400	0.106	0.290			
697	1.802	0.330	0.080	0.244			
698	2.508	0.400	0.114	0.284			
699	3.776	0.235	0.030	0.204			
700	1.798	0.212	0.064	0.149			
701	1.928	0.208	0.064	0.140			
702	1.746	0.490	0.156	0.324			
703	3.086	0.488	0.170	0.306			
704	3.022	0.352	0.110	0.232			
705	1.582	0.208	0.074	0.128			
706	1.410	0.210	0.066	0.142			
707	2.130	0.280	0.082	0.194			
708	2.922	0.410	0.108	0.292			
709	3.720	0.544	0.144	0.396			

Sample (depth, cm)	Sample weight	weight >63µm	weight >63<150µm	weight >150µm	Pteropods	Ash	Comments
710	2.058	0.261	0.072	0.187			
711	2.520	0.346	0.106	0.228			
712	2.128	0.342	0.122	0.212			
713	1.980	0.202	0.064	0.136			
714	3.228	0.412	0.130	0.276			
715	1.696	0.234	0.068	0.160			
716	1.696	0.258	0.064	0.188			
717	2.900	0.440	0.124	0.310			
718	3.168	0.452	0.120	0.322			
719	5.044	0.808	0.228	0.572			
720	2.203	0.322	0.088	0.229			
721	1.924	0.346	0.092	0.246			
722	2.178	0.334	0.092	0.236			
723	2.652	0.428	0.122	0.300			
724	2.576	0.392	0.104	0.282			
725	2.704	0.410	0.122	0.284			
726	2.290	0.452	0.124	0.324			
727	1.960	0.334	0.096	0.232			
728	2.882	0.542	0.148	0.386			
729	4.032	0.654	0.196	0.450			
730	2.312	0.369	0.085	0.243			
731	2.524	0.430	0.104	0.322			
732	2.548	0.510	0.124	0.384			
733	3.016	0.494	0.126	0.362			
734	4.042	0.490	0.144	0.336			
735	1.774	0.287	0.068	0.208			
736	2.500	0.378	0.120	0.254			
737	3.566	0.492	0.134	0.352			
738	2.904	0.380	0.118	0.260			
739	3.074	0.458	0.122	0.332			
740	2.632	0.395	0.088	0.302			
741	2.690	0.370	0.098	0.266			
742	2.666	0.334	0.074	0.246			
743	2.128	0.338	0.108	0.228			
744	3.082	0.480	0.124	0.348			
745	3.220	0.594	0.136	0.450			
746	1.658	0.246	0.062	0.162			
747	2.344	0.352	0.098	0.244			
748	3.184	0.564	0.110	0.452			
749	2.740	0.348	0.086	0.252			
750	2.187	0.327	0.077	0.250			
751	2.376	0.342	0.082	0.256			
752	1.724	0.208	0.058	0.148			
753	2.204	0.298	0.076	0.216			
754	2.752	0.374	0.096	0.278			
755	1.826	0.238	0.060	0.176			
756	3.048	0.422	0.092	0.324			
757	2.162	0.338	0.074	0.260			

Sample (depth, cm)	Sample weight	weight >63µm	weight >63<150µm	weight >150µm	Pteropods	Ash	Comments
758	2.118	0.244	0.058	0.184			
759	1.994	0.284	0.066	0.214			
760	2.313	0.271	0.074	0.195			
761	2.678	0.246	0.070	0.178			
762	2.438	0.376	0.088	0.284			
763	2.038	0.286	0.074	0.208			
764	2.066	0.302	0.086	0.214			
765	1.470	0.206	0.052	0.150			
766	0.980	0.172	0.040	0.130			
767	2.520	0.438	0.096	0.334			
768	2.386	0.400	0.088	0.302			
769	3.316	0.580	0.122	0.456			
770	1.757	0.250	0.065	0.179			
771	1.302	0.252	0.066	0.182			
772	1.798	0.320	0.074	0.242			
773	2.116	0.402	0.088	0.308			
774	2.190	0.420	0.092	0.322			
775	1.250	0.226	0.046	0.176			
776	1.648	0.252	0.066	0.184			
777	3.316	0.468	0.106	0.358			
778	1.898	0.318	0.086	0.228			
779	1.758	0.320	0.080	0.236			
780	1.498	0.275	0.058	0.213			
781	1.548	0.306	0.070	0.234			
782	2.288	0.456	0.108	0.346			
783	2.130	0.346	0.082	0.262			
784	3.272	0.550	0.126	0.420			
785	1.586	0.238	0.052	0.178			silica spikes, sponge
786	2.246	0.436	0.084	0.352			silica spikes, sponge
787	1.458	0.298	0.052	0.242			
788	2.136	0.355	0.094	0.250			
789	2.072	0.316	0.084	0.226			
790	1.856	0.231	0.055	0.173			
791	2.566	0.398	0.098	0.296			
792	2.008	0.300	0.074	0.222			
793	2.290	0.286	0.074	0.214			
794	1.512	0.204	0.066	0.138			
795	2.042	0.370	0.090	0.278			
796	2.428	0.496	0.102	0.388			
797	2.800	0.566	0.118	0.436			
798	3.164	0.410	0.094	0.314			
799	2.360	0.816	0.126	0.684			
800	2.213	0.475	0.109	0.364			
801	2.264	0.524	0.096	0.424			
802	1.788	0.338	0.078	0.260			
803	1.868	0.378	0.078	0.302			
804	1.842	0.366	0.080	0.284			
805	2.270	0.392	0.090	0.292			

Sample (depth, cm)	Sample weight	weight >63µm	weight >63<150µm	weight >150µm	Pteropods	Ash	Comments
806	2.030	0.356	0.084	0.264			
807	1.836	0.284	0.076	0.204			
808	1.804	0.400	0.074	0.316			
809	3.784	0.796	0.154	0.632			
810	1.886	0.417	0.080	0.330			
811	3.102	0.528	0.122	0.400			
812	2.056	0.384	0.084	0.294			
813	3.392	0.600	0.138	0.456			
814	2.904	0.536	0.122	0.356			
815	3.084	0.542	0.124	0.416			
816	3.300	0.584	0.142	0.440			
817	2.388	0.438	0.114	0.320			
818	3.582	0.630	0.144	0.480			
819	2.514	0.422	0.100	0.314			
820	2.016	0.383	0.103	0.278			
821	2.904	0.558	0.124	0.428			
822	2.530	0.522	0.104	0.416			
823	3.392	0.628	0.154	0.468			
824	4.270	0.670	0.160	0.506			
825	3.622	0.620	0.146	0.462			
826	2.690	0.436	0.096	0.338			
827	2.276	0.380	0.096	0.282			
828	2.312	0.368	0.092	0.270			
829	3.402	0.398	0.092	0.300			
830	2.690	0.438	0.106	0.330			
831	3.394	0.444	0.070	0.370			
832	2.842	0.520	0.124	0.394			
833	4.222	0.578	0.144	0.432			
834	3.216	0.472	0.142	0.338			
835	3.232	0.558	0.132	0.420			
836	3.014	0.550	0.146	0.404			
837	3.954	0.768	0.162	0.604			
838	2.224	0.294	0.076	0.216			
839	4.576	1.076	0.154	0.918			
840	2.111	0.489	0.096	0.388			
841	4.250	0.786	0.188	0.594			
842	2.322	0.616	0.118	0.494			
843	3.510	0.752	0.136	0.610			
844	2.754	0.608	0.134	0.474			
845	3.440	0.640	0.180	0.456			
846	2.472	0.358	0.094	0.260			
847	4.216	0.602	0.156	0.442			
848	3.840	0.606	0.168	0.434			
849	3.894	0.556	0.172	0.380			
850	1.809	0.297	0.103	0.191			
851	3.452	0.494	0.150	0.338			
852	2.806	0.424	0.130	0.294			
853	3.662	0.468	0.136	0.326			

Sample (depth, cm)	Sample weight	weight >63µm	weight >63<150µm	weight >150µm	Pteropods	Ash	Comments
854	3.188	0.488	0.120	0.352			
855	3.232	0.480	0.144	0.330			
856	2.104	0.310	0.082	0.220			
857	2.710	0.426	0.106	0.308			
858	2.764	0.674	0.122	0.306			
859	4.404	0.827	0.210	0.614			
860	1.717	0.274	0.076	0.196			
861	3.638	0.534	0.152	0.376			
862	1.850	0.310	0.088	0.220			
863	3.502	0.680	0.152	0.524			
864	2.636	0.488	0.114	0.360			
865	2.682	0.382	0.104	0.268			
866	1.946	0.424	0.088	0.336			ash (?)
867	2.112	0.410	0.114	0.294			
868	2.576	0.476	0.105	0.368			
869	1.696	0.320	0.078	0.234			
870	3.149	0.573	0.139	0.431			
871	2.028	0.370	0.082	0.278			
872	2.930	0.524	0.116	0.398			
873	2.442	0.296	0.078	0.212			
874	2.628	0.224	0.056	0.162			
875	2.580	0.258	0.076	0.180			
876	2.346	0.278	0.074	0.202			
877	2.616	0.312	0.084	0.224			
878	3.014	0.470	0.124	0.346			
879	3.266	0.498	0.136	0.358			
880	2.455	0.327	0.101	0.225			
881	2.718	0.386	0.106	0.270			
882	1.806	0.308	0.074	0.228			pteropods
883	2.962	0.422	0.116	0.284			
884	3.604	0.662	0.168	0.494			
885	2.132	0.336	0.086	0.246			pteropods
886	4.376	0.786	0.168	0.606			pteropods
887	3.102	0.698	0.154	0.528			
888	2.310	0.484	0.110	0.370			
889	3.906	0.710	0.166	0.540			
890	2.136	0.460	0.138	0.320			
891	4.030	0.854	0.206	0.640			
892	1.856	0.330	0.094	0.236			
893	3.078	0.582	0.140	0.434			
894	2.932	0.600	0.154	0.436			
895	2.328	0.466	0.116	0.348			
896	2.408	0.530	0.132	0.386			
897	1.828	0.356	0.102	0.242			
898	2.992	0.590	0.176	0.398			
899	1.398	0.356	0.106	0.242			
900	1.883	0.415	0.097	0.318			
901	1.640	0.408	0.096	0.308			

Sample (depth, cm)	Sample weight	weight >63µm	weight >63<150µm	weight >150µm	Pteropods	Ash	Comments
902	1.986	0.378	0.092	0.282			
903	2.440	0.502	0.136	0.360			
904	2.692	0.478	0.166	0.310		√	ash
905	4.124	0.744	0.258	0.478		√	ash
906	2.498	0.398	0.240	0.158		√	ash
907	2.666	0.620	0.200	0.412		√	ash
908	3.402	0.544	0.134	0.408			
909	1.854	0.646	0.148	0.494			
910	2.000	0.394	0.092	0.301			
911	2.186	0.524	0.138	0.380			
912	1.606	0.300	0.078	0.216			
913	2.418	0.458	0.126	0.326			
914	1.928	0.406	0.144	0.260			
915	1.558	0.292	0.080	0.208			
916	1.804	0.298	0.098	0.198			
917	2.216	0.414	0.116	0.292			
918	2.194	0.364	0.106	0.256			
919	2.772	0.452	0.132	0.314			
920	3.010	0.563	0.150	0.411			
921	2.122	0.288	0.084	0.196			
922	2.932	0.544	0.128	0.414			
923	2.542	0.424	0.108	0.308			
924	2.464	0.400	0.106	0.290			
925	2.302	0.370	0.096	0.264			
926	1.814	0.262	0.070	0.192			
927	1.170	0.206	0.048	0.150			
928	1.706	0.352	0.062	0.280			
929	2.176	0.286	0.078	0.204			
930	1.983	0.331	0.086	0.244			
931	2.234	0.240	0.072	0.166			
932	1.840	0.228	0.052	0.168			
933							missing
934							missing
935							missing
936	1.792	0.278	0.066	0.212			
937							missing
938							missing
939							missing
940	2.915	0.472	0.123	0.349			
941	2.380	0.404	0.092	0.310			
942	2.058	0.340	0.078	0.256			
943	2.444	0.326	0.084	0.236			
944	2.454	0.330	0.094	0.230			
945	2.768	0.516	0.114	0.400			
946	1.374	0.238	0.056	0.182			
947	1.920	0.354	0.080	0.266			
948	2.174	0.446	0.096	0.348			
949	1.992	0.354	0.084	0.264			

Sample (depth, cm)	Sample weight	weight >63µm	weight >63<150µm	weight >150µm	Pteropods	Ash	Comments
950	2.341	0.417	0.105	0.311			
951	2.142	0.372	0.092	0.278			
952	2.810	0.514	0.124	0.388			
953	1.638	0.292	0.070	0.220			
954	3.118	0.416	0.118	0.296			
955	1.894	0.314	0.078	0.230			
956	1.920	0.318	0.076	0.236			
957	1.480	0.268	0.054	0.212			
958	1.610	0.254	0.052	0.198			
959	2.258	0.344	0.078	0.266			
960	1.645	0.326	0.067	0.257			
961	2.742	0.380	0.088	0.284			
962	2.058	0.342	0.080	0.260			
963	2.040	0.236	0.060	0.174			
964	2.242	0.150	0.050	0.098			
965	2.516	0.174	0.066	0.100			
966	2.002	0.214	0.070	0.142			
967	1.396	0.126	0.040	0.082			
968	2.324	0.270	0.072	0.192			
969	2.404	0.288	0.074	0.212			
970	2.500	0.413	0.101	0.308			
971	2.238	0.176	0.052	0.118			
972	1.848	0.242	0.062	0.170			
973	2.600	0.392	0.082	0.308			
974	2.536	0.372	0.084	0.278			
975	2.876	0.430	0.106	0.318			
976	2.112	0.296	0.068	0.222			
977	2.370	0.326	0.076	0.242			
978	1.950	0.242	0.062	0.172			
979	1.790	0.372	0.086	0.284			
980	2.382	0.339	0.084	0.253			
981	1.700	0.242	0.060	0.180			
982	2.378	0.242	0.060	0.178			
983	3.062	0.500	0.110	0.382			
984	2.018	0.310	0.072	0.232			
985	1.706	0.250	0.054	0.190			
986	1.742	0.298	0.060	0.226			
987	2.242	0.378	0.076	0.296			
988	2.834	0.648	0.110	0.530			
989	2.596	0.530	0.096	0.428			
990	2.042	0.423	0.078	0.342			
991	1.640	0.338	0.064	0.266			
992	2.620	0.518	0.092	0.418			
993	1.448	0.236	0.054	0.180			
994	2.682	0.492	0.092	0.392			
995	1.976	0.304	0.062	0.238			
996	2.514	0.224	0.062	0.154			
997	2.292	0.352	0.080	0.272			

Sample (depth, cm)	Sample weight	weight >63µm	weight >63<150µm	weight >150µm	Pteropods	Ash	Comments
998	2.316	0.332	0.076	0.254			
999	3.194	0.396	0.100	0.290			
1000	2.154	0.282	0.073	0.209			
1001	2.790	0.384	0.090	0.288			silica spikes, mollusk shells, sponge
1002	2.694	0.298	0.076	0.218			silica spikes, sponge
1003	3.028	0.268	0.074	0.184			
1004	3.362	0.320	0.092	0.224			silica spikes, sponge
1005	3.034	0.432	0.096	0.326			
1006	2.614	0.368	0.090	0.274			
1007	2.532	0.354	0.080	0.266			
1008	3.580	0.408	0.120	0.286			
1009	4.172	0.524	0.132	0.386			
1010	1.466	0.261	0.057	0.201			
1011	2.234	0.338	0.080	0.256			
1012	2.406	0.332	0.076	0.250			
1013	3.386	0.526	0.110	0.408			
1014	3.512	0.582	0.118	0.450			
1015	2.788	0.414	0.082	0.322			
1016	1.988	0.352	0.072	0.274			
1017	1.636	0.304	0.068	0.234			
1018	3.760	0.564	0.130	0.430			
1019	1.916	0.304	0.064	0.232			
1020	1.759	0.291	0.066	0.224			
1021	2.168	0.394	0.084	0.314			
1022	1.976	0.582	0.108	0.474			
1023	2.690	0.660	0.118	0.540			
1024	3.034	0.788	0.138	0.644			
1025	1.982	0.376	0.078	0.296			
1026	2.260	0.388	0.080	0.300			
1027	1.914	0.336	0.080	0.256			silica spikes
1028	2.296	0.332	0.062	0.268			
1029	2.652	0.336	0.066	0.266			
1030	1.728	0.240	0.046	0.192			
1031	3.342	0.336	0.074	0.260			
1032	1.898	0.270	0.048	0.216			
1033	2.272	0.304	0.060	0.242			
1034	2.476	0.348	0.066	0.282			
1035	1.964	0.306	0.066	0.232			
1036	2.340	0.364	0.058	0.300			
1037	2.460	0.402	0.074	0.322			
1038	2.940	0.444	0.086	0.356			
1039	2.570	0.350	0.064	0.280			
1040	1.020	0.189	0.033	0.155			
1041	3.000	0.400	0.074	0.326			
1042	1.702	0.288	0.052	0.230			
1043	2.592	0.382	0.068	0.312			
1044	2.236	0.312	0.058	0.250			

Sample (depth, cm)	Sample weight	weight >63µm	weight >63<150µm	weight >150µm	Pteropods	Ash	Comments
1045	2.238	0.328	0.068	0.252			
1046	1.944	0.268	0.056	0.212			
1047	1.552	0.234	0.048	0.184			
1048	2.068	0.288	0.048	0.234			
1049	2.542	0.414	0.074	0.340			
1050	1.389	0.230	0.049	0.181			
1051	2.502	0.464	0.078	0.382			
1052	2.252	0.318	0.062	0.250			
1053	2.696	0.434	0.072	0.360			
1054	2.406	0.342	0.064	0.274			
1055	2.730	0.418	0.080	0.330			
1056	2.180	0.318	0.062	0.250			
1057	1.884	0.274	0.060	0.214			
1058	2.102	0.308	0.062	0.242			
1059	1.910	0.264	0.056	0.206			
1060	1.660	0.356	0.086	0.267			
1061	2.960	0.246	0.044	0.196			
1062	3.348	0.304	0.058	0.246			
1063	2.368	0.272	0.054	0.216			
1064	2.214	0.300	0.060	0.238			
1065	2.826	0.358	0.060	0.290			
1066	3.836	0.516	0.100	0.410			
1067	2.042	0.274	0.060	0.214			
1068	2.754	0.390	0.080	0.306			
1069	2.110	0.316	0.064	0.248			
1070	2.008	0.346	0.061	0.280			
1071	2.292	0.338	0.068	0.264			
1072	3.334	0.548	0.108	0.436			
1073	2.206	0.284	0.062	0.218			
1074	2.446	0.324	0.070	0.260			
1075	2.624	0.384	0.082	0.296			
1076	1.802	0.240	0.058	0.182			
1077	3.778	0.566	0.112	0.452			
1078	1.502	0.220	0.046	0.174			
1079	5.144	0.748	0.156	0.588			
1080	1.564	0.284	0.054	0.230			
1081	2.482	0.342	0.072	0.264			
1082	3.280	0.454	0.108	0.340			
1083	2.520	0.318	0.074	0.238			
1084	2.518	0.360	0.078	0.276			
1085	1.922	0.278	0.054	0.218			
1086	1.588	0.194	0.046	0.146			
1087	2.934	0.358	0.088	0.268			
1088	4.442	0.614	0.128	0.472			
1089	3.756	0.512	0.106	0.396			
1090	1.746	0.298	0.062	0.236			
1091	3.102	0.434	0.094	0.338			
1092	3.580	0.444	0.098	0.338			

Sample (depth, cm)	Sample weight	weight >63µm	weight >63<150µm	weight >150µm	Pteropods	Ash	Comments
1093	2.532	0.312	0.074	0.242			
1094	2.478	0.286	0.068	0.214			
1095	2.228	0.216	0.056	0.160			
1096	3.170	0.404	0.086	0.314			
1097	2.340	0.296	0.062	0.224			
1098	4.722	0.524	0.120	0.398			
1099	4.916	0.586	0.128	0.452			
1100	2.359	0.370	0.084	0.286			
1101	4.302	0.500	0.120	0.372			
1102	4.220	0.476	0.114	0.360			
1103	2.500	0.326	0.078	0.240			
1104	4.318	0.594	0.134	0.458			
1105	3.400	0.452	0.106	0.344			
1106	3.798	0.494	0.118	0.372			
1107	2.546	0.304	0.070	0.232			
1108	2.926	0.304	0.074	0.228			
1109	3.278	0.278	0.068	0.202			
1110	1.138	0.112	0.032	0.080			
1111	1.346	0.070	0.024	0.042			
1112	2.290	0.164	0.046	0.116			
1113	3.384	0.286	0.068	0.216			
1114	2.522	0.238	0.062	0.174			
1115	1.476	0.092	0.030	0.058			
1116	2.432	0.176	0.054	0.118			
1117	2.374	0.182	0.050	0.132			
1118	3.650	0.182	0.060	0.118			
1119	2.812	0.382	0.082	0.296			many broken shells, few whole forams
1120	0.982	0.190	0.046	0.146		√	ash
1121	2.290	0.202	0.052	0.148		√	ash
1122	2.136	0.290	0.066	0.224		√	ash
1123	6.926	0.600	0.148	0.442		√	ash
1124	3.430	0.266	0.078	0.188		√	ash
1125	2.392	0.158	0.046	0.110		√	ash
1126	2.310	0.210	0.062	0.148		√	ash
1127	1.438	0.108	0.032	0.072		√	ash
1128	2.902	0.154	0.046	0.100		√	ash
1129	2.860	0.144	0.046	0.096		√	ash
1130	1.041	0.128	0.030	0.094			
1131	1.856	0.094	0.032	0.056			few whole forams
1132	3.518	0.290	0.076	0.212			silica spikes -> sponge
1133	3.384	0.248	0.060	0.184			
1134	2.244	0.084	0.026	0.052			
1135	3.642	0.168	0.060	0.106			
1136	2.548	0.140	0.040	0.100		√	ash, many broken shells
1137	2.744	0.106	0.040	0.066		√	ash, many broken shells
1138	2.876	0.084	0.030	0.052		√	ash, many broken shells
1139	2.672	0.164	0.056	0.108		√	ash

Sample (depth, cm)	Sample weight	weight >63µm	weight >63<150µm	weight >150µm	Pteropods	Ash	Comments
1140	1.724	0.226	0.052	0.164			
1141	3.466	0.328	0.096	0.230			
1142	3.114	0.262	0.084	0.172			silica spikes - ash
1143	4.346	0.372	0.108	0.260			silica spikes - ash
1144	3.744	0.416	0.098	0.310			silica spikes - ash
1145	1.664	0.150	0.046	0.104			silica spikes
1146	2.558	0.210	0.056	0.150			many broken shells, silica spikes
1147	2.170	0.140	0.056	0.078			many broken shells, silica spikes
1148	3.594	0.184	0.072	0.108			many broken shells, silica spikes
1149	2.982	0.148	0.060	0.084			many broken shells, silica spikes
1150	2.255	0.366	0.064	0.300			many broken shells
1151	1.974	0.142	0.050	0.086			many broken shells
1152	1.304	0.068	0.026	0.040			many broken shells
1153	3.612	0.252	0.086	0.164			many broken shells
1154	3.024	0.166	0.058	0.106			many broken shells
1155	2.198	0.072	0.036	0.030			many broken shells
1156	1.536	0.054	0.028	0.022			many broken shells
1157	2.288	0.082	0.048	0.032			many broken shells
1158	3.394	0.146	0.066	0.082			many broken shells
1159	3.508	0.196	0.068	0.126			many broken shells
1160	1.859	0.362	0.060	0.298			many broken shells
1161	2.362	0.160	0.056	0.102			many broken shells
1162	3.056	0.202	0.062	0.130		√	ash, many broken shells
1163	3.850	0.244	0.074	0.160		√	ash, many broken shells
1164	2.314	0.118	0.044	0.068		√	ash, many broken shells
1165	3.520	0.168	0.062	0.102		√	ash, many broken shells
1166	1.922	0.110	0.040	0.066		√	ash, many broken shells
1167	2.254	0.156	0.052	0.100		√	ash
1168	2.478	0.204	0.064	0.132		√	ash
1169	3.658	0.126	0.046	0.078		√	ash
1170	2.432	0.408	0.086	0.318			
1171	3.026	0.202	0.054	0.142		√	ash
1172	2.036	0.088	0.026	0.058		√	ash
1173	2.466	0.104	0.032	0.072		√	ash
1174	1.956	0.090	0.028	0.056		√	ash
1175	2.718	0.140	0.044	0.092		√	ash
1176	3.198	0.136	0.048	0.088		√	ash
1177	4.236	0.192	0.062	0.126		√	ash
1178	3.706	0.220	0.058	0.160		√	ash
1179	3.128	0.128	0.048	0.078		√	ash
1180	1.893	0.220	0.036	0.184			
1181	2.734	0.132	0.034	0.088			
1182	2.016	0.102	0.034	0.066			many broken shells
1183	1.530	0.056	0.026	0.028			many broken shells

Sample (depth, cm)	Sample weight	weight >63µm	weight >63<150µm	weight >150µm	Pteropods	Ash	Comments
1184	3.092	0.130	0.038	0.086		√	ash
1185	2.170	0.094	0.032	0.058		√	ash
1186	2.328	0.142	0.046	0.092		√	ash
1187	2.808	0.148	0.048	0.096		√	ash
1188	2.792	0.174	0.062	0.108		√	ash
1189	2.692	0.246	0.062	0.174			
1190	2.232	0.314	0.050	0.264			
1191	2.552	0.142	0.048	0.090		√	ash
1192	1.364	0.070	0.026	0.040		√	ash
1193	2.560	0.184	0.054	0.128		√	ash
1194	2.366	0.140	0.046	0.094		√	ash
1195	1.980	0.180	0.050	0.128		√	ash
1196	2.474	0.122	0.048	0.072		√	ash
1197	2.234	0.154	0.054	0.100		√	ash
1198	2.536	0.100	0.034	0.064		√	ash
1199	2.356	0.116	0.040	0.070		√	ash
1200	1.512	0.118	0.018	0.100		√	ash
1201	2.664	0.142	0.050	0.088		√	ash
1202	2.278	0.108	0.038	0.066		√	ash
1203	3.760	0.194	0.064	0.128		√	ash
1204	2.704	0.200	0.060	0.140		√	ash
1205	2.920	0.100	0.040	0.058		√	ash, many broken shells
1206	2.614	0.112	0.038	0.072		√	ash
1207	2.716	0.136	0.040	0.082			
1208	2.992	0.132	0.050	0.082			
1209	2.870	0.172	0.050	0.116		√	ash, many broken shells
1210	2.483	0.330	0.064	0.266			
1211	2.304	0.268	0.074	0.190			
1212	3.412	0.452	0.106	0.344			
1213	3.634	0.458	0.102	0.352			
1214	3.782	0.506	0.108	0.396			
1215	2.674	0.432	0.088	0.342			
1216	3.122	0.404	0.092	0.310			
1217	3.236	0.464	0.106	0.358			
1218	2.434	0.344	0.080	0.264			
1219	2.672	0.364	0.094	0.266			
1220	1.430	0.230	0.026	0.204			
1221	2.216	0.288	0.076	0.210			
1222	1.568	0.190	0.062	0.128			
1223	2.750	0.344	0.080	0.248			
1224	2.140	0.190	0.058	0.132			
1225	1.734	0.192	0.056	0.132			
1254	1.520	0.102	0.030	0.066		√	ash, many broken shells
1255	2.614	0.172	0.052	0.120			
1256	3.800	0.122	0.038	0.078			
1257	4.260	0.170	0.048	0.118		√	ash, many broken shells
1258	5.526	0.458	0.096	0.362		√	ash, many broken shells
1259	4.864	0.624	0.114	0.502			

Sample (depth, cm)	Sample weight	weight >63µm	weight >63<150µm	weight >150µm	Pteropods	Ash	Comments
1260	1.920	0.268	0.038	0.230			
1261	2.728	0.330	0.080	0.250			
1262	2.552	0.244	0.060	0.176			
1263	5.068	0.984	0.156	0.820			
1264	5.064	0.820	0.130	0.684			
1265	2.540	0.608	0.124	0.474			
1266	3.458	0.882	0.140	0.738			
1267	4.412	0.968	0.172	0.786			
1268	5.564	1.106	0.196	0.908			
1269	6.250	1.098	0.230	0.864			
1270	2.240	0.298	0.052	0.246			
1271	2.310	0.350	0.088	0.260			
1272	3.532	0.588	0.160	0.424			
1273	3.344	0.610	0.110	0.494			
1274	3.542	0.696	0.110	0.582			
1275	3.480	0.606	0.116	0.488			
1276	3.232	0.502	0.098	0.404			
1277	4.148	0.866	0.132	0.728			
1278	4.530	0.984	0.160	0.818			
1279	5.434	1.248	0.218	1.024			
1280	2.137	0.448	0.064	0.384			
1281	3.042	0.656	0.124	0.528			
1282	2.898	0.662	0.138	0.516			
1283	4.214	0.974	0.222	0.750			
1284	3.312	0.564	0.124	0.418			
1285	3.490	0.450	0.108	0.338			
1286	2.610	0.390	0.094	0.288			
1287	2.954	0.608	0.118	0.484			
1288	3.142	0.592	0.114	0.478			
1289	3.802	0.748	0.140	0.600			
1290	2.062	0.416	0.050	0.366			
1291	3.390	0.434	0.094	0.330			
1292	2.774	0.338	0.060	0.274			
1293	4.256	0.568	0.114	0.452			
1294	2.382	0.300	0.060	0.230			
1295	2.752	0.284	0.058	0.220			
1296	3.142	0.508	0.092	0.408			
1297	4.288	0.818	0.108	0.694			
1298	4.800	0.782	0.142	0.636			
1299	5.390	0.760	0.162	0.594			
1300	3.081	0.482	0.076	0.408			
1301	3.826	0.536	0.114	0.412			
1302	4.002	0.648	0.136	0.506			
1303	3.648	0.618	0.124	0.488			
1304	3.442	0.466	0.112	0.356			
1305	2.828	0.434	0.096	0.336			
1306	2.344	0.304	0.088	0.214			
1307	3.918	0.422	0.112	0.306			

Sample (depth, cm)	Sample weight	weight >63µm	weight >63<150µm	weight >150µm	Pteropods	Ash	Comments
1308	3.302	0.574	0.154	0.412			
1309	4.678	0.582	0.144	0.434			
1310	1.594	0.254	0.078	0.176			
1311	3.654	0.396	0.110	0.284			
1312	2.414	0.260	0.062	0.188			
1313	1.290	0.150	0.034	0.112			
1314	4.864	0.670	0.140	0.526			
1315	3.306	0.372	0.098	0.268			
1316	2.448	0.248	0.060	0.182			
1317	2.342	0.186	0.054	0.132			
1318	3.944	0.384	0.092	0.284			
1319	1.844	0.128	0.036	0.090			
1320	2.716	0.514	0.116	0.398			
1321	2.558	0.268	0.066	0.198			
1322	2.952	0.328	0.086	0.240			
1323	3.346	0.352	0.086	0.262			
1324	3.724	0.240	0.074	0.162			
1325	2.432	0.182	0.048	0.128			
1326	2.844	0.242	0.074	0.168			
1327	3.716	0.356	0.082	0.268			
1328	3.094	0.206	0.052	0.150			
1329	2.510	0.184	0.046	0.134			
1330	4.192	0.782	0.176	0.602			
1331	4.112	0.492	0.100	0.388			
1332	3.056	0.280	0.072	0.208			
1333	5.148	0.304	0.068	0.234			
1334	3.078	0.130	0.030	0.100			
1335	2.632	0.102	0.022	0.082			
1336	3.670	0.168	0.046	0.122			
1337	2.326	0.086	0.014	0.072			
1338	4.208	0.092	0.022	0.066			many broken shells
1339	3.970	0.084	0.018	0.066			many broken shells
1340	2.765	0.402	0.092	0.304			many broken shells
1341	3.012	0.150	0.038	0.112			many broken shells
1342	3.044	0.158	0.054	0.104			many broken shells
1343	2.866	0.172	0.058	0.114			many broken shells
1344	4.172	0.166	0.056	0.102			many broken shells
1345	1.868	0.110	0.042	0.064			many broken shells
1346	2.384	0.092	0.038	0.052			many broken shells
1347	2.842	0.142	0.058	0.078		√	ash
1348	3.084	0.130	0.060	0.068		√	ash
1349	4.592	0.338	0.112	0.222		√	ash
1350	1.737	0.332	0.080	0.252		√	ash
1351	2.294	0.120	0.056	0.060		√	ash
1352	2.604	0.170	0.080	0.094		√	ash
1353	1.466	0.122	0.038	0.080		√	ash
1354	3.278	0.240	0.108	0.162		√	ash
1355	1.546	0.090	0.042	0.050		√	ash

Sample (depth, cm)	Sample weight	weight >63µm	weight >63<150µm	weight >150µm	Pteropods	Ash	Comments
1356	0.842	0.084	0.024	0.050		√	ash
1357	2.266	0.216	0.070	0.140		√	ash
1358	1.888	0.118	0.044	0.074		√	ash
1359	2.136	0.098	0.040	0.054		√	ash
1360	1.508	0.228	0.044	0.180			
1361	1.404	0.078	0.028	0.050			
1362	2.430	0.154	0.058	0.092			
1363	2.142	0.326	0.076	0.250			
1364	1.440	0.136	0.038	0.098			
1365	1.846	0.252	0.048	0.204			
1366	2.368	0.222	0.060	0.168			
1367	1.508	0.120	0.032	0.090			
1368	1.692	0.130	0.036	0.096			
1369	1.966	0.174	0.060	0.116			
1370	1.168	0.196	0.040	0.154			
1371	1.470	0.066	0.020	0.046			
1372	2.640	0.192	0.050	0.140			
1373	2.166	0.160	0.056	0.106			
1374	2.778	0.196	0.044	0.154			
1375	2.664	0.250	0.056	0.194			
1376	2.684	0.222	0.054	0.166			
1377	2.302	0.208	0.048	0.156			
1378	3.088	0.310	0.056	0.256			
1379	2.340	0.226	0.036	0.188			
1380	1.445	0.230	0.046	0.178			
1393	2.356	0.360	0.084	0.278			
1394	2.414	0.246	0.052	0.190			
1395	1.924	0.206	0.042	0.160			
1396	2.658	0.278	0.050	0.220			
1397	2.062	0.252	0.056	0.206			
1398	3.344	0.420	0.088	0.330			
1399	3.740	0.474	0.086	0.386			
1400	2.118	0.310	0.072	0.236			
1401	2.544	0.170	0.048	0.120			
1402	4.066	0.328	0.060	0.274			
1403	4.000	0.318	0.082	0.240			
1404	4.856	0.512	0.204	0.310		√	ash
1405	3.800	0.440	0.140	0.298		√	ash
1406	4.382	0.442	0.172	0.280		√	ash
1407	3.670	0.372	0.104	0.286		√	ash
1408	3.878	0.420	0.110	0.308		√	ash
1409	4.026	0.402	0.076	0.328			
1410	2.677	0.472	0.096	0.374			
1411	2.998	0.392	0.068	0.322			
1412	2.010	0.264	0.050	0.212			
1413	2.732	0.344	0.054	0.284			
1414	3.388	0.588	0.096	0.490			
1415	2.706	0.380	0.052	0.322			

Sample (depth, cm)	Sample weight	weight >63µm	weight >63<150µm	weight >150µm	Pteropods	Ash	Comments
1416	3.856	0.456	0.070	0.384			
1417	2.880	0.376	0.062	0.310			
1418	3.178	0.414	0.066	0.346			
1419	2.280	0.314	0.048	0.264			
1420	2.119	0.486	0.076	0.408			
1421	2.584	0.424	0.068	0.350			
1422	3.280	0.532	0.070	0.458			
1423	2.196	0.282	0.042	0.236			
1424	3.414	0.382	0.068	0.312			
1425	2.820	0.326	0.042	0.280			
1426	3.996	0.384	0.064	0.304			
1427	3.514	0.350	0.060	0.288			
1428	3.386	0.414	0.062	0.346			
1429	4.134	0.442	0.082	0.356			
1430	3.656	0.600	0.106	0.492			
1431	3.534	0.496	0.060	0.432			
1432	2.750	0.308	0.042	0.264			
1433	3.690	0.588	0.068	0.512			
1434	2.772	0.340	0.044	0.292			
1435	3.346	0.360	0.030	0.104			many broken shells
1436	3.154	0.226	0.040	0.180			
1437	3.980	0.274	0.048	0.226			
1438	3.390	0.130	0.028	0.100			few whole forams, broken shells
1439	2.770	0.214	0.040	0.170			
1440	1.906	0.402	0.062	0.338			
1441	3.294	0.428	0.070	0.350			
1442	2.814	0.602	0.070	0.528			
1443	3.344	0.690	0.092	0.596			
1444	2.958	0.530	0.072	0.456			
1445	2.978	0.522	0.076	0.444			
1446	2.986	0.288	0.042	0.246			
1447	3.184	0.406	0.056	0.292			
1448	2.096	0.124	0.028	0.094			few whole forams - broken shells
1449	2.304	0.292	0.048	0.230			
1450	2.418	0.124	0.022	0.102			
1451	2.730	0.084	0.020	0.062			
1452	1.830	0.156	0.030	0.120			
1453	4.366	0.348	0.064	0.278			
1454	3.224	0.386	0.054	0.324			
1455	3.028	0.328	0.050	0.276			
1456	2.664	0.320	0.050	0.266			
1457	2.734	0.446	0.066	0.374			
1458	2.932	0.242	0.050	0.190			
1459	3.300	0.294	0.058	0.234			
1460	1.908	0.244	0.056	0.186			
1461	2.646	0.246	0.044	0.196			

Sample (depth, cm)	Sample weight	weight >63µm	weight >63<150µm	weight >150µm	Pteropods	Ash	Comments
1462	3.226	0.174	0.030	0.130			
1463	2.632	0.254	0.046	0.204			
1464	2.304	0.254	0.056	0.192			
1465	3.834	0.624	0.110	0.512			
1466	1.638	0.272	0.050	0.218			
1467	3.476	0.600	0.096	0.500			
1468	2.348	0.450	0.066	0.382			
1469	2.186	0.218	0.042	0.170			
1470	2.349	0.378	0.072	0.302			
1471	2.302	0.366	0.052	0.302			
1472	2.364	0.432	0.072	0.356			
1473	3.114	0.472	0.098	0.368			
1474	1.892	0.338	0.076	0.256			
1475	3.124	0.552	0.148	0.394			
1476	4.002	0.462	0.194	0.266		√	ash; silica spikes,sponge
1477	4.440	0.702	0.396	0.298		√	ash
1478	2.704	0.430	0.128	0.296		√	ash
1479	4.090	0.582	0.112	0.468			
1480	1.680	0.346	0.054	0.288			
1481	3.364	0.564	0.080	0.478			
1482	0.688	0.076	0.018	0.054		√	few whole forams, ash
1483	2.442	0.116	0.020	0.088			few whole forams, broken shells
1484	2.880	0.276	0.050	0.224			
1485	2.338	0.192	0.042	0.150		√	few whole forams, broken shells
1486	3.346	0.196	0.050	0.144		√	no *G. ruber*
1487	2.398	0.122	0.030	0.090		√	no *G. ruber*
1488	3.820	0.172	0.044	0.126		√	
1489	2.818	0.118	0.026	0.090		√	
1490	1.562	0.194	0.040	0.154		√	
1491	1.504	0.092	0.018	0.070			
1492	1.874	0.140	0.026	0.112			
1493	3.456	0.302	0.052	0.238			
1494	2.174	0.256	0.036	0.220			
1495	2.990	0.206	0.048	0.156			
1496	2.214	0.080	0.024	0.054			
1497	2.954	0.084	0.022	0.056			
1498	3.134	0.142	0.032	0.106			
1499	2.398	0.086	0.026	0.058			
1500	1.404	0.194	0.038	0.156			
1501	2.420	0.148	0.038	0.106			
1502	1.436	0.148	0.036	0.108			
1503	1.400	0.104	0.032	0.068			
1504	2.288	0.106	0.030	0.074			
1505	2.290	0.138	0.040	0.096			
1506	2.044	0.102	0.034	0.068			few whole forams, many broken shells

Sample (depth, cm)	Sample weight	weight >63µm	weight >63<150µm	weight >150µm	Pteropods	Ash	Comments
1507	2.262	0.136	0.042	0.096			
1508	2.156	0.082	0.022	0.060			
1509							missing
1510	1.962	0.166	0.028	0.138			
1511	1.674	0.052	0.016	0.034		√	few whole whole forams
1512	1.296	0.044	0.014	0.028		√	no *G. ruber*, ash
1513	2.602	0.128	0.046	0.082		√	no *G. ruber*, ash
1514	1.664	0.056	0.026	0.028		√	no *G. ruber*, ash
1515	1.780	0.068	0.032	0.032		√	no *G. ruber*, ash
1516	3.128	0.188	0.126	0.054		√	ash
1517	3.582	0.456	0.374	0.066		√	ash, not enough forams
1518	1.590	0.166	0.118	0.046		√	ash, not enough forams
1519	2.882	0.330	0.206	0.124		√	ash "frosted"
1520	2.335	0.332	0.164	0.164		√	ash
1521	1.488	0.144	0.060	0.050		√	ash
1522	1.880	0.114	0.050	0.062		√	ash
1523	3.024	0.206	0.078	0.120		√	ash
1524	3.236	0.184	0.068	0.112		√	ash
1525	1.762	0.074	0.022	0.046		√	ash
1526	1.454	0.126	0.038	0.086		√	ash
1527	0.949	0.152	0.044	0.102		√	ash
1528	3.344	0.216	0.068	0.142		√	ash
1529	3.006	0.156	0.042	0.112		√	ash, not enough forams
1530	1.148	0.100	0.028	0.072		√	ash
1531	2.116	0.118	0.026	0.088		√	ash
1532	3.850	0.322	0.066	0.256		√	ash
1533	2.798	0.204	0.062	0.142		√	ash
1534	2.044	0.194	0.042	0.150		√	ash
1535	1.998	0.136	0.040	0.100		√	ash, not enough forams
1536	1.482	0.176	0.052	0.116		√	ash, many broken shells
1537	2.102	0.214	0.056	0.152		√	ash
1538	2.474	0.280	0.060	0.214		√	ash
1539	2.012	0.210	0.040	0.164			
1540	1.688	0.258	0.048	0.204			
1541	2.358	0.412	0.068	0.338			
1542	2.300	0.426	0.102	0.324			
1543	1.954	0.346	0.076	0.260			
1544	1.832	0.298	0.078	0.212			
1545	2.270	0.372	0.102	0.266			
1546	1.798	0.386	0.072	0.306			
1547	2.276	0.362	0.066	0.288			
1548	2.534	0.356	0.078	0.276			
1549	1.466	0.344	0.068	0.270			
1550	2.556	0.672	0.102	0.562		√	ash
1551	3.124	0.960	0.154	0.756			
1552	1.490	0.212	0.056	0.150			
1553	2.888	0.484	0.098	0.376			
1554	2.726	0.558	0.112	0.442			

Sample (depth, cm)	Sample weight	weight >63µm	weight >63<150µm	weight >150µm	Pteropods	Ash	Comments
1555	2.118	0.570	0.102	0.456			
1556	2.196	0.558	0.102	0.448			
1557	3.494	0.868	0.164	0.672			
1558	2.108	0.588	0.112	0.470			
1559	1.670	0.498	0.088	0.396			
1560	2.366	0.888	0.166	0.718			
1561	3.072	0.922	0.170	0.746			
1562	2.340	0.752	0.126	0.510			
1563	2.652	0.580	0.122	0.448			
1564	2.232	0.508	0.092	0.410			
1565	3.098	0.754	0.134	0.614			
1566	1.774	0.422	0.088	0.320			
1567	2.356	0.486	0.072	0.394			
1568	2.714	0.696	0.106	0.576			
1569	2.314	0.606	0.104	0.500			
1570	2.202	0.782	0.134	0.636			
1571	2.044	0.550	0.104	0.436			
1572	2.640	0.694	0.132	0.562			
1573	2.194	0.528	0.116	0.408			
1574	2.486	0.608	0.110	0.494			
1575	2.374	0.586	0.118	0.464			
1576	1.910	0.450	0.094	0.354			
1577	2.459	0.456	0.082	0.368			
1578	2.196	0.404	0.094	0.310			
1579	3.124	0.504	0.106	0.388			
1580	1.870	0.586	0.132	0.444			
1581	1.772	0.296	0.062	0.228			
1582	2.180	0.308	0.058	0.240			
1583	2.676	0.494	0.100	0.386			
1584	3.452	0.726	0.170	0.552			
1585	2.130	0.368	0.108	0.256			
1586	1.940	0.284	0.052	0.226			
1587	3.724	0.536	0.228	0.306		√	ash
1588	3.510	0.550	0.336	0.204		√	ash
1589	3.762	0.436	0.226	0.206		√	ash
1590	3.450	0.702	0.296	0.388		√	ash
1591	2.380	0.386	0.166	0.214		√	ash
1592	3.104	0.522	0.224	0.294		√	ash
1593	2.976	0.466	0.206	0.254		√	ash, pink ruber datum
1594	3.762	0.536	0.296	0.234		√	ash
1595	2.226	0.502	0.182	0.314		√	ash
1596	3.564	0.492	0.166	0.322		√	ash
1597	1.816	0.314	0.098	0.214		√	ash
1598	2.238	0.496	0.090	0.400			
1599	2.758	0.634	0.102	0.526			
1600	1.782	0.550	0.118	0.390			
1601	2.636	0.600	0.108	0.486			
1602	2.346	0.594	0.098	0.494			

Sample (depth, cm)	Sample weight	weight >63µm	weight >63<150µm	weight >150µm	Pteropods	Ash	Comments
1603	2.306	0.614	0.118	0.492			
1604	3.678	0.786	0.146	0.634			
1605	2.258	0.516	0.110	0.402			
1606	3.542	0.892	0.164	0.724			
1607	1.948	0.586	0.066	0.510			
1608	3.010	0.802	0.132	0.664			
1609	3.116	0.848	0.130	0.716			
1610	1.408	0.384	0.076	0.298			
1611	2.674	0.574	0.114	0.454			
1612	2.560	0.574	0.092	0.490			
1613	2.624	0.610	0.082	0.528			
1614	1.888	0.542	0.086	0.450			
1615	2.004	0.624	0.074	0.550			
1616	1.942	1.312	0.174	1.132			
1617	2.478	1.066	0.158	0.902			
1618	2.058	0.678	0.080	0.592			
1619	1.980	0.984	0.118	0.864			
1620	1.530	1.016	0.170	0.844			
1621	1.682	0.838	0.132	0.700			
1622	1.672	1.106	0.090	0.932			
1623	1.376	0.746	0.066	0.676			
1624	2.192	1.118	0.074	1.040			
1625	3.254	0.818	0.150	0.666			
1626	2.774	0.578	0.091	0.484			
1627	1.730	0.500	0.080	0.412			
1628	1.836	0.478	0.102	0.370			
1629	1.918	0.388	0.094	0.290			
1630	1.404	0.496	0.128	0.364			
1631	2.188	0.392	0.078	0.306			
1632	1.578	0.280	0.070	0.202			
1633	1.254	0.230	0.060	0.170			
1634	2.156	0.350	0.082	0.262			
1635	2.084	0.250	0.062	0.182			
1636	1.472	0.368	0.076	0.284			
1637	2.028	0.322	0.086	0.232			
1638	2.776	0.510	0.124	0.380			
1639	1.894	0.342	0.064	0.272			
1640	2.262	0.336	0.092	0.238			
1641							missing
1642	1.766	0.240	0.082	0.152			
1643	2.298	0.312	0.084	0.224			
1644	2.466	0.328	0.092	0.232			
1645	1.728	0.244	0.060	0.180			
1646	1.576	0.230	0.066	0.162			
1647	1.862	0.260	0.072	0.184			
1648	2.582	0.446	0.208	0.230			
1649	2.094	0.264	0.094	0.168			
1650	3.600	0.652	0.182	0.468			

Sample (depth, cm)	Sample weight	weight >63µm	weight >63<150µm	weight >150µm	Pteropods	Ash	Comments
1651	3.138	0.468	0.120	0.322			
1652	1.224	0.178	0.034	0.134			
1653	3.030	0.410	0.092	0.316			
1654	2.992	0.446	0.132	0.308			
1655	2.116	0.318	0.080	0.236			
1656	1.500	0.220	0.060	0.154			
1657	3.636	0.482	0.148	0.330			
1658	3.274	0.464	0.106	0.352			
1659	2.306	0.316	0.096	0.214			
1660	2.460	0.322	0.114	0.206			
1661	3.554	0.548	0.136	0.410			
1662	2.180	0.280	0.088	0.188			
1663	3.642	0.352	0.100	0.250			
1664	2.088	0.236	0.078	0.152			
1665	2.232	0.280	0.086	0.192			
1666	2.674	0.234	0.054	0.174			
1667	2.786	0.446	0.126	0.314			
1668	3.500	0.526	0.124	0.396			
1669	3.296	0.446	0.130	0.312			
1670	2.410	0.356	0.118	0.238			
1671	2.754	0.316	0.114	0.200			
1672	2.856	0.372	0.116	0.254			
1673	2.878	0.372	0.132	0.232			
1674	3.714	0.454	0.144	0.306			
1675	3.658	0.316	0.122	0.190			
1676	3.288	0.352	0.112	0.238			
1677	3.930	0.548	0.198	0.344			
1678	3.234	0.328	0.130	0.192			
1679	2.886	0.254	0.084	0.168			
1680	3.286	0.522	0.206	0.314			
1681	3.036	0.380	0.146	0.234			
1682	2.300	0.278	0.074	0.198			
1683	2.992	0.262	0.106	0.156			
1684	2.518	0.238	0.104	0.132			
1685	2.708	0.190	0.070	0.116			
1686	2.212	0.202	0.090	0.110			
1687	2.832	0.266	0.088	0.176			
1688	2.840	0.406	0.146	0.256			
1689	3.818	0.400	0.126	0.272			
1690	2.344	0.420	0.120	0.296			
1691	2.608	0.406	0.126	0.280			
1692	2.588	0.386	0.110	0.270			
1693	2.896	0.336	0.132	0.202			
1694	1.664	0.148	0.062	0.088			
1695	1.732	0.098	0.052	0.042			
1696	2.068	0.130	0.064	0.062		√	ash
1697	2.834	0.292	0.114	0.174		√	ash
1698	1.374	0.152	0.058	0.090		√	ash

Sample (depth, cm)	Sample weight	weight >63µm	weight >63<150µm	weight >150µm	Pteropods	Ash	Comments
1699	3.208	0.312	0.122	0.184		√	ash
1700	2.228	0.358	0.128	0.230		√	ash
1701	2.260	0.286	0.126	0.152		√	ash
1702	2.662	0.244	0.084	0.156		√	ash
1703	2.024	0.244	0.100	0.136		√	ash
1704	2.668	0.308	0.134	0.166		√	ash
1705	1.672	0.184	0.076	0.110		√	ash
1706	2.278	0.298	0.132	0.162		√	ash
1707	2.546	0.252	0.114	0.132		√	ash
1708	2.470	0.214	0.110	0.100		√	ash
1709	4.064	0.166	0.090	0.072			
1710	3.880	0.428	0.260	0.166			
1711	4.214	0.378	0.202	0.168			
1712	1.706	0.160	0.074	0.082			
1713	2.698	0.232	0.086	0.138			
1714	2.432	0.380	0.126	0.246			
1715	2.062	0.292	0.110	0.178			
1716	2.336	0.182	0.080	0.106			
1717	1.848	0.072	0.030	0.042			
1718	2.904	0.214	0.096	0.114			
1719	2.074	0.128	0.070	0.056			
1720	2.214	0.310	0.092	0.212			
1721	2.050	0.092	0.048	0.042			
1722	1.810	0.142	0.052	0.084			
1723	2.990	0.170	0.078	0.086			
1724	1.888	0.118	0.052	0.060			
1725	2.104	0.140	0.054	0.086			
1726	3.060	0.166	0.082	0.078			
1727	2.182	0.116	0.062	0.046			
1728	1.804	0.142	0.066	0.072			
1729	1.800	0.104	0.052	0.052			
1730	1.982	0.246	0.084	0.160			
1731	2.288	0.176	0.084	0.086			
1732	2.104	0.098	0.042	0.052			
1733	2.774	0.130	0.054	0.076			
1734	2.370	0.136	0.064	0.065			
1735	2.286	0.134	0.054	0.074			
1736	2.020	0.110	0.052	0.056			
1737	2.668	0.142	0.060	0.072			
1738	1.988	0.122	0.050	0.070			
1739	1.510	0.098	0.042	0.048			
1740	2.280	0.364	0.108	0.254			
1741	2.946	0.098	0.066	0.088			
1742	2.096	0.122	0.064	0.064			
1743	0.960	0.132	0.052	0.078			
1744	2.208	0.142	0.056	0.086			
1745	2.418	0.168	0.048	0.116			
1746	2.720	0.194	0.078	0.110			

Sample (depth, cm)	Sample weight	weight >63µm	weight >63<150µm	weight >150µm	Pteropods	Ash	Comments
1747	2.364	0.134	0.042	0.088			
1748	2.190	0.102	0.040	0.058			
1749	1.716	0.114	0.016	0.098			
1750	0.962	0.314	0.094	0.212			
1751	1.326	0.092	0.008	0.086			
1752	2.000	0.156	0.024	0.130			
1753	2.374	0.162	0.020	0.140			
1754	1.972	0.156	0.024	0.128			
1755	1.474	0.120	0.022	0.094			
1756	1.332	0.240	0.022	0.102			
1757	2.860	0.070	0.026	0.046			
1758	2.362	0.110	0.026	0.084			
1759	1.080	0.302	0.010	0.040			
1760	2.798	0.326	0.146	0.178			
1761	3.720	0.212	0.054	0.154			
1762	2.578	0.200	0.026	0.168			
1763	2.570	0.172	0.022	0.148			
1764	3.112	0.352	0.064	0.288			
1765	2.286	0.114	0.086	0.026			
1766	1.898	0.160	0.034	0.126			
1767	1.820	0.102	0.058	0.040			
1768	2.706	0.140	0.076	0.058			
1769	2.398	0.110	0.056	0.052			
1770	3.334	0.436	0.260	0.174	√	√	ash, pteropods
1771	2.790	0.232	0.174	0.054			
1772	2.708	0.188	0.170	0.016			
1773	2.284	0.074	0.048	0.024			
1774	2.824	0.138	0.086	0.052			
1775	2.572	0.064	0.028	0.028			
1776	1.670	0.094	0.046	0.042			
1777	1.794	0.132	0.060	0.068			
1778	1.758	0.122	0.040	0.082			
1779	2.232	0.136	0.062	0.068			
1780	1.438	0.240	0.064	0.174	√	√	ash, pteropods
1781	2.038	0.120	0.046	0.072			
1782	2.622	0.188	0.068	0.114			
1783	2.462	0.104	0.044	0.066			
1784	1.748	0.050	0.020	0.026			
1785	1.826	0.122	0.018	0.104			
1786	2.220	0.110	0.046	0.056			
1787	2.212	0.106	0.054	0.046			
1788	1.934	0.082	0.034	0.042			
1789	2.842	0.116	0.052	0.060			
1790	2.956	0.418	0.114	0.304	√	√	ash, pteropods
1791	2.238	0.062	0.030	0.030			
1792	2.316	0.094	0.046	0.044			
1793	1.764	0.026	0.010	0.014			
1793	2.478	0.092	0.038	0.044			

Sample (depth, cm)	Sample weight	weight >63µm	weight >63<150µm	weight >150µm	Pteropods	Ash	Comments
1794	1.912	0.082	0.040	0.040			
1795	1.780	0.040	0.018	0.022			
1796	1.632	0.092	0.038	0.050			
1797	2.722	0.078	0.028	0.042			
1798	2.090	0.060	0.024	0.038			
1799	1.934	0.054	0.024	0.034			
1800	1.536	0.204	0.056	0.146			

Note:
samples: 662-672,1226-1253,
1381-1392 are voids in original core
samples: 370, 933-935,
937-939,1509,
and 1641 are lost in mail